

EUROPEAN ORGANISATION FOR NUCLEAR RESEARCH (CERN)



JHEP 08 (2019) 033
DOI: [10.1007/JHEP08\(2019\)033](https://doi.org/10.1007/JHEP08(2019)033)



CERN-EP-2019-011
13th November 2019

Measurement of jet-substructure observables in top quark, W boson and light jet production in proton-proton collisions at $\sqrt{s} = 13$ TeV with the ATLAS detector

The ATLAS Collaboration

A measurement of jet substructure observables is presented using data collected in 2016 by the ATLAS experiment at the LHC with proton-proton collisions at $\sqrt{s} = 13$ TeV. Large-radius jets groomed with the trimming and soft-drop algorithms are studied. Dedicated event selections are used to study jets produced by light quarks or gluons, and hadronically decaying top quarks and W bosons. The observables measured are sensitive to substructure, and therefore are typically used for tagging large-radius jets from boosted massive particles. These include the energy correlation functions and the N -subjettiness variables. The number of subjets and the Les Houches angularity are also considered. The distributions of the substructure variables, corrected for detector effects, are compared to the predictions of various Monte Carlo event generators. They are also compared between the large-radius jets originating from light quarks or gluons, and hadronically decaying top quarks and W bosons.

1 Introduction

Increasing the centre-of-mass energy of proton–proton (pp) collisions from 7 and 8 TeV in Run 1 to 13 TeV in Run 2 of the Large Hadron Collider (LHC) leads to a larger fraction of heavy particles such as top quarks, vector bosons and Higgs bosons being produced with large transverse momenta. This large transverse momentum leads to collimated decay products. They are usually reconstructed in a large-radius jet, whose internal (sub)structure shows interesting features that can be used to identify the particle that initiated the jet formation [1, 2].

This is relevant for a host of measurements and searches, which involve identifying the large-radius jets coming from top quarks [3–7], or Higgs bosons [8–11], for example in Run 2 in ATLAS. Usually a two step procedure is employed. In the first step, termed grooming, the effect of soft, uncorrelated radiation contained in the large-radius jet is reduced. Then jet substructure observables, which describe the spatial energy distribution inside the jets, are used to classify the jets originating from different particles. This process is called jet tagging and the algorithms are referred to as taggers.

Most of the grooming algorithms and jet substructure observables were developed on the basis of theoretical calculations or Monte Carlo (MC) simulation programs and then they are applied to data. Given that often large differences have been seen between predictions from MC and data, large correction factors need to be applied to simulation results. Additionally, taggers suffer from large systematic uncertainties as the modelling of the substructure observables is not well constrained [2, 12]. Most of these variables have never been measured in data, and performing a proper unfolded measurement is a common request from the theory community. Measuring these observables will help in optimising and developing current and future substructure taggers, as well as tuning hadronization models in the important but still relatively unexplored regime of jet substructure. The choice of variables measured in this paper prioritized jet shapes commonly used in jet tagging, as well as those most useful for model tuning.

The ATLAS Collaboration has performed measurements of jet mass and substructure variables at the pp centre-of-mass energies of $\sqrt{s} = 7, 8$ and 13 TeV [13–19] in inclusive jet events, and the CMS Collaboration has performed measurements of jet mass and substructure in dijet, W/Z boson, and $t\bar{t}$ events [20–24] at $\sqrt{s} = 7, 8$ and 13 TeV. This paper presents measurements of substructure variables in large-radius jets produced in inclusive multijet events and in $t\bar{t}$ events at $\sqrt{s} = 13$ TeV using 33 fb^{-1} of data collected in 2016 by the ATLAS experiment. In this analysis, the lepton+jets decay mode of $t\bar{t}$ events is selected, where one W boson decays into a muon and a neutrino, and the other W boson decays into a pair of quarks. Then the large-radius jets are separated into those that contain all the decay products of a hadronically decaying top quark and those containing only hadronic W boson decay products.

The contents of this paper are organised as follows. First, a description of the ATLAS detector is presented in Section 2 and then the MC samples used in the analysis are discussed in Section 3. In Section 4, event and object selections are summarised. The measured jet substructure observables are defined in Section 5. The background estimation is described in Section 6 and the systematic uncertainties are assessed in Section 7. In Section 8, detector-level mass and p_T distributions corresponding to selected large-radius jets are shown, and the unfolding is described in Section 9. Finally, the unfolded results are presented in Section 10, and the conclusions in Section 11.

2 ATLAS detector

The ATLAS experiment uses a multipurpose particle detector [25, 26] with a forward–backward symmetric cylindrical geometry and a near 4π coverage in solid angle.¹ It consists of an inner tracking detector (ID) surrounded by a thin superconducting solenoid providing a 2 T axial magnetic field, electromagnetic (EM) and hadron calorimeters, and a muon spectrometer. The ID consists of silicon pixel, silicon microstrip, and straw-tube transition-radiation tracking detectors, covering the pseudorapidity range $|\eta| < 2.5$. The calorimeter system covers the pseudorapidity range $|\eta| < 4.9$. Electromagnetic calorimetry is performed with barrel and endcap high-granularity lead/liquid-argon (LAr) sampling calorimeters, within the region $|\eta| < 3.2$. There is an additional thin LAr presampler covering $|\eta| < 1.8$, to correct for energy loss in material upstream of the calorimeters. For $|\eta| < 2.5$, the LAr calorimeters are divided into three layers in depth. Hadronic calorimetry is performed with a steel/scintillator-tile calorimeter, segmented into three barrel structures within $|\eta| < 1.7$, and two copper/LAr hadronic endcap calorimeters, which cover the region $1.5 < |\eta| < 3.2$. The forward solid angle up to $|\eta| = 4.9$ is covered by copper/LAr and tungsten/LAr calorimeter modules, which are optimised for energy measurements of electrons/photons and hadrons, respectively. The muon spectrometer consists of separate trigger and high-precision tracking chambers that measure the deflection of muons in a magnetic field generated by superconducting air-core toroids.

The ATLAS detector selects events using a tiered trigger system [27]. The first level is implemented in custom electronics. The second level is implemented in software running on a general-purpose processor farm which processes the events and reduces the rate of recorded events to 1 kHz.

3 Monte Carlo samples

Simulated events are used to optimise the event selection, correct the data for detector effects and estimate systematic uncertainties. The predictions of different phenomenological models implemented in the Monte Carlo (MC) generators are compared with the data corrected to the particle level (i.e. observables constructed from final-state particles within the detector acceptance).

The generators used to produce the samples are listed in Table 1. The dijet (to obtain multijet events), $t\bar{t}$ and single-top-quark samples are considered to be signal processes in this analysis, corresponding to the dedicated selections. The background is estimated using $Z/W+\text{jets}$ and diboson samples. The $t\bar{t}$ samples are scaled to next-to-next-to-leading order (NNLO) in perturbative QCD, including soft-gluon resummation to next-to-next-to-leading-log order (NNLL) [28] in cross-section, assuming a top quark mass $m_t = 172.5$ GeV. The PowHEG model [29] resummation damping parameter, h_{damp} , which controls the matching of matrix elements to parton showers and regulates the high- p_T radiation, was set to $1.5m_t$ [30]. The single-top-quark [31–36] and W/Z samples [37] are scaled to the NNLO theoretical cross-sections.

The predicted shape of jet substructure distributions depends on the modelling of final-state radiation (FSR), and fragmentation and hadronisation, as well as on the merging/matching between matrix element (ME) and parton shower (PS) generators. The PYTHIA8 and the SHERPA generators use a dipole shower ordered

¹ ATLAS uses a right-handed coordinate system with its origin at the nominal interaction point (IP) in the centre of the detector and the z -axis along the beam pipe. The x -axis points from the IP to the centre of the LHC ring, and the y -axis points upwards. Cylindrical coordinates (r, ϕ) are used in the transverse plane, ϕ being the azimuthal angle around the z -axis. The pseudorapidity is defined in terms of the polar angle θ as $\eta = -\ln \tan(\theta/2)$. An angular separation between two objects is defined as $\Delta R \equiv \sqrt{(\Delta\eta)^2 + (\Delta\phi)^2}$, where $\Delta\eta$ and $\Delta\phi$ are the separations in η and ϕ . Momentum in the transverse plane is denoted by p_T .

in transverse momentum, with the Lund string [38] and cluster hadronisation model [39] respectively. The HERWIG7 generator uses an angle-ordered shower, with the cluster hadronisation model. For comparison purposes in dijet events, a sample was generated with SHERPA using the string hadronisation model.

| Process | Generator | Version | PDF | Tune | Use |
|------------|--------------------|---------|----------------|-------------------|--|
| Dijet | PYTHIA8 [40, 41] | 8.186 | NNPDF23LO [42] | A14 [43] | Nominal for unfolding |
| | SHERPA [44] | 2.2.1 | CT10 [45] | Default | Validation of unfolding (with two different hadronisation models) |
| | HERWIG7 [46] | 7.0.4 | MMHT2014 | H7UE [46] | Comparison |
| $t\bar{t}$ | POWHEG [47] | v2 | NNPDF30NLO | | Nominal for unfolding |
| | + PYTHIA8 | 8.186 | NNPDF23LO | A14 | |
| | POWHEG | v2 | CT10 | | Validation of unfolding |
| | +HERWIG++ [48] | 2.7 | CTEQ6L1 | UE-EE-5 tune [49] | |
| | POWHEG | v2 | CT10 | | Comparison |
| | +HERWIG7 | 7.0.4 | MMHT2014 | H7UE | |
| | MG5_aMC@NLO [50] | 2.6.0 | NNPDF30NLO | | Comparison |
| | + PYTHIA8 | 8.186 | NNPDF23LO | A14 | |
| | SHERPA | 2.2.1 | CT10 | Default | Comparison |
| Single top | POWHEG | v1 | CT10 | | Nominal for unfolding |
| | + PYTHIA6 [51, 52] | 6.428 | CTEQ6L1 [45] | Perugia2012 [53] | |
| Z+jets | SHERPA | 2.2.1 | CT10 | Default | Background estimation |
| W+jets | SHERPA | 2.2.1 | CT10 | Default | Background estimation (nominal) |
| W+jets | MG5_aMC@NLO | 2.2.5 | CT10 | | Background estimation (cross-check) |
| + PYTHIA8 | | 8.186 | NNPDF23LO | A14 | |
| Diboson | SHERPA | 2.2.1 | CT10 | Default | Background estimation |

Table 1: Main features of the Monte Carlo models used to simulate signal and background samples, and to produce predictions to be compared with data. The nominal samples listed are used for comparisons with corrected data at particle level as well. For convenience, MG5_aMC@NLO is referred to as MG5_aMC in Figures 3–9.

The MC samples were processed through the full ATLAS detector simulation [54] based on Geant4 [55], and then reconstructed and analysed using the same procedure and software that are used for the data. Additional pp collisions generated by PYTHIA8, with parameter values set to the A2 tune [56] and using the MSTW2008 [57] PDF set, were overlaid to simulate the effects of additional collisions from the same and nearby bunch crossings (pile-up), with a distribution of the number of extra collisions matching that of data.

4 Object and event selection

This analysis uses pp collision data at $\sqrt{s} = 13$ TeV collected by the ATLAS detector in 2016, that satisfy a number of criteria to ensure that the ATLAS detector was in good operating condition. All selected events must have at least one vertex with at least two associated tracks with $p_T > 400$ MeV. The vertex with the highest $\sum p_{T,\text{track}}^2$, where $p_{T,\text{track}}$ is the transverse momentum of a track associated with the vertex, is chosen as the primary vertex.

Jets are reconstructed from the EM-scale or locally-calibrated topological energy clusters [58] in both the EM and hadronic calorimeters using the anti- k_t algorithm [59] with a radius parameter of $R = 0.4$ or $R = 1.0$, referred to as small-radius and large-radius jets respectively. These clusters are assumed to be massless when computing the jet four-vectors and substructure variables. A trimming algorithm [60] is employed for the large-radius jets to mitigate the impact of initial-state radiation, underlying-event activity,

and pile-up. Trimming removes subjets of radius $R_{\text{sub}} = 0.2$ with $p_T^i/p_T^{\text{jet}} < f_{\text{cut}}$, where p_T^i is the transverse momentum of the i^{th} subjet, p_T^{jet} is the transverse momentum of the jet under consideration, and $f_{\text{cut}} = 0.05$. All large-radius jets used in this paper are trimmed before applying the selection criteria. The energies of jets are calibrated by applying p_T - and rapidity-dependent corrections derived from Monte Carlo simulation with additional correction factors for residual non-closure in data determined from data [58, 61].

In order to reduce the contamination by small-radius jets originating from pile-up, a requirement is imposed on the output of the Jet Vertex Tagger (JVT) [62]. The JVT algorithm is a multivariate algorithm that uses tracking information to reject jets which do not originate from the primary vertex, and is applied to jets with $p_T < 60$ GeV and $|\eta| < 2.4$. Small-radius jets containing b -hadrons are tagged using a neural-network-based algorithm [63–65] that combines information from the track impact parameters, secondary vertex location, and decay topology inside the jets. The operating point corresponds to an overall 70% b -tagging efficiency in simulated $t\bar{t}$ events, and to a probability of mis-tagging light-flavour jets of approximately 1%.

Muons are reconstructed from high-quality muon spectrometer track segments matched to ID tracks. Muons with a transverse momentum greater than 30 GeV and within $|\eta| < 2.5$ are selected if the associated track has a longitudinal impact parameter $|z_0 \sin(\theta)| < 0.5$ mm and a transverse impact parameter significance $|d_0|/\sigma(d_0) < 3$. The impact parameter d_0 is measured relative to the beam line. The muon candidates are also required to be isolated from nearby hadronic activity [66]. The muon isolation criteria remove muons that lie a distance $\Delta R(\mu, \text{jet}) < 0.04 + 10 \text{ GeV}/p_{T,\mu}$ from a small-radius jet axis, where $p_{T,\mu}$ is the p_T of the muon. Since muons deposit energy in the calorimeters, an overlap removal procedure is applied in order to avoid double counting of leptons and small-radius jets.

Electrons are reconstructed from energy deposits measured in the EM calorimeter which are matched to ID tracks. They are required to be isolated from nearby hadronic activity by using a set of p_T - and η -dependent criteria based on calorimeter and track information as described in Ref. [67]. Their selection also requires $p_T > 30$ GeV and $|\eta| < 2.5$, excluding the region $1.37 < |\eta| < 1.52$ which corresponds to the transition region between the barrel and end-cap calorimeters. Photon candidates are reconstructed from clusters of energy deposited in the EM calorimeter, and must have $p_T > 30$ GeV and $|\eta| < 2.5$. Photon identification is based primarily on shower shapes in the calorimeter [68].

The missing transverse momentum, with magnitude E_T^{miss} , is calculated as the negative vectorial sum of the transverse momenta of calibrated photons, electrons, muons and jets associated with the primary vertex [69]. The transverse mass of the leptonically decaying W boson, m_T^W , is defined using the absolute value of E_T^{miss} as $m_T^W = \sqrt{2p_{T,\mu}E_T^{\text{miss}}(1 - \cos \Delta\phi(\mu, E_T^{\text{miss}}))}$.

In order to examine large-radius jets originating from light quarks and gluons, from top quarks and from W bosons, three event selections are defined. These are referred to as *dijet*, *top* and *W selections*, and are indicative of the origin of the large-radius jet.

In the dijet selection, the events are accepted by a single-large-radius-jet trigger that becomes fully efficient for jets with $p_T > 400$ GeV. The offline dijet selection requires a leading trimmed large-radius jet with $p_T > 450$ GeV and $|\eta| < 1.5$, and at least one other trimmed large-radius jet with $p_T > 200$ GeV and $|\eta| < 2.5$, and rejects the event if an electron or muon is present.

For both the top and W selections, events are collected with a set of single-muon triggers that become fully efficient for muon $p_T > 28$ GeV. The top quarks and the W bosons are identified from their decay products. A geometrical separation between the decay products of the two top quark candidates is required.

Additional requirements are applied to separate large-radius jets containing all decay products of the top quark from those where the large-radius jet only contains the hadronic W boson decays, with the b -tagged small-radius jet reconstructed independently. These form the top selection and the W selection respectively. The selections are described in Table 2. After these requirements the data sample contains about 3.2×10^7 events in the dijet selection, and roughly 6800 and 4500 events in the top and W selection respectively.

Particle-level observables in Monte Carlo simulation are constructed from stable particles, defined as those with proper lifetimes $c\tau \gtrsim 10$ mm. Muons at particle level are dressed by including contributions from photons with an angular distance $\Delta R < 0.1$ from the muon. Particle-level jets do not include muons or neutrinos. Particle-level b -tagging is performed by requiring a prompt b -hadron to be ghost-associated [70] with the jet.

5 Definition of the jet observables

All large-radius jets are trimmed before being used in the selections, and subsequently only the leading trimmed large-radius is considered in the analysis. Then the large-radius jet constructed from the original constituents of the selected jet before the trimming step is groomed using the soft-drop algorithm, and the jet substructure observables studies are constructed from that soft-dropped large-radius jet.

Soft-drop [71, 72] is an extension of the original split-filtering technique [73] and relies on reclustering the jet constituents using the angle-ordered Cambridge–Aachen jet algorithm and then sequentially considering each splitting in order to remove soft and wide-angle radiation. At each step the jet is split into two proto-jets. The removal of proto-jets in a splitting is controlled by two parameters: a measure of the energy balance of the pair, z_{cut} , and the significance of the angular separation of the proto-jets, β^{SD} . These are used to define the soft-drop condition:

$$\frac{\min(p_{\text{T}1}, p_{\text{T}2})}{p_{\text{T}1} + p_{\text{T}2}} > z_{\text{cut}} \left(\frac{\Delta R_{12}}{R} \right)^{\beta^{\text{SD}}}$$

where R_{12} is the angular distance between the two proto-jets and R is the radius of the large jet. In this analysis, values of $z_{\text{cut}} = 0.1$ and $\beta^{\text{SD}} = 0.0$ are used, based on previous ATLAS studies [18], which is equivalent to modified mass drop tagger [74]. An important feature of soft-drop is that groomed observables are analytically calculable to high-order resummation accuracy [75–77].

The following substructure variables are measured in this analysis:

- Number of subjets with $p_{\text{T}} > 10$ GeV, reconstructed from the selected large-radius jet constituents using the k_t algorithm [78] with $R = 0.2$.
- Generalised angularities defined as:

$$\lambda_{\beta^{\text{LHA}}}^\kappa = \sum_{i \in J} z_i^\kappa \theta_i^{\beta^{\text{LHA}}},$$

where z_i is the transverse momentum of jet constituent i as a fraction of the scalar sum of the p_{T} of all constituents and θ_i is the angle of the i^{th} constituent relative to the jet axis, normalised by the jet radius. The exponents κ and β^{LHA} probe different aspects of the jet fragmentation. The ($\kappa = 1, \beta^{\text{LHA}} = 0.5$) variant is termed the Les Houches angularity (LHA) [79] and used in this analysis. It is an infrared-safe version of the jet-shape angularity, and provides a measure of the broadness of a jet.

| | Detector level | Particle level |
|--|--|---|
| Dijet selection: | | |
| Two trimmed anti- k_t $R = 1.0$ jets | $p_T > 200 \text{ GeV}$ $ \eta < 2.5$ | $p_T > 200 \text{ GeV}$ $ \eta < 2.5$ |
| Leading- p_T trimmed anti- k_t $R = 1.0$ jet | | $p_T > 450 \text{ GeV}$ |
| Top and W selections: | | |
| Exactly one muon | $p_T > 30 \text{ GeV}$ $ \eta < 2.5$ $ z_0 \sin(\theta) < 0.5 \text{ mm}$ and $ d_0/\sigma(d_0) < 3$ | $p_T > 30 \text{ GeV}$ $ \eta < 2.5$ |
| Anti- k_t $R = 0.4$ jets | $p_T > 25 \text{ GeV}$ $ \eta < 4.4$ JVT output > 0.5 (if $p_T < 60 \text{ GeV}$) | $p_T > 25 \text{ GeV}$ $ \eta < 4.4$ |
| Muon isolation criteria | If $\Delta R(\mu, \text{jet}) < 0.04 + 10 \text{ GeV}/p_{T,\mu}$: muon is removed, so the event is discarded | None |
| E_T^{miss}, m_T^W | $E_T^{\text{miss}} > 20 \text{ GeV}, E_T^{\text{miss}} + m_T^W > 60 \text{ GeV}$ | |
| Leptonic top | At least one small-radius jet with $0.4 < \Delta R(\mu, \text{jet}) < 1.5$ | |
| Top selection: | | |
| Leading- p_T trimmed anti- k_t $R = 1.0$ jet | $ \eta < 1.5, p_T > 350 \text{ GeV}$, mass $> 140 \text{ GeV}$ $\Delta R(\text{large-radius jet}, b\text{-tagged jet}) < 1$ $\Delta\phi(\mu, \text{large-radius jet}) > 2.3$ | |
| W selection: | | |
| Leading- p_T trimmed anti- k_t $R = 1.0$ jet | $ \eta < 1.5, p_T > 200 \text{ GeV}$, mass $> 60 \text{ GeV}$ and mass $< 100 \text{ GeV}$ $1 < \Delta R(\text{large-radius jet}, b\text{-tagged jet}) < 1.8$ $\Delta\phi(\mu, \text{large-radius jet}) > 2.3$ | |

Table 2: Summary of object event selections for detector-level and particle-level dijet and $t\bar{t}$ events. ‘‘Leptonic top’’ refers to the top quark that decays into a leptonically decaying W boson, while ‘‘ b -tagged jet’’ refers to small-radius jets that pass a b -tagging requirement. The top and W selections are common up to the requirement on the leptonic top, then they differ on the requirements on the leading- p_T trimmed large-radius jet. All selections are inclusive, unless otherwise mentioned.

- Energy correlation functions ECF2 and ECF3 [80], and related ratios C_2, D_2 [81]. The 1-point, 2-point and 3-point energy correlation functions for a jet J are given by:

$$\begin{aligned} \text{ECF1} &= \sum_{i \in J} p_{T,i}, \\ \text{ECF2}(\beta^{\text{ECF}}) &= \sum_{i < j \in J} p_{T,i} p_{T,j} (\Delta R_{ij})^{\beta^{\text{ECF}}}, \\ \text{ECF3}(\beta^{\text{ECF}}) &= \sum_{i < j < k \in J} p_{T,i} p_{T,j} p_{T,k} (\Delta R_{ij} \Delta R_{ik} \Delta R_{jk})^{\beta^{\text{ECF}}}, \end{aligned}$$

where the parameter β^{ECF} weights the angular separation of the jet constituents. In the above functions, the sum is over the i constituents in the jet J , such that the 1-point correlation function ECF1 is approximately the jet p_T . Likewise, if one takes $\beta^{\text{ECF}} = 2$, the 2-point correlation functions scale as the mass of a particle undergoing a two-body decay in collider coordinates. In this analysis, $\beta^{\text{ECF}} = 1$ is used, and for brevity, β^{ECF} is not explicitly mentioned hereafter.

The ratios of some of these quantities (written in an abbreviated form) are defined as :

$$\begin{aligned} e_2 &= \frac{\text{ECF2}}{(\text{ECF1})^2}, \\ e_3 &= \frac{\text{ECF3}}{(\text{ECF1})^3}. \end{aligned}$$

The observables e_2 and e_3 are measured, and are later referred to as $ECF2^{\text{norm}}$ and $ECF3^{\text{norm}}$. These ratios are then used to generate the variable C_2 [80], and its modified version D_2 [79, 81], which have been shown to be particularly useful in identifying two-body structures within jets [82]. The C_2 and D_2 variables as defined below are measured in this analysis:

$$\begin{aligned} C_2 &= \frac{e_3}{(e_2)^2}, \\ D_2 &= \frac{e_3}{(e_2)^3}. \end{aligned}$$

- Ratios of N -subjettiness [83], τ_{21} and τ_{32} . The N -subjettiness describes to what degree the substructure of a given jet is compatible with being composed of N or fewer subjets.

In order to calculate τ_N , first N subjet axes are defined within the jet by using the exclusive k_t algorithm, where the jet reconstruction continues until a desired number of jets are found. The 0-, 1-,

2-, and 3-subjettiness are defined as:

$$\tau_0(\beta^{\text{NS}}) = \sum_{i \in J} p_{T_i} R^{\beta^{\text{NS}}}, \quad (1\text{a})$$

$$\tau_1(\beta^{\text{NS}}) = \frac{1}{\tau_0(\beta^{\text{NS}})} \sum_{i \in J} p_{T_i} \Delta R_{a_1, i}^{\beta^{\text{NS}}}, \quad (1\text{b})$$

$$\tau_2(\beta^{\text{NS}}) = \frac{1}{\tau_0(\beta^{\text{NS}})} \sum_{i \in J} p_{T_i} \min(\Delta R_{a_1, i}^{\beta^{\text{NS}}}, \Delta R_{a_2, i}^{\beta^{\text{NS}}}), \quad (1\text{c})$$

$$\tau_3(\beta^{\text{NS}}) = \frac{1}{\tau_0(\beta^{\text{NS}})} \sum_{i \in J} p_{T_i} \min(\Delta R_{a_1, i}^{\beta^{\text{NS}}}, \Delta R_{a_2, i}^{\beta^{\text{NS}}} \Delta R_{a_3, i}^{\beta^{\text{NS}}}), \quad (1\text{d})$$

where ΔR is the angular distance between constituent i and the jet axis, a_i , and $\Delta R_{a,n}$ is the angular distance between constituent i and the axis of the n^{th} subjet. The term R in equation 1a is the radius parameter of the jet. The parameter β^{NS} gives a weight to the angular separation of the jet constituents. In the studies presented here, the value of $\beta^{\text{NS}} = 1$ is used. In the above functions, the sum is performed over the constituents i in the jet J , and a normalisation factor τ_0 (Eq. (1a)) is used. The ratios of the N -subjettiness functions, $\tau_{21} = \tau_2/\tau_1$ and $\tau_{32} = \tau_3/\tau_2$ have been shown to be particularly useful in identifying two-body and three-body structures within jets.

Studies presented in Ref. [84] have shown that an alternative axis definition can increase the discrimination power of these variables. The winner-takes-all (WTA) axis uses the direction of the hardest constituent in the subjet obtained from the exclusive k_t algorithm instead of the subjet axis, such that the distance measure $\Delta R_{a_1, i}$ changes in the calculation. In this analysis, the same observables calculated with the WTA axis definition, τ_{21}^{WTA} and τ_{32}^{WTA} , are used.

6 Data-driven background estimation

The largest non- $t\bar{t}$ contributions to the W and top selections come from the W +jets and single-top processes. Additionally non-prompt and mis-reconstructed muons are a separate source of background for the top and W selections. Contributions from other processes were considered and found to be negligible. A data-driven method, following Ref. [85], is used to estimate the contribution from the W +jets process while the single-top process is considered part of the signal.

At the LHC the production rate of W^+ +jets events is larger than that of W^- +jets due to the higher density of u -quarks than d -quarks in the proton. This results in more events with positively charged leptons. Other processes do not contribute significantly to this charge asymmetry. The data are used to derive scale factors that correct the normalisation and flavour fraction given by the MC simulation [86].

Normalisation scale factors are determined by comparing the charge asymmetry in data with the asymmetry estimated by simulation. Contributions to the asymmetry from other processes are estimated by simulation and subtracted. A selection that contains the full top and W selection criteria without any b -tagging requirements is initially used. The total number of W +jets events in data, $N_{W^+} + N_{W^-}$, is given by

$$N_{W^+} + N_{W^-} = \left(\frac{r_{\text{MC}} + 1}{r_{\text{MC}} - 1} \right) (D_+ - D_-)$$

where r_{MC} is the ratio of the number of events with positive muons to the number of events with negative muons obtained from the MC simulation while D_+ and D_- are the number of events with positive and negative muons in data, respectively, after using simulation to subtract the estimated background contribution of all processes other than $W+\text{jets}$. From the above equation the scale factor C_A is extracted which is defined as the ratio of $W+\text{jets}$ events evaluated from data to the number predicted by the simulation

$$C_A = \left(\frac{r_{MC} + 1}{r_{MC} - 1} \right) (D_+ - D_-) \cdot \frac{1}{N_W^{\text{MC}}}$$

where N_W^{MC} is the predicted number of $W+\text{jets}$ events.

Scale factors correcting the relative fractions of W bosons produced in association with jets of different flavour are also estimated using data. The fractions of $W + b\bar{b}$, $W + c\bar{c}$, $W + c$ and $W+\text{light-quark}$ events are initially estimated from simulation in a selection without the b -tagging requirements, which corresponds to the selection mentioned in Table 2 without the ΔR requirement imposed during the top and W selections. A system of three equations is used to fit the fractions estimated from simulation to the selection with full b -tagging requirements:

$$\begin{pmatrix} C_A(N_{bb}^- + N_{cc}^-) & C_A N_c^- & C_A N_{\text{light}}^- \\ f_{bb} + f_{cc} & f_c & f_{\text{light}} \\ C_A(N_{bb}^+ + N_{cc}^+) & C_A N_c^+ & C_A N_{\text{light}}^+ \end{pmatrix} \cdot \begin{pmatrix} K_{bb,cc} \\ K_c \\ K_{\text{light}} \end{pmatrix} = \begin{pmatrix} D_{W^-} \\ 1 \\ D_{W^+} \end{pmatrix}, \quad (2)$$

where f_{bb} , f_{cc} , f_c and f_{light} are flavour factors estimated from simulation while K_{bb} , K_{cc} , K_c and K_{light} are the respective correction factors. The corresponding number of events estimated by simulation with positive (negative) leptons are given by $N_{bb}^{+(-)}$, $N_{cc}^{+(-)}$, $N_c^{+(-)}$ and $N_{\text{light}}^{+(-)}$. The terms D_{W^\pm} are the expected numbers of $W+\text{jets}$ events with positively or negatively charged leptons in the data. An iterative process is used to find the K_{flavour} correction factors which are used to correct the associated f_{flavour} fractions used in the calculation of C_A . The correction factors are determined by inverting Eq. (2) and then the process is repeated with a new C_A calculated using the corrected flavour fractions. This process is repeated 10 times and further iterations produce negligible changes in C_A .

This process is repeated individually for all variables in the top and W selections since, depending on the substructure of the selected large-radius jet, events can fall out of the acceptance for a subset of the variables. The final calculated scale factors are, however, consistent across both selections and all variables. These scale factors are 0.84 ± 0.02 , where the uncertainty is statistical, and the overall contribution to the final selections is shown in Table 3. In order to determine the uncertainty in the shape of the subtracted $W+\text{jets}$ distribution, the contribution from an alternative MC generator (MG5_aMC@NLO+Pythia8 as opposed to default SHERPA) was used. Both MC samples were scaled to the estimated number of events and the envelope of the shape difference was taken as an uncertainty.

There is also a contribution from events where a jet is misreconstructed as a muon or when a non-prompt muon is misidentified as a prompt muon which satisfies the selection criteria. This contribution is estimated using the matrix method, comparing the yields of muons and non-prompt muons that pass a loose selection with the yields of those that pass a tight selection. The efficiency for real muon selection ($\varepsilon_{\text{real}}$) is measured using a tag-and-probe method with muons from $Z \rightarrow \mu\mu$ events. The efficiency for misreconstructed muon selection ($\varepsilon_{\text{fake}}$) is measured in control regions dominated by background from multijet processes, after using simulation to subtract the contribution of other processes. Event weights are computed using the

above efficiencies, which are parameterised in the kinematics of the event. The weight for event i , where the muons satisfy the loose criteria, is given by

$$w_i = \frac{\varepsilon_{\text{fake}}}{\varepsilon_{\text{real}} - \varepsilon_{\text{fake}}} (\varepsilon_{\text{real}} - \delta_i)$$

where δ_i equals unity if the muon in event i satisfies the tight criteria and zero otherwise. The background estimate in a given bin is therefore the total sum of weights in that bin. The estimated contributions to the yield from misreconstructed or non-prompt muons for the top and W selections are shown in Table 3. These corrections have very little effect on the shape of the distributions considered.

| Background | Top selection (Percent contributions) | W selection |
|---------------------------------------|--|---------------|
| $W+\text{jets}$ | 4.0 ± 0.1 | 2.6 ± 0.1 |
| Misreconstructed and non-prompt muons | 6.6 ± 0.1 | 5.5 ± 0.1 |

Table 3: Contributions from background processes which are subtracted in the top and W selections. The uncertainties are statistical only.

7 Systematic uncertainties

7.1 Large-radius jet uncertainties

As jets are built from topological clusters reconstructed in the calorimeter, systematic uncertainties in the jet substructure observables are calculated using a bottom-up approach applied to the clusters forming each jet [18]. The following components of the uncertainty are considered:

- Cluster reconstruction efficiency (CE): Accounts for low energy particles that fail to seed a cluster based on the fraction of inner-detector tracks matched to no clusters in low μ data. The uncertainty is the observed difference between simulation and data. Since the efficiency reaches 100% for cluster energy above 2.5 GeV, no uncertainty is assumed above this value.
- Cluster energy scale variation (CESu/CESd): The cluster energy scale is determined by studying clusters matched to isolated tracks in data events with low pile-up. A fit of the E/p distribution is used to extract an overall energy scale. The uncertainty in the scale is given by taking the difference of the ratio of the scales calculated in data and simulation from unity. Clusters are independently scaled up and down and the resulting variations in observables are added in quadrature.
- Cluster energy smearing (CES): The difference in quadrature of the width of the E/p distribution measured in data and given by simulation is defined as the uncertainty in the energy resolution. The cluster energies are smeared by this value and the effect on the observables is taken as an uncertainty.
- Cluster angular resolution (CAR): The radial distance between clusters and their matched tracks (extrapolated to the corresponding calorimeter layer) is measured in bins of η and as a function of E , to account for the resolution in various regions of the calorimeter. A conservative uncertainty of 5 mrad is used to smear cluster positions.

Uncertainties in the jet p_T and mass are derived by the R_{trk} method [87], comparing the variables calculated using the energy deposited in the calorimeter with those using the momenta of charged-particle tracks. The largest effect on the majority of measured distributions comes from cluster energy smearing for the top and W selections, typically around 8% but can be as high as 16% in some regions. The other cluster uncertainty components contribute between 1% and 6% in the statistically significant part of the distributions for the top and W selections. For the dijet selection, the typical values are between 2% and 4% for all observables, but reach 10% in some bins. The dominant large-radius jet uncertainties for a subset of variables are shown in Figure 1.

In addition to the above uncertainties the sensitivity of the measured distributions to other detector effects was considered. This are summarised as follows:

- Energy scaling correlation scheme: applying the variations to clusters with different kinematics and with different properties, assuming them to be uncorrelated.
- Since the cluster energy calibration is based on pion energy deposition, additional tests are carried out to account for the different energy deposited by non-pion hadrons, such as K_L , and the impact on the distributions under study.
- Cluster merging and splitting: topo-clusters can be split or merged during the clustering procedure and this process can be sensitive to noise fluctuations.

In all cases, very conservative variations were applied in order to ensure that the distributions considered were not sensitive to the above effects. For the majority of the distributions the observed variations due to other detector effects were smaller than the cluster uncertainties. However, it was found that N -subjettiness variables in the dijet selection had shifts of about 50% when some of the cluster merging and splitting variations were applied. Using a different axis definition, rather than the WTA variant, did not sufficiently reduce the sensitivity of the variables to this effect. While these variations were conservative, in order to ensure that no systematic uncertainties are being underestimated the N -subjettiness variables and their ratios were not used in the dijet selection.

7.2 Other sources of uncertainties

Systematic uncertainties are also derived for other reconstructed objects which are considered in the top and the W selections [88]. Uncertainties associated with small-radius jets, b -tagged jets, reconstructed muons and E_T^{miss} are all considered and are found to be subdominant. The theory normalisation uncertainties are also found to be negligible.

Finally, uncertainties in the shape of the subtracted W +jets component are derived by comparing, for each variable, the shapes obtained using the nominal MC sample and an alternative sample, as listed in Table 1. The envelope is taken as an uncertainty in the subtracted shape, and results in uncertainties which are smaller than 1%. The uncertainties due to signal modelling in MC generators are accounted for in unfolding, as described in Section 9.

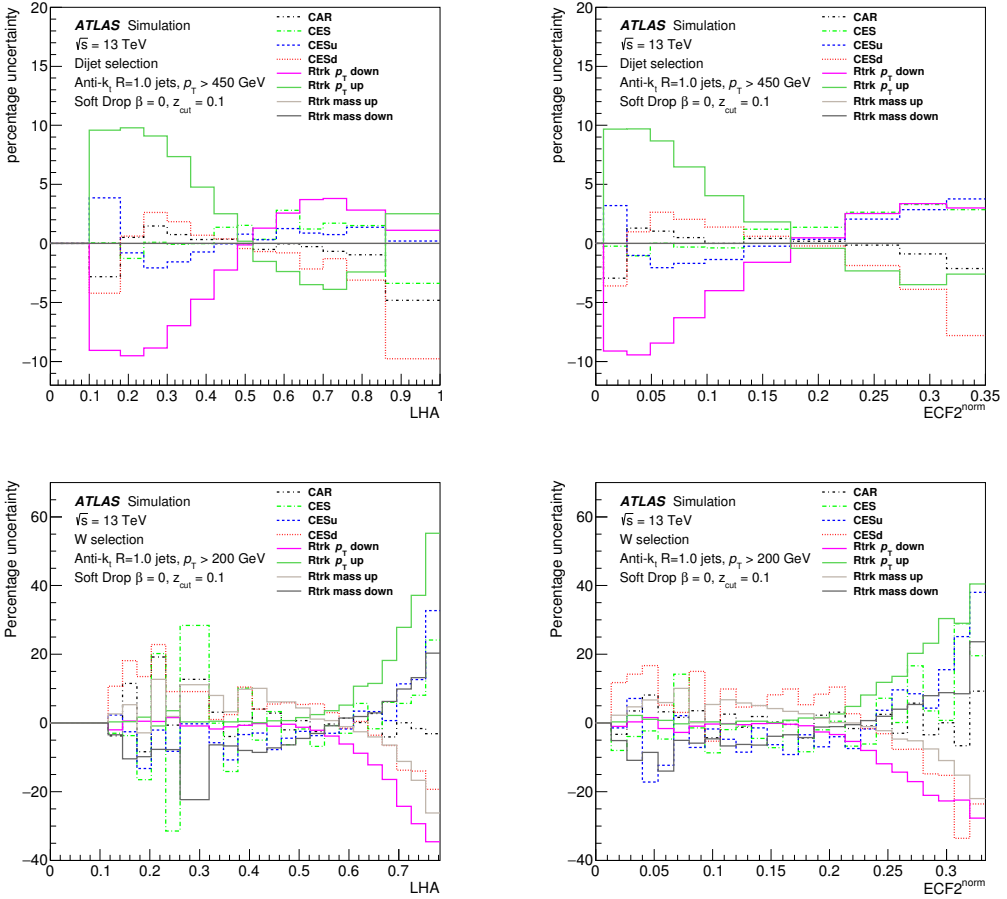


Figure 1: Bin-by-bin systematic uncertainties due to large-radius jet reconstruction uncertainties associated with cluster, Rtrk and jet mass calibrations in the dijet (top) and W (bottom) selections for the soft-drop groomed Les Houches angularity variable (left) and the normalised ECF2 variable (right).

8 Detector-level results

The distributions of the trimmed large-radius jet mass and p_T at detector level are shown in Figure 2 for dijet, top and W selections. The peaks in the distributions due to the top and W masses are clearly visible. In general, good agreement is observed between data and simulation for the distribution of transverse momenta, while a shift is observed for the distributions of mass. This is a known effect [2], due to the lack of in situ calibrations of jet mass, and to jet mass scale uncertainties in the detector-level plots.

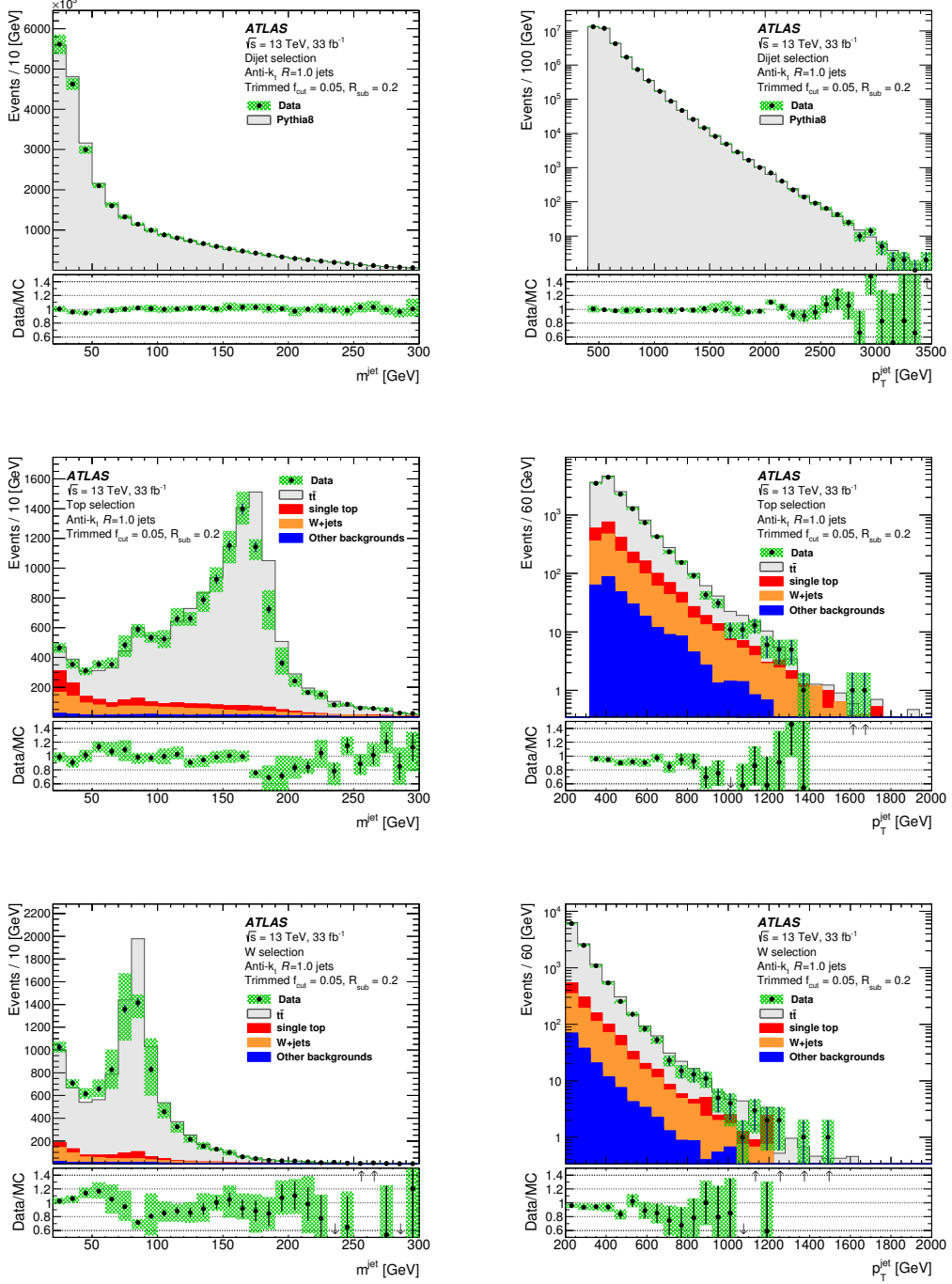


Figure 2: Comparison of detector-level distributions in data and MC simulation for trimmed large-radius jets for dijet (top row), top (middle row), and W (bottom row) selections. For the top and W selections, jet mass requirements have not been applied. The mass is shown in the left column, while the transverse momentum is in the right column. The shaded bands represent the combined statistical and systematic uncertainty. Contributions from dominant backgrounds are shown for the top and W selections, while the smaller contributions from other processes are grouped under other backgrounds.

9 Unfolding

The measured distributions are unfolded to correct for detector effects. The Iterative Bayesian (IB) unfolding method [89] with three iterations (as implemented in RooUnfold [90]) is used to correct detector-level data to particle level, as defined in Section 4. Response matrices (a_{ji}) for each distribution are derived from MC simulation and used in order to estimate the probability for a given event at particle level (T), contributing to bin i , to be reconstructed in a given detector-level (D) bin j , also defined as $P(D_j|T_i)$. Rather than using a simple matrix inversion, IB unfolding uses a probabilistic approach. In order to do this, the unfolding matrix (θ_{ij}) is defined such that the number of events in a particle-level bin, T_i , is given by

$$T_i = \sum_j \theta_{ij} d_j \quad (3)$$

where d_j is the number of data events measured in bin j . Using Bayes' theorem, one can define the unfolding matrix as:

$$\theta_{ij} = P(T_i|D_j) = \frac{P(D_j|T_i) \cdot P(T_i)}{\sum_i P(D_j|T_i) \cdot P(T_i)} = \frac{a_{ji} \cdot P(T_i)}{\sum_i a_{ji} \cdot P(T_i)},$$

where $P(T_i)$ is the input prior. The unfolding matrix can therefore be constructed using the response matrix obtained from simulation. After corrections are applied for detector acceptance and reconstruction efficiency, Eq. (3) can be used to perform the unfolding. To ensure that the final distributions are not biased by the shape predicted by simulation the process is iterated, each subsequent iteration using the previous estimate for the final corrected distribution as $P(T_i)$. The number of iterations is chosen such that differences between multiple subsequent iterations are smaller than data-driven cross-closure uncertainties, described below.

The consistency of the unfolding procedure was tested using several closure and cross-closure tests.

- MC closure: a test where the distributions from the nominal MC generator are unfolded using the nominal method. Uncertainties are found to be negligible.
- Cross-closure: accounts for modelling differences between two different MC generators. The distributions from an alternative generator are unfolded using the nominal method and the differences account for differences in the predicted shape. These result in the largest uncertainties and are typically around 5% in the dijet selection and around 14% in the top and W selections, depending on the observable and the bin.
- Data-driven cross-closure: accounts for the sensitivity of the unfolding method to differences between the shape of the observable seen in data and in simulation. The particle-level substructure distributions are reweighted such that the corresponding detector-level distributions match the data. These reweighted distributions are unfolded using the nominal method and uncertainties are estimated as the differences between the reweighted particle-level and unfolded distributions.

The binning of variables in the dijet selection was chosen to reduce uncertainties from the above effects by increasing the bin purity. For the top and W selections binning was determined based on the statistical uncertainty of the dominant systematic uncertainties.

10 Particle-level results

The results are presented in two sets of distributions: substructure observables in data are compared with MC predictions, and distributions measured in data corresponding to different selections are compared with each other. For the latter, it must be noted that the comparisons are performed in different large-radius jet p_T ranges; however, in each instance the most inclusive selection is used. They are indicative of different substructures of the large-radius jets according to their origin even with somewhat different kinematic ranges. All plots with soft-drop grooming are shown; the trimmed versions have very similar characteristics [91]. The dominant systematic uncertainties in the measurement are the large-radius jet uncertainties resulting from the bottom-up approach using clusters, and modelling uncertainties affecting the unfolding closure and cross-closure.

In Figure 3, the subjet multiplicity inside the large-radius jets from the three different selections is compared with different MC predictions, and the data are compared between the three selections. While for the dijet selection most events have one subjet, for the top selection and W selection the distributions peak at three and two subjets respectively, as expected. In both cases a non-negligible fraction of events have more subjets, indicating the presence of semi-hard gluon radiation. In the W selection, the instances with one subjet are few, while for the top selection, some fraction of events have two subjets, indicating either non-containment of the top quark decay products, or overlapping subjets that get reconstructed as a single subjet. For the dijet selection, PYTHIA8 and SHERPA describe the data the best, while for the top selection and W selection, there is more spread among MC predictions. Predictions from HERWIG7 are very different from data for the dijet selection, a trend which is consistent across all observables. The difference between the different hadronisation models used in SHERPA is negligible. Although these observables depend on hadronisation modelling, it can be inferred that both models can be tuned to give a good description of data.

In Figure 4, the Les Houches angularity (LHA) is compared between large-radius jets for the three selections and with MC model predictions. For the dijet selection, all models except HERWIG7 describe the data, while for the top and W selections, the level of agreement between all models and data is worse, and the peaks of the distributions in the models are shifted relative to those in data. While in the case of the top and W selections the shapes are similar, the distribution for the dijet selection peaks at the lowest value. This indicates that the additional radiation in quark/gluon jets is soft, with little activity away from the large-radius jet axis, while for the large-radius jets from top quarks and W bosons, there are hard emissions separated by appreciable angles.

In Figure 5, a comparison of C_2 among the three different selections with MC is presented, as well as a comparisons of data and MC predictions for each selection. For the dijet selection, all models except HERWIG7 describe the data well, while for the top and W selections, the models predict shapes that differ from data, with Powheg+HERWIG7 performing somewhat worse than the rest. The three distributions have distinct peaks, corresponding to their substructure. The value of C_2 increases as the number of subjets inside the large-radius jets increases.

In Figure 6, comparisons of the data with MC predictions for D_2 reveal some interesting features. For the dijet selection, most of the models describe the data well, and for the top selection the some differences can be seen. For the W selection, all MC predictions have a peak shifted relative to data, suggesting that the models are overestimating gluon radiation. The distributions in data for the three selections are also compared in Figure 6 (bottom right), where peaks at different values are observed.

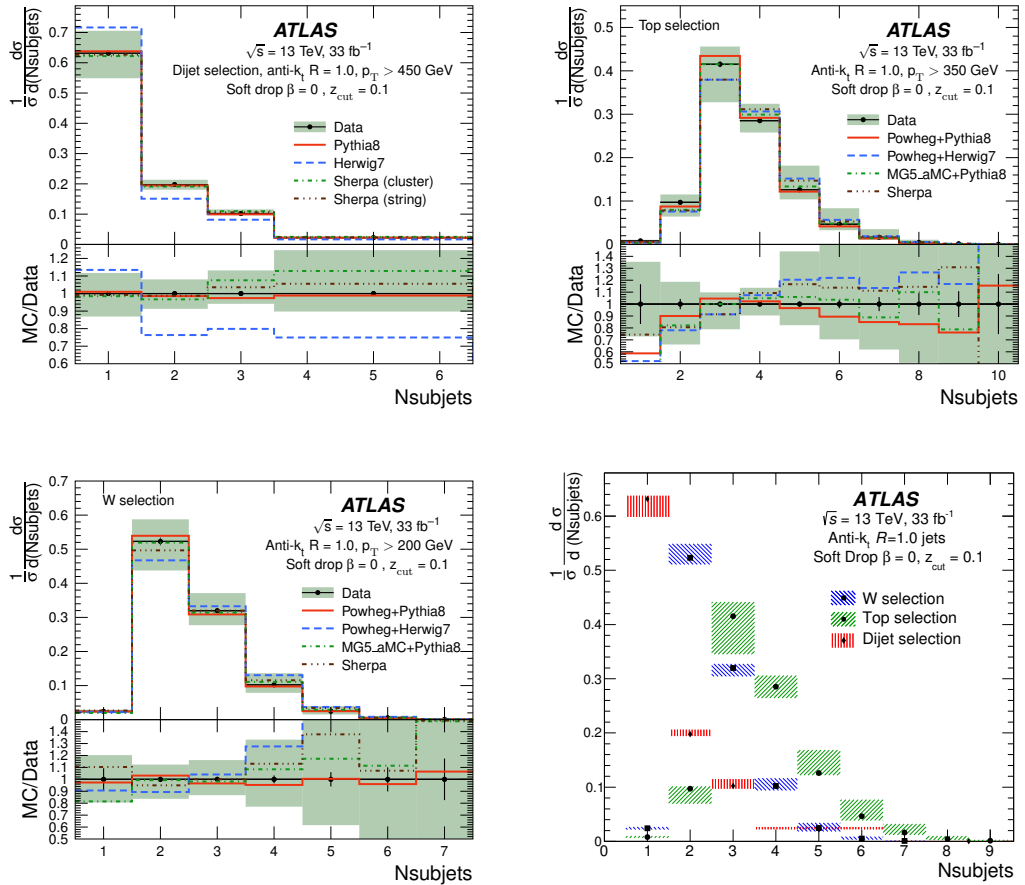


Figure 3: Subjet multiplicity distributions compared with different MC predictions for soft-dropped large-radius jets from dijet (top left), top (top right), and W (bottom left) selections. For the dijet selection, SHERPA is tested with two different hadronisation models. Data are compared between the soft-dropped large-radius jets for the three selections mentioned above (bottom right). The shaded bands represent the total uncertainty, while the error bars show the statistical uncertainty, except in the bottom right plot, where the shaded areas represent the total uncertainty.

The distributions of $ECF2^{\text{norm}}$, as shown in Figure 7 for the different selections, can discriminate between events with two and three prong decays as opposed to one prong decay. Similarly to C_2 , for the dijet selection, all models except HERWIG7 describe the data well, while for the top and W selections, the models predict shapes that differ somewhat from data, with agreement being worse for the W selection case.

The modelling of $ECF3^{\text{norm}}$ in the dijet selection is better for PYTHIA8 than for the other generators, as shown in Figure 8. For the top and W selections, none of the models describe the shape of the data distribution well, with noticeable differences at low values. The three different selections again show distinct shapes.

Finally, in Figure 9, a comparison of τ_{21}^{WTA} and τ_{32}^{WTA} among top quark and W selections is presented. The distribution of τ_{21}^{WTA} peaks at lower values for the W selection than for the top selection, indicating the two-prong decay of the former. In general, τ_{21}^{WTA} distributions are modelled well by the MC models, except POWHEG + HERWIG7. Although most of the models also describe the τ_{32}^{WTA} distributions well, differences can be observed between them, especially in the W selection.

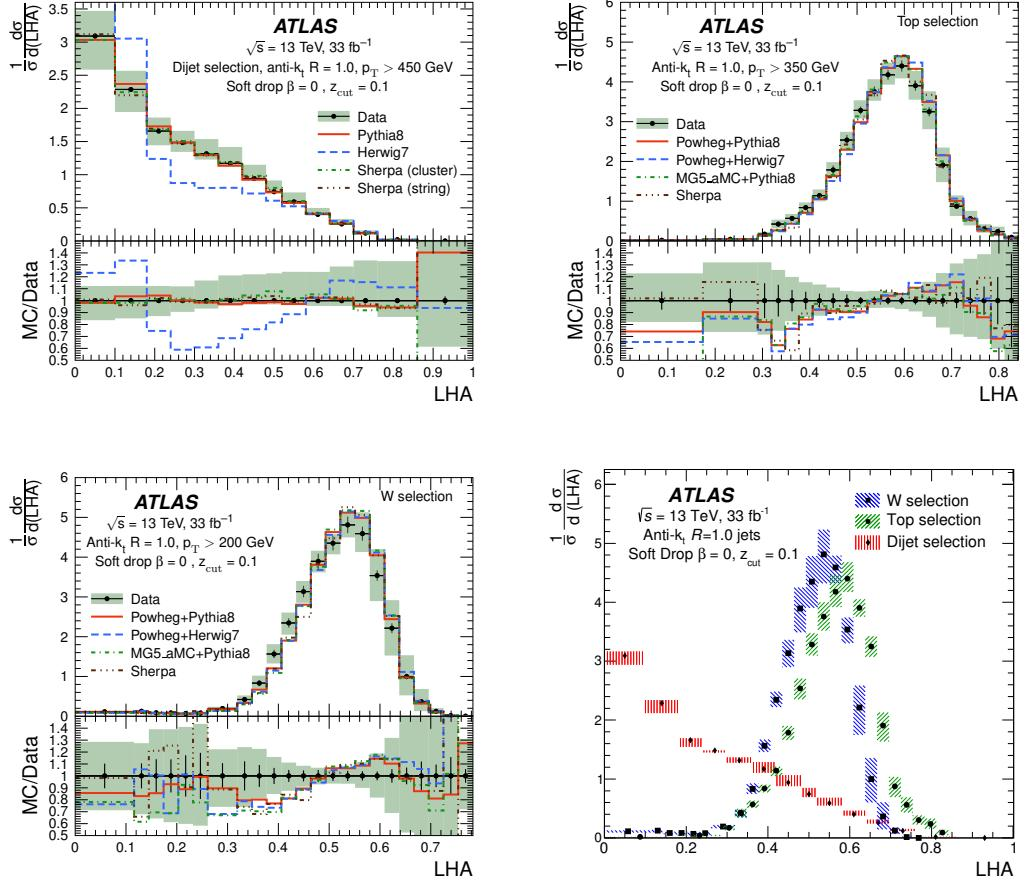


Figure 4: Les Houches angularity is compared with different MC predictions for soft-dropped large-radius jets from dijet (top left), top (top right), and W (bottom left) selections. For the dijet selection, SHERPA is tested with two different hadronisation models. Data are compared between the soft-dropped large-radius jets for the three selections mentioned above (bottom right). The shaded bands represent the total uncertainty, while the error bars show the statistical uncertainty, except in the bottom right plot, where the shaded areas represent the total uncertainty.

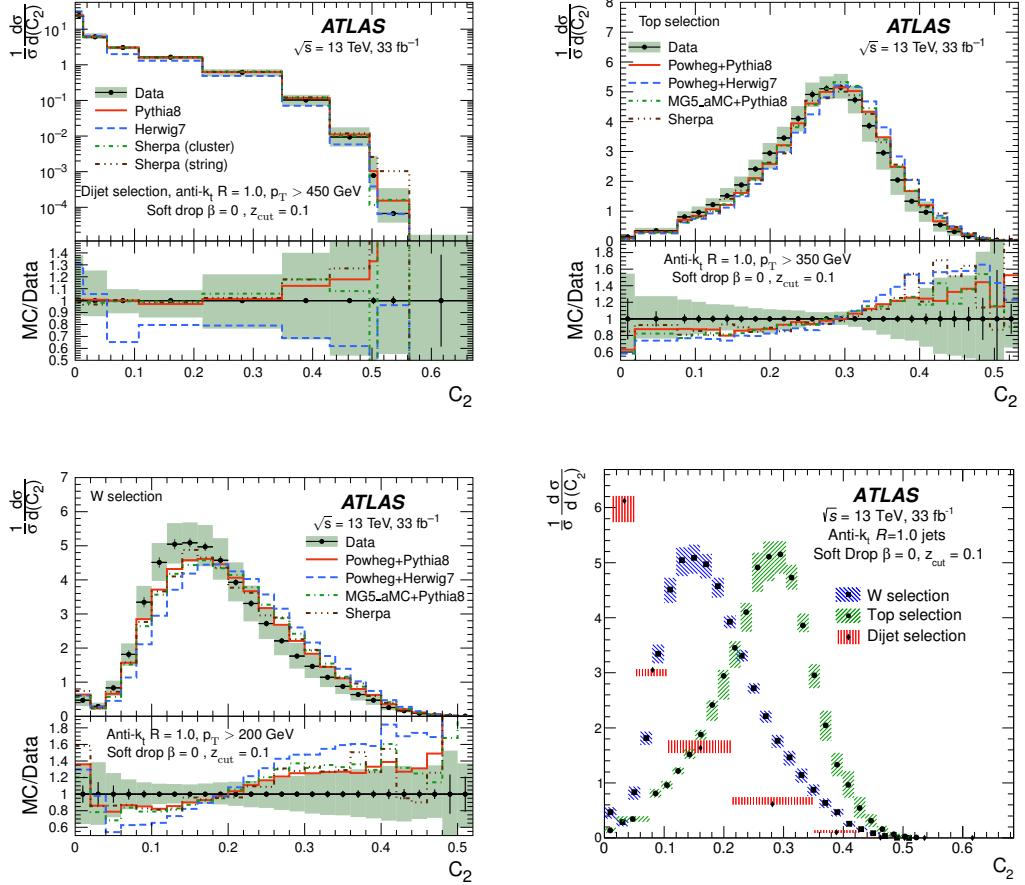


Figure 5: The distributions of C_2 compared with different MC predictions for soft-dropped large-radius jets from dijet (top left), top (top right), and W (bottom left) selections. For the dijet selection, SHERPA is tested with two different hadronisation models. Data are compared between the soft-dropped large-radius jets for the three selections mentioned above (bottom right). The shaded bands represent the total uncertainty, while the error bars show the statistical uncertainty, except in the bottom right plot, where the shaded areas represent the total uncertainty.

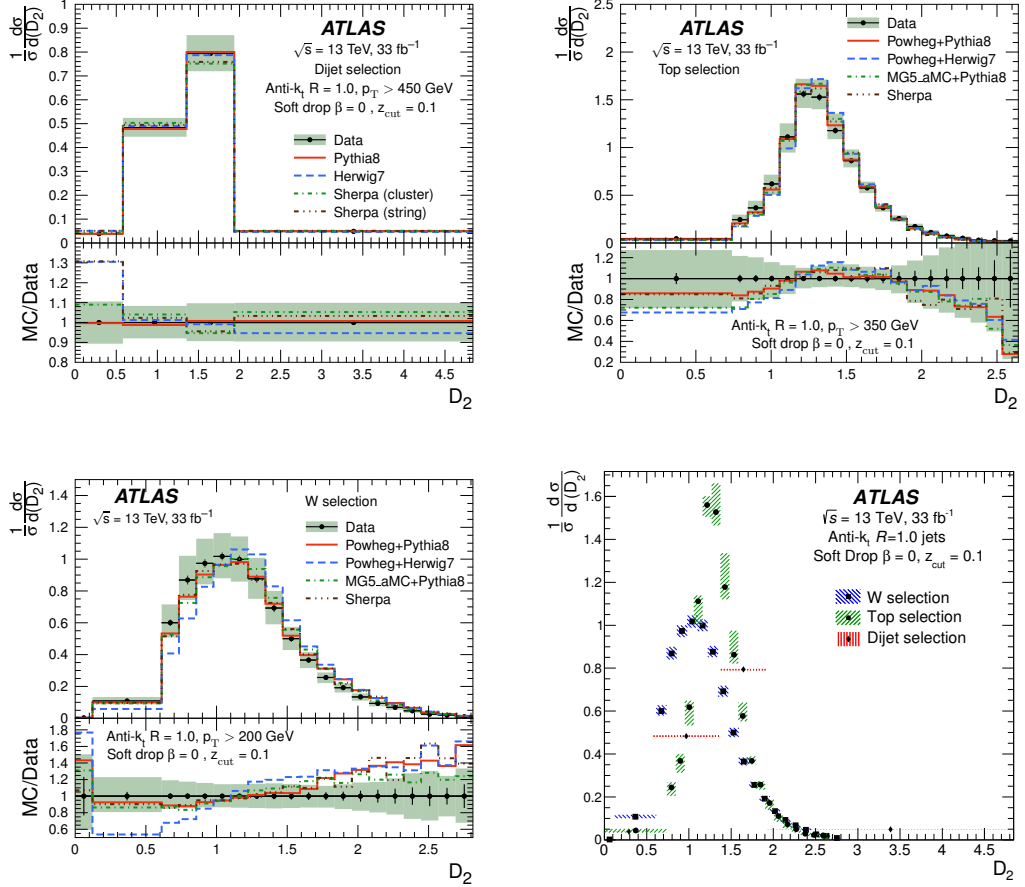


Figure 6: The distributions of D_2 compared with different MC predictions for soft-dropped large-radius jets from dijet (top left), top (top right), and W (bottom left) selections. For the dijet selection, SHERPA is tested with two different hadronisation models. Data are compared between the soft-dropped large-radius jets for the three selections mentioned above (bottom right). The shaded bands represent the total uncertainty, while the error bars show the statistical uncertainty, except in the bottom right plot, where the shaded areas represent the total uncertainty.

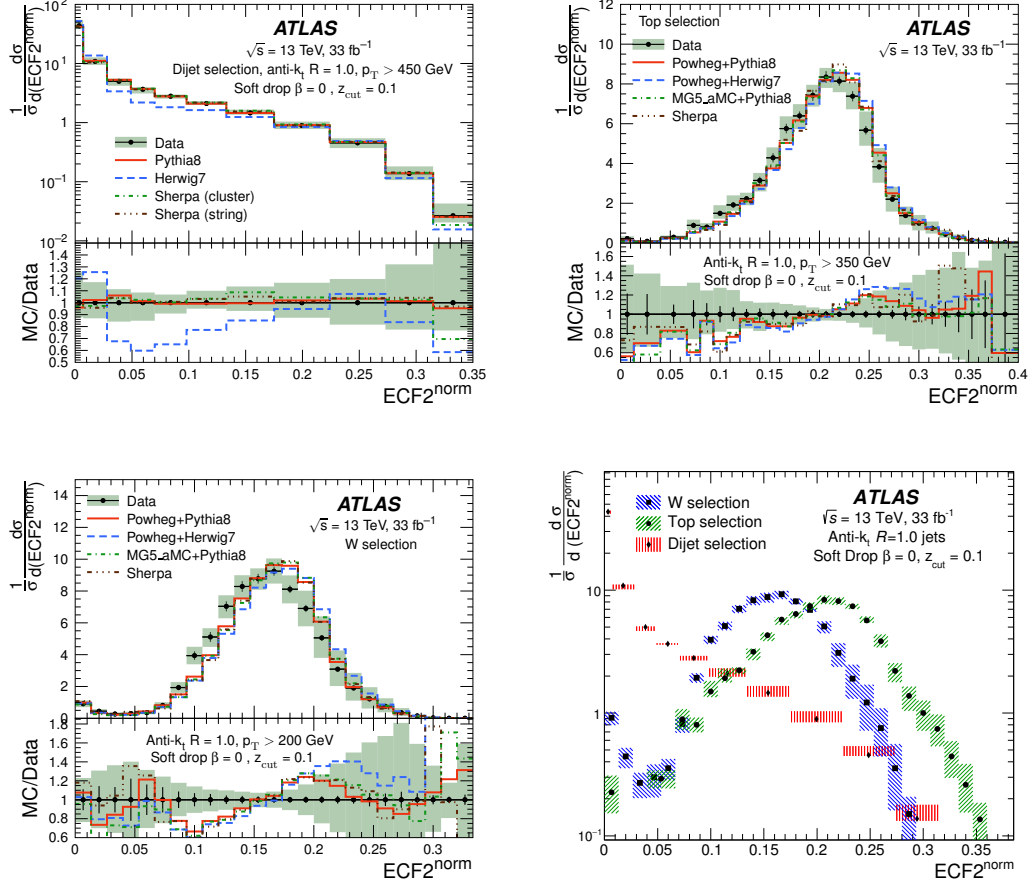


Figure 7: The distributions of $ECF2^{\text{norm}}$ compared with different MC predictions for soft-dropped large-radius jets from dijet (top left), top (top right), and W (bottom left) selections. For the dijet selection, SHERPA is tested with two different hadronisation models. Data are compared between the soft-dropped large-radius jets for the three selections mentioned above (bottom right). The subscript norm indicates that normalised versions of $ECF2^{\text{norm}}$ are used. The shaded bands represent the total uncertainty, while the error bars show the statistical uncertainty, except in the bottom right plot, where the shaded areas represent the total uncertainty.

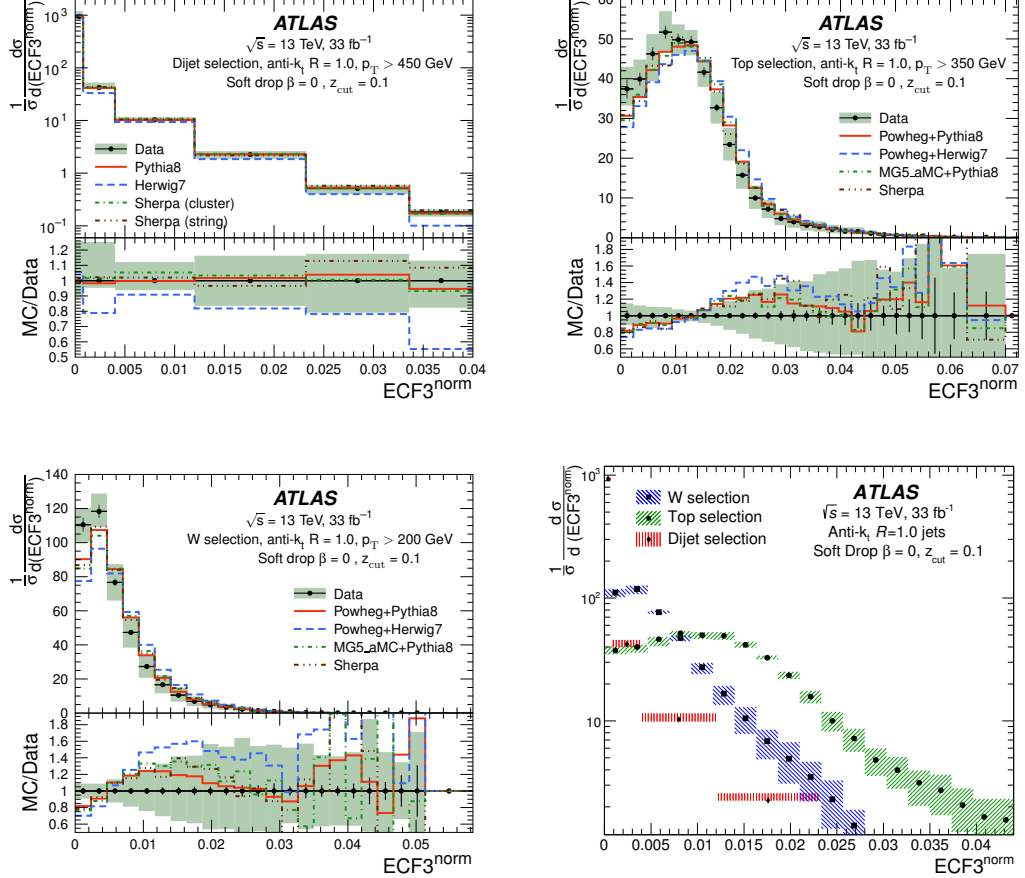


Figure 8: The distributions of $ECF3^{\text{Norm}}$ are compared with different MC predictions for soft-dropped large-radius jets from dijet (top left), top (top right), and W (bottom left) selections. For the dijet selection, SHERPA is tested with two different hadronisation models. Data are compared between the soft-dropped large-radius jets for the three selections mentioned above (bottom right). The superscript “norm” indicates that normalised versions of $ECF3^{\text{Norm}}$ are used. The shaded bands represent the total uncertainty, while the error bars show the statistical uncertainty, except in the bottom right plot, where the shaded areas represent the total uncertainty.

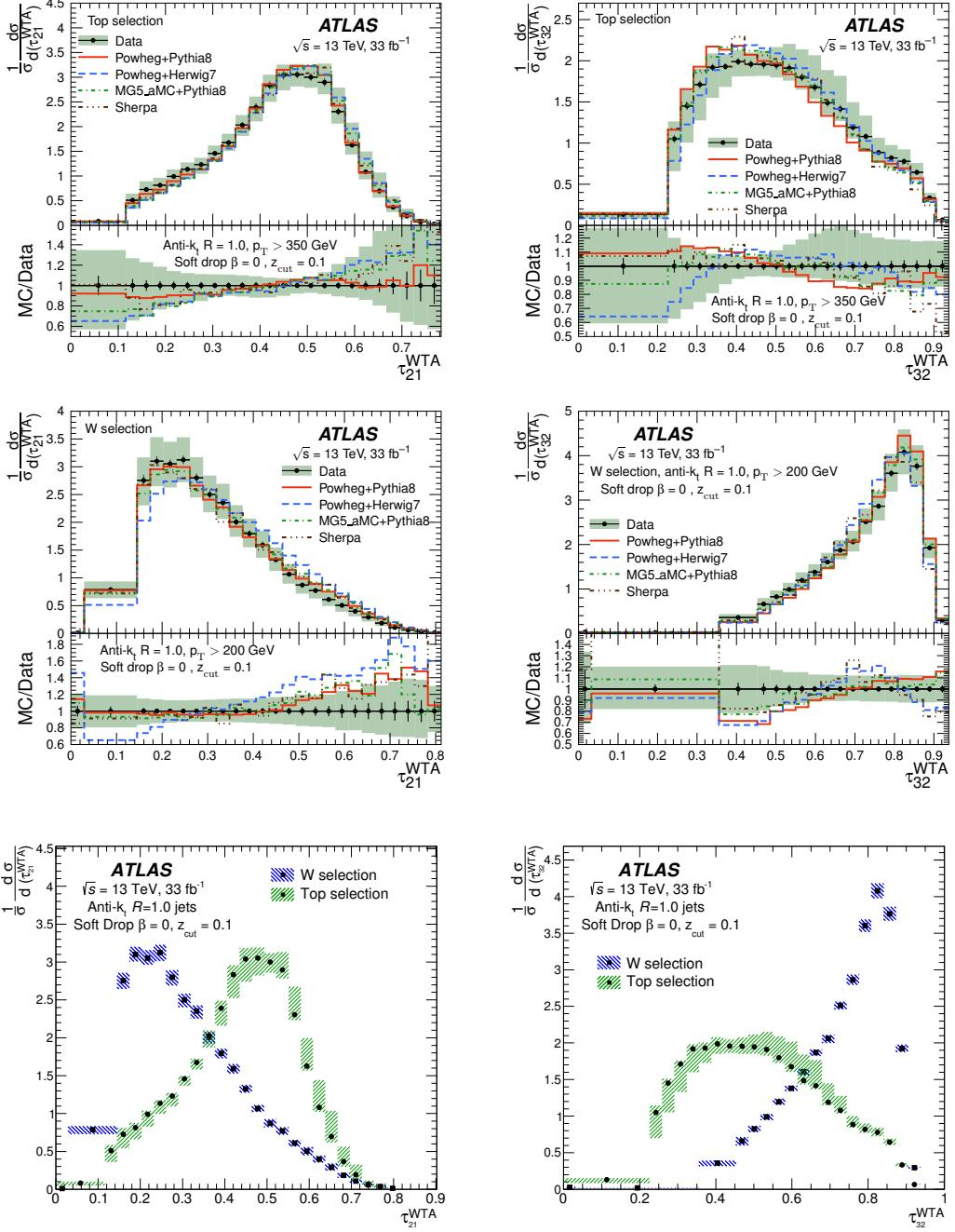


Figure 9: The distributions of τ_{21}^{WTA} (left) and τ_{32}^{WTA} (right) are compared with different MC predictions for large-radius jets from top (top row) and W (bottom row) selections. The distributions of τ_{21}^{WTA} (bottom left) and τ_{32}^{WTA} (bottom right) in data are compared between the soft-dropped large-radius jets for the two selections mentioned above. The subscript WTA indicates that WTA axis was used in calculating these observables. The shaded bands represent the total uncertainty, while the error bars show the statistical uncertainty, except in the bottom plots, where the shaded areas represent the total uncertainty.

11 Conclusions

A measurement of jet substructure observables using groomed large-radius jets from light quarks or gluons, hadronically decaying top quarks and W bosons is presented using 33 fb^{-1} of $\sqrt{s} = 13\text{ TeV}$ proton–proton collision data taken with the ATLAS detector at the LHC. The data discriminate between the various MC models probed. In general, PYTHIA8 for light-quark/gluon large-radius jet observables, and POWHEG+PYTHIA8, SHERPA as well as MG5_aMC@NLO+PYTHIA8 for top quark and W boson large-radius jet observables, describe the data better than other models. The different hadronisation models in SHERPA in the dijet selection result in similar predictions. For most observables, HERWIG7 in the dijet selection, and POWHEG+HERWIG7 in the top and W selections do not describe the data well. These measurements will be useful in improving the modelling of these substructure variables in MC generators. Since searches that utilise boosted topologies use these observables, or combinations of them, in tagging large-radius jets, a better modelling of them will help to increase the sensitivity of such searches.

Acknowledgements

We thank CERN for the very successful operation of the LHC, as well as the support staff from our institutions without whom ATLAS could not be operated efficiently.

We acknowledge the support of ANPCyT, Argentina; YerPhI, Armenia; ARC, Australia; BMWFW and FWF, Austria; ANAS, Azerbaijan; SSTC, Belarus; CNPq and FAPESP, Brazil; NSERC, NRC and CFI, Canada; CERN; CONICYT, Chile; CAS, MOST and NSFC, China; COLCIENCIAS, Colombia; MSMT CR, MPO CR and VSC CR, Czech Republic; DNRF and DNSRC, Denmark; IN2P3-CNRS, CEA-DRF/IRFU, France; SRNSFG, Georgia; BMBF, HGF, and MPG, Germany; GSRT, Greece; RGC, Hong Kong SAR, China; ISF and Benoziyo Center, Israel; INFN, Italy; MEXT and JSPS, Japan; CNRST, Morocco; NWO, Netherlands; RCN, Norway; MNiSW and NCN, Poland; FCT, Portugal; MNE/IFA, Romania; MES of Russia and NRC KI, Russian Federation; JINR; MESTD, Serbia; MSSR, Slovakia; ARRS and MIZŠ, Slovenia; DST/NRF, South Africa; MINECO, Spain; SRC and Wallenberg Foundation, Sweden; SERI, SNSF and Cantons of Bern and Geneva, Switzerland; MOST, Taiwan; TAEK, Turkey; STFC, United Kingdom; DOE and NSF, United States of America. In addition, individual groups and members have received support from BCKDF, CANARIE, CRC and Compute Canada, Canada; COST, ERC, ERDF, Horizon 2020, and Marie Skłodowska-Curie Actions, European Union; Investissements d’Avenir Labex and Idex, ANR, France; DFG and AvH Foundation, Germany; Herakleitos, Thales and Aristeia programmes co-financed by EU-ESF and the Greek NSRF, Greece; BSF-NSF and GIF, Israel; CERCA Programme Generalitat de Catalunya, Spain; The Royal Society and Leverhulme Trust, United Kingdom.

The crucial computing support from all WLCG partners is acknowledged gratefully, in particular from CERN, the ATLAS Tier-1 facilities at TRIUMF (Canada), NDGF (Denmark, Norway, Sweden), CC-IN2P3 (France), KIT/GridKA (Germany), INFN-CNAF (Italy), NL-T1 (Netherlands), PIC (Spain), ASGC (Taiwan), RAL (UK) and BNL (USA), the Tier-2 facilities worldwide and large non-WLCG resource providers. Major contributors of computing resources are listed in Ref. [92].

References

- [1] A. Abdesselam et al. ‘Boosted objects: a probe of beyond the standard model physics’. In: *Eur. Phys. J. C* 71 (2011), p. 1661. doi: [10.1140/epjc/s10052-011-1661-y](https://doi.org/10.1140/epjc/s10052-011-1661-y). arXiv: [1012.5412 \[hep-ph\]](https://arxiv.org/abs/1012.5412).
- [2] ATLAS Collaboration. ‘Performance of top-quark and W -boson tagging with ATLAS in Run 2 of the LHC’. In: (2018). arXiv: [1808.07858 \[hep-ex\]](https://arxiv.org/abs/1808.07858).
- [3] ATLAS Collaboration. ‘Measurements of top-quark pair differential cross-sections in the lepton+jets channel in pp collisions at $\sqrt{s} = 13$ TeV using the ATLAS detector’. In: *JHEP* 11 (2017), p. 191. doi: [10.1007/JHEP11\(2017\)191](https://doi.org/10.1007/JHEP11(2017)191). arXiv: [1708.00727 \[hep-ex\]](https://arxiv.org/abs/1708.00727).
- [4] ATLAS Collaboration. ‘Measurements of $t\bar{t}$ differential cross-sections of highly boosted top quarks decaying to all-hadronic final states in pp collisions at $\sqrt{s} = 13$ TeV using the ATLAS detector’. In: *Phys. Rev. D* 98.1 (2018), p. 012003. doi: [10.1103/PhysRevD.98.012003](https://doi.org/10.1103/PhysRevD.98.012003). arXiv: [1801.02052 \[hep-ex\]](https://arxiv.org/abs/1801.02052).
- [5] ATLAS Collaboration. ‘Top-quark mass measurement in the all-hadronic $t\bar{t}$ decay channel at $\sqrt{s} = 8$ TeV with the ATLAS detector’. In: *JHEP* 09 (2017), p. 118. doi: [10.1007/JHEP09\(2017\)118](https://doi.org/10.1007/JHEP09(2017)118). arXiv: [1702.07546 \[hep-ex\]](https://arxiv.org/abs/1702.07546).
- [6] ATLAS Collaboration. ‘Search for heavy particles decaying into a top-quark pair in the fully hadronic final state in pp collisions at $\sqrt{s} = 13$ TeV with the ATLAS detector’. In: *Phys. Rev. D* 99.9 (2019), p. 092004. doi: [10.1103/PhysRevD.99.092004](https://doi.org/10.1103/PhysRevD.99.092004). arXiv: [1902.10077 \[hep-ex\]](https://arxiv.org/abs/1902.10077).
- [7] ATLAS Collaboration. ‘Search for $W' \rightarrow tb$ decays in the hadronic final state using pp collisions at $\sqrt{s} = 13$ TeV with the ATLAS detector’. In: *Phys. Lett. V* 781 (2018), pp. 327–348. doi: [10.1016/j.physletb.2018.03.036](https://doi.org/10.1016/j.physletb.2018.03.036). arXiv: [1801.07893 \[hep-ex\]](https://arxiv.org/abs/1801.07893).
- [8] ATLAS Collaboration. ‘Search for the standard model Higgs boson produced in association with top quarks and decaying into a $b\bar{b}$ pair in pp collisions at $\sqrt{s} = 13$ TeV with the ATLAS detector’. In: *Phys. Rev. D* 97.7 (2018), p. 072016. doi: [10.1103/PhysRevD.97.072016](https://doi.org/10.1103/PhysRevD.97.072016). arXiv: [1712.08895 \[hep-ex\]](https://arxiv.org/abs/1712.08895).
- [9] ATLAS Collaboration. ‘Observation of $H \rightarrow b\bar{b}$ decays and VH production with the ATLAS detector’. In: *Phys. Lett. B* 786 (2018), pp. 59–86. doi: [10.1016/j.physletb.2018.09.013](https://doi.org/10.1016/j.physletb.2018.09.013). arXiv: [1808.08238 \[hep-ex\]](https://arxiv.org/abs/1808.08238).
- [10] ATLAS Collaboration. ‘Search for pair production of Higgs bosons in the $b\bar{b}b\bar{b}$ final state using proton-proton collisions at $\sqrt{s} = 13$ TeV with the ATLAS detector’. In: *JHEP* 01 (2019), p. 030. doi: [10.1007/JHEP01\(2019\)030](https://doi.org/10.1007/JHEP01(2019)030). arXiv: [1804.06174 \[hep-ex\]](https://arxiv.org/abs/1804.06174).
- [11] ATLAS Collaboration. ‘Search for Higgs boson pair production in the $b\bar{b}WW^*$ decay mode at $\sqrt{s} = 13$ TeV with the ATLAS detector’. In: *JHEP* 04 (2019), p. 092. doi: [10.1007/JHEP04\(2019\)092](https://doi.org/10.1007/JHEP04(2019)092). arXiv: [1811.04671 \[hep-ex\]](https://arxiv.org/abs/1811.04671).
- [12] P. Gras et al. ‘Systematics of quark/gluon tagging’. In: *JHEP* 07 (2017), p. 091. doi: [10.1007/JHEP07\(2017\)091](https://doi.org/10.1007/JHEP07(2017)091). arXiv: [1704.03878 \[hep-ph\]](https://arxiv.org/abs/1704.03878).
- [13] ATLAS Collaboration. ‘Jet mass and substructure of inclusive jets in $\sqrt{s} = 7$ TeV pp collisions with the ATLAS experiment’. In: *JHEP* 05 (2012), p. 128. doi: [10.1007/JHEP05\(2012\)128](https://doi.org/10.1007/JHEP05(2012)128). arXiv: [1203.4606 \[hep-ex\]](https://arxiv.org/abs/1203.4606).

- [14] ATLAS Collaboration. ‘ATLAS measurements of the properties of jets for boosted particle searches’. In: *Phys. Rev. D* 86 (2012), p. 072006. doi: [10.1103/PhysRevD.86.072006](https://doi.org/10.1103/PhysRevD.86.072006). arXiv: [1206.5369 \[hep-ex\]](https://arxiv.org/abs/1206.5369).
- [15] ATLAS Collaboration. ‘Measurement of colour flow with the jet pull angle in $t\bar{t}$ events using the ATLAS detector at $\sqrt{s} = 8$ TeV’. In: *Phys. Lett. B* 750 (2015), p. 475. doi: [10.1016/j.physletb.2015.09.051](https://doi.org/10.1016/j.physletb.2015.09.051). arXiv: [1506.05629 \[hep-ex\]](https://arxiv.org/abs/1506.05629).
- [16] ATLAS Collaboration. ‘Measurement of jet charge in dijet events from $\sqrt{s} = 8$ TeV pp collisions with the ATLAS detector’. In: *Phys. Rev. D* 93 (2016), p. 052003. doi: [10.1103/PhysRevD.93.052003](https://doi.org/10.1103/PhysRevD.93.052003). arXiv: [1509.05190 \[hep-ex\]](https://arxiv.org/abs/1509.05190).
- [17] ATLAS Collaboration. ‘Measurement of the charged-particle multiplicity inside jets from $\sqrt{s} = 8$ TeV pp collisions with the ATLAS detector’. In: *Eur. Phys. J. C* 76.6 (2016), p. 322. doi: [10.1140/epjc/s10052-016-4126-5](https://doi.org/10.1140/epjc/s10052-016-4126-5). arXiv: [1602.00988 \[hep-ex\]](https://arxiv.org/abs/1602.00988).
- [18] ATLAS Collaboration. ‘Measurement of the Soft-Drop Jet Mass in pp Collisions at $\sqrt{s} = 13$ TeV with the ATLAS detector’. In: *Phys. Rev. Lett.* 121.9 (2018), p. 092001. doi: [10.1103/PhysRevLett.121.092001](https://doi.org/10.1103/PhysRevLett.121.092001). arXiv: [1711.08341 \[hep-ex\]](https://arxiv.org/abs/1711.08341).
- [19] ATLAS Collaboration. ‘Measurement of colour flow using jet-pull observables in $t\bar{t}$ events with the ATLAS experiment at $\sqrt{s} = 13$ TeV’. In: *Eur. Phys. J. C* 78.10 (2018), p. 847. doi: [10.1140/epjc/s10052-018-6290-2](https://doi.org/10.1140/epjc/s10052-018-6290-2). arXiv: [1805.02935 \[hep-ex\]](https://arxiv.org/abs/1805.02935).
- [20] CMS Collaboration. ‘Shape, Transverse Size, and Charged Hadron Multiplicity of Jets in pp Collisions at 7 TeV’. In: *JHEP* 06 (2012), p. 160. doi: [10.1007/JHEP06\(2012\)160](https://doi.org/10.1007/JHEP06(2012)160). arXiv: [1204.3170 \[hep-ex\]](https://arxiv.org/abs/1204.3170).
- [21] CMS Collaboration. ‘Studies of jet mass in dijet and W/Z + jet events’. In: *JHEP* 05 (2013), p. 090. doi: [10.1007/JHEP05\(2013\)090](https://doi.org/10.1007/JHEP05(2013)090). arXiv: [1303.4811 \[hep-ex\]](https://arxiv.org/abs/1303.4811).
- [22] CMS Collaboration. ‘Measurements of jet charge with dijet events in pp collisions at $\sqrt{s} = 8$ TeV’. In: *JHEP* 10 (2017), p. 131. doi: [10.1007/JHEP10\(2017\)131](https://doi.org/10.1007/JHEP10(2017)131). arXiv: [1706.05868 \[hep-ex\]](https://arxiv.org/abs/1706.05868).
- [23] CMS Collaboration. ‘Measurements of the differential jet cross section as a function of the jet mass in dijet events from proton-proton collisions at $\sqrt{s} = 13$ TeV’. In: *JHEP* 11 (2018), p. 113. doi: [10.1007/JHEP11\(2018\)113](https://doi.org/10.1007/JHEP11(2018)113). arXiv: [1807.05974 \[hep-ex\]](https://arxiv.org/abs/1807.05974).
- [24] CMS Collaboration. ‘Measurement of jet substructure observables in $t\bar{t}$ events from proton-proton collisions at $\sqrt{s} = 13$ TeV’. In: *Phys. Rev. D* 98.9 (2018), p. 092014. doi: [10.1103/PhysRevD.98.092014](https://doi.org/10.1103/PhysRevD.98.092014). arXiv: [1808.07340 \[hep-ex\]](https://arxiv.org/abs/1808.07340).
- [25] ATLAS Collaboration. ‘The ATLAS Experiment at the CERN Large Hadron Collider’. In: *JINST* 3 (2008), S08003. doi: [10.1088/1748-0221/3/08/S08003](https://doi.org/10.1088/1748-0221/3/08/S08003).
- [26] M. Capeans et al. *ATLAS Insertable B-Layer Technical Design Report*. Tech. rep. CERN-LHCC-2010-013. ATLAS-TDR-19. Sept. 2010. URL: <https://cds.cern.ch/record/1291633>.
- [27] ATLAS Collaboration. ‘Performance of the ATLAS trigger system in 2015’. In: *Eur. Phys. J. C* 77.5 (2017), p. 317. doi: [10.1140/epjc/s10052-017-4852-3](https://doi.org/10.1140/epjc/s10052-017-4852-3). arXiv: [1611.09661 \[hep-ex\]](https://arxiv.org/abs/1611.09661).
- [28] M. Czakon and A. Mitov. ‘Top++: A program for the calculation of the top-pair cross-section at hadron colliders’. In: *Comput. Phys. Commun.* 185 (2014), p. 2930. doi: [10.1016/j.cpc.2014.06.021](https://doi.org/10.1016/j.cpc.2014.06.021). arXiv: [1112.5675 \[hep-ph\]](https://arxiv.org/abs/1112.5675).
- [29] S. Frixione, P. Nason and G. Ridolfi. ‘A Positive-weight next-to-leading-order Monte Carlo for heavy flavour hadroproduction’. In: *JHEP* 09 (2007), p. 126. doi: [10.1088/1126-6708/2007/09/126](https://doi.org/10.1088/1126-6708/2007/09/126). arXiv: [0707.3088 \[hep-ph\]](https://arxiv.org/abs/0707.3088).

- [30] ATLAS Collaboration. *Studies on top-quark Monte Carlo modelling for Top2016*. ATL-PHYS-PUB-2016-020. 2016. URL: <https://cds.cern.ch/record/2216168>.
- [31] E. Re. ‘Single-top Wt-channel production matched with parton showers using the POWHEG method’. In: *Eur. Phys. J. C* 71 (2011), p. 1547. doi: [10.1140/epjc/s10052-011-1547-z](https://doi.org/10.1140/epjc/s10052-011-1547-z). arXiv: [1009.2450 \[hep-ph\]](https://arxiv.org/abs/1009.2450).
- [32] S. Alioli et al. ‘NLO single-top production matched with shower in POWHEG: s- and t-channel contributions’. In: *JHEP* 09 (2009). [Erratum: *JHEP* 02 (2010)] 011, p. 111. doi: [10.1007/JHEP02\(2010\)011](https://doi.org/10.1007/JHEP02(2010)011). arXiv: [0907.4076 \[hep-ph\]](https://arxiv.org/abs/0907.4076).
- [33] R. Frederix, E. Re and P. Torrielli. ‘Single-top t-channel hadroproduction in the four-flavour scheme with POWHEG and aMC@NLO’. In: *JHEP* 09 (2012), p. 130. doi: [10.1007/JHEP09\(2012\)130](https://doi.org/10.1007/JHEP09(2012)130). arXiv: [1207.5391 \[hep-ph\]](https://arxiv.org/abs/1207.5391).
- [34] N. Kidonakis. ‘Next-to-next-to-leading-order collinear and soft gluon corrections for t-channel single top quark production’. In: *Phys. Rev. D* 83 (2011), p. 091503. doi: [10.1103/PhysRevD.83.091503](https://doi.org/10.1103/PhysRevD.83.091503). arXiv: [1103.2792 \[hep-ph\]](https://arxiv.org/abs/1103.2792).
- [35] N. Kidonakis. ‘Two-loop soft anomalous dimensions for single top quark associated production with a W- or H-’. In: *Phys. Rev. D* 82 (2010), p. 054018. doi: [10.1103/PhysRevD.82.054018](https://doi.org/10.1103/PhysRevD.82.054018). arXiv: [1005.4451 \[hep-ph\]](https://arxiv.org/abs/1005.4451).
- [36] N. Kidonakis. ‘NNLL resummation for s-channel single top quark production’. In: *Phys. Rev. D* 81 (2010), p. 054028. doi: [10.1103/PhysRevD.81.054028](https://doi.org/10.1103/PhysRevD.81.054028). arXiv: [1001.5034 \[hep-ph\]](https://arxiv.org/abs/1001.5034).
- [37] C. Anastasiou et al. ‘High precision QCD at hadron colliders: Electroweak gauge boson rapidity distributions at NNLO’. In: *Phys. Rev. D* 69 (2004), p. 094008. doi: [10.1103/PhysRevD.69.094008](https://doi.org/10.1103/PhysRevD.69.094008). arXiv: [hep-ph/0312266 \[hep-ph\]](https://arxiv.org/abs/hep-ph/0312266).
- [38] B. Andersson et al. ‘Parton Fragmentation and String Dynamics’. In: *Phys. Rept.* 97 (1983), pp. 31–145. doi: [10.1016/0370-1573\(83\)90080-7](https://doi.org/10.1016/0370-1573(83)90080-7).
- [39] G. Marchesini et al. ‘HERWIG: A Monte Carlo event generator for simulating hadron emission reactions with interfering gluons. Version 5.1 - April 1991’. In: *Comput. Phys. Commun.* 67 (1992), pp. 465–508. doi: [10.1016/0010-4655\(92\)90055-4](https://doi.org/10.1016/0010-4655(92)90055-4).
- [40] T. Sjöstrand, S. Mrenna and P. Skands. ‘A brief introduction to PYTHIA 8.1’. In: *Comput. Phys. Commun.* 178 (2008), pp. 852–867. doi: [10.1016/j.cpc.2008.01.036](https://doi.org/10.1016/j.cpc.2008.01.036). arXiv: [0710.3820 \[hep-ph\]](https://arxiv.org/abs/0710.3820).
- [41] T. Sjöstrand et al. ‘An introduction to PYTHIA 8.2’. In: *Comput. Phys. Commun.* 191 (2015), pp. 159–177. doi: [10.1016/j.cpc.2015.01.024](https://doi.org/10.1016/j.cpc.2015.01.024). arXiv: [1410.3012 \[hep-ph\]](https://arxiv.org/abs/1410.3012).
- [42] R. D. Ball et al. ‘Parton distributions with LHC data’. In: *Nucl. Phys. B* 867 (2013), pp. 244–289. doi: [10.1016/j.nuclphysb.2012.10.003](https://doi.org/10.1016/j.nuclphysb.2012.10.003). arXiv: [1207.1303 \[hep-ph\]](https://arxiv.org/abs/1207.1303).
- [43] ATLAS Collaboration. *ATLAS Pythia 8 tunes to 7 TeV data*. ATL-PHYS-PUB-2014-021. 2014. URL: <https://cds.cern.ch/record/1966419>.
- [44] T. Gleisberg et al. ‘Event generation with SHERPA 1.1’. In: *JHEP* 02 (2009), p. 007. doi: [10.1088/1126-6708/2009/02/007](https://doi.org/10.1088/1126-6708/2009/02/007). arXiv: [0811.4622 \[hep-ph\]](https://arxiv.org/abs/0811.4622).
- [45] J. Pumplin et al. ‘New Generation of Parton Distributions with Uncertainties from Global QCD Analysis’. In: *JHEP* 07 (2002), p. 012. doi: [10.1088/1126-6708/2002/07/012](https://doi.org/10.1088/1126-6708/2002/07/012). arXiv: [hep-ph/0201195 \[hep-ph\]](https://arxiv.org/abs/hep-ph/0201195).

- [46] J. Bellm et al. ‘Herwig 7.0/Herwig++ 3.0 release note’. In: *Eur. Phys. J. C* 76.4 (2016), p. 196. doi: [10.1140/epjc/s10052-016-4018-8](https://doi.org/10.1140/epjc/s10052-016-4018-8). arXiv: [1512.01178 \[hep-ph\]](https://arxiv.org/abs/1512.01178).
- [47] S. Alioli et al. ‘A general framework for implementing NLO calculations in shower Monte Carlo programs: the POWHEG BOX’. In: *JHEP* 06 (2010), p. 043. doi: [10.1007/JHEP06\(2010\)043](https://doi.org/10.1007/JHEP06(2010)043). arXiv: [1002.2581 \[hep-ph\]](https://arxiv.org/abs/1002.2581).
- [48] M. Bahr et al. ‘Herwig++ physics and manual’. In: *Eur. Phys. J. C* 58 (2008), pp. 639–707. doi: [10.1140/epjc/s10052-008-0798-9](https://doi.org/10.1140/epjc/s10052-008-0798-9). arXiv: [0803.0883 \[hep-ph\]](https://arxiv.org/abs/0803.0883).
- [49] M. H. Seymour and A. Siodmok. ‘Constraining MPI models using σ_{eff} and recent Tevatron and LHC Underlying Event data’. In: *JHEP* 10 (2013), p. 113. doi: [10.1007/JHEP10\(2013\)113](https://doi.org/10.1007/JHEP10(2013)113). arXiv: [1307.5015 \[hep-ph\]](https://arxiv.org/abs/1307.5015).
- [50] J. Alwall et al. ‘The automated computation of tree-level and next-to-leading order differential cross sections, and their matching to parton shower simulations’. In: *JHEP* 07 (2014), p. 079. doi: [10.1007/JHEP07\(2014\)079](https://doi.org/10.1007/JHEP07(2014)079). arXiv: [1405.0301 \[hep-ph\]](https://arxiv.org/abs/1405.0301).
- [51] T. Sjöstrand et al. ‘High-energy physics event generation with PYTHIA 6.1’. In: *Comput. Phys. Commun.* 135 (2001), pp. 238–259. doi: [10.1016/S0010-4655\(00\)00236-8](https://doi.org/10.1016/S0010-4655(00)00236-8). arXiv: [hep-ph/0010017 \[hep-ph\]](https://arxiv.org/abs/hep-ph/0010017).
- [52] T. Sjöstrand, S. Mrenna and P. Z. Skands. ‘PYTHIA 6.4 Physics and Manual’. In: *JHEP* 05 (2006), p. 026. doi: [10.1088/1126-6708/2006/05/026](https://doi.org/10.1088/1126-6708/2006/05/026). arXiv: [hep-ph/0603175 \[hep-ph\]](https://arxiv.org/abs/hep-ph/0603175).
- [53] P. Z. Skands. ‘Tuning Monte Carlo generators: The Perugia tunes’. In: *Phys. Rev. D* 82 (2010), p. 074018. doi: [10.1103/PhysRevD.82.074018](https://doi.org/10.1103/PhysRevD.82.074018). arXiv: [1005.3457 \[hep-ph\]](https://arxiv.org/abs/1005.3457).
- [54] ATLAS Collaboration. ‘The ATLAS Simulation Infrastructure’. In: *Eur. Phys. J. C* 70 (2010), pp. 823–874. doi: [10.1140/epjc/s10052-010-1429-9](https://doi.org/10.1140/epjc/s10052-010-1429-9). arXiv: [1005.4568 \[physics.ins-det\]](https://arxiv.org/abs/1005.4568).
- [55] S. Agostinelli et al. ‘Geant4—a simulation toolkit’. In: *Nucl. Instrum. Meth. A* 506 (2003), pp. 250–303. doi: [10.1016/S0168-9002\(03\)01368-8](https://doi.org/10.1016/S0168-9002(03)01368-8).
- [56] ATLAS Collaboration. *Further ATLAS tunes of Pythia 6 and Pythia 8*. ATL-PHYS-PUB-2011-014. 2011. URL: <https://cds.cern.ch/record/1400677>.
- [57] A. D. Martin et al. ‘Parton distributions for the LHC’. In: *Eur. Phys. J. C* 63 (2009), pp. 189–285. doi: [10.1140/epjc/s10052-009-1072-5](https://doi.org/10.1140/epjc/s10052-009-1072-5). arXiv: [0901.0002 \[hep-ph\]](https://arxiv.org/abs/0901.0002).
- [58] ATLAS Collaboration. *Monte Carlo Calibration and Combination of In-situ Measurements of Jet Energy Scale, Jet Energy Resolution and Jet Mass in ATLAS*. ATLAS-CONF-2015-037. 2015. URL: <https://cds.cern.ch/record/2044941>.
- [59] M. Cacciari, G. P. Salam and G. Soyez. ‘The anti- k_t jet clustering algorithm’. In: *JHEP* 04 (2008), p. 063. doi: [10.1088/1126-6708/2008/04/063](https://doi.org/10.1088/1126-6708/2008/04/063). arXiv: [0802.1189 \[hep-ph\]](https://arxiv.org/abs/0802.1189).
- [60] D. Krohn, J. Thaler and L.-T. Wang. ‘Jet trimming’. In: *JHEP* 02 (2010), p. 084. doi: [10.1007/JHEP02\(2010\)084](https://doi.org/10.1007/JHEP02(2010)084). arXiv: [0912.1342 \[hep-ph\]](https://arxiv.org/abs/0912.1342).
- [61] ATLAS Collaboration. ‘Jet energy scale measurements and their systematic uncertainties in proton-proton collisions at $\sqrt{s} = 13$ TeV with the ATLAS detector’. In: *Phys. Rev. D* 96.7 (2017), p. 072002. doi: [10.1103/PhysRevD.96.072002](https://doi.org/10.1103/PhysRevD.96.072002). arXiv: [1703.09665 \[hep-ex\]](https://arxiv.org/abs/1703.09665).
- [62] ATLAS Collaboration. ‘Performance of pile-up mitigation techniques for jets in pp collisions at $\sqrt{s} = 8$ TeV using the ATLAS detector’. In: *Eur. Phys. J. C* 76.11 (2016), p. 581. doi: [10.1140/epjc/s10052-016-4395-z](https://doi.org/10.1140/epjc/s10052-016-4395-z). arXiv: [1510.03823 \[hep-ex\]](https://arxiv.org/abs/1510.03823).

- [63] ATLAS Collaboration. ‘Performance of b-jet identification in the ATLAS experiment’. In: *JINST* 11.04 (2016), P04008. doi: [10.1088/1748-0221/11/04/P04008](https://doi.org/10.1088/1748-0221/11/04/P04008). arXiv: [1512.01094](https://arxiv.org/abs/1512.01094) [hep-ex].
- [64] ATLAS Collaboration. *Optimisation of the ATLAS b-tagging performance for the 2016 LHC Run*. ATL-PHYS-PUB-2016-012. 2016. URL: <https://cds.cern.ch/record/2160731>.
- [65] ATLAS Collaboration. ‘Measurements of b-jet tagging efficiency with the ATLAS detector using $t\bar{t}$ events at $\sqrt{s} = 13$ TeV’. In: *JHEP* 08 (2018), p. 089. doi: [10.1007/JHEP08\(2018\)089](https://doi.org/10.1007/JHEP08(2018)089). arXiv: [1805.01845](https://arxiv.org/abs/1805.01845) [hep-ex].
- [66] ATLAS Collaboration. ‘Muon reconstruction performance of the ATLAS detector in proton–proton collision data at $\sqrt{s} = 13$ TeV’. In: *Eur. Phys. J. C* 76.5 (2016), p. 292. doi: [10.1140/epjc/s10052-016-4120-y](https://doi.org/10.1140/epjc/s10052-016-4120-y). arXiv: [1603.05598](https://arxiv.org/abs/1603.05598) [hep-ex].
- [67] ATLAS Collaboration. ‘Electron reconstruction and identification in the ATLAS experiment using the 2015 and 2016 LHC proton-proton collision data at $\sqrt{s} = 13$ TeV’. In: *Submitted to: Eur. Phys. J. C* (2019). arXiv: [1902.04655](https://arxiv.org/abs/1902.04655) [physics.ins-det].
- [68] ATLAS Collaboration. ‘Measurement of the photon identification efficiencies with the ATLAS detector using LHC Run 2 data collected in 2015 and 2016’. In: *Submitted to: Eur. Phys. J. C* (2018). arXiv: [1810.05087](https://arxiv.org/abs/1810.05087) [hep-ex].
- [69] ATLAS Collaboration. ‘Performance of missing transverse momentum reconstruction with the ATLAS detector using proton-proton collisions at $\sqrt{s} = 13$ TeV’. In: *Eur. Phys. J. C* 78.11 (2018), p. 903. doi: [10.1140/epjc/s10052-018-6288-9](https://doi.org/10.1140/epjc/s10052-018-6288-9). arXiv: [1802.08168](https://arxiv.org/abs/1802.08168) [hep-ex].
- [70] M. Cacciari, G. P. Salam and G. Soyez. ‘The catchment area of jets’. In: *JHEP* 04 (2008), p. 005. doi: [10.1088/1126-6708/2008/04/005](https://doi.org/10.1088/1126-6708/2008/04/005). arXiv: [0802.1188](https://arxiv.org/abs/0802.1188) [hep-ph].
- [71] A. J. Larkoski et al. ‘Soft drop’. In: *JHEP* 05 (2014), p. 146. doi: [10.1007/JHEP05\(2014\)146](https://doi.org/10.1007/JHEP05(2014)146). arXiv: [1402.2657](https://arxiv.org/abs/1402.2657) [hep-ph].
- [72] S. Marzani, L. Schunk and G. Soyez. ‘The jet mass distribution after Soft Drop’. In: *Eur. Phys. J. C* 78.2 (2018), p. 96. doi: [10.1140/epjc/s10052-018-5579-5](https://doi.org/10.1140/epjc/s10052-018-5579-5). arXiv: [1712.05105](https://arxiv.org/abs/1712.05105) [hep-ph].
- [73] J. M. Butterworth et al. ‘Jet Substructure as a New Higgs-Search Channel at the Large Hadron Collider’. In: *Phys. Rev. Lett.* 100 (2008), p. 242001. doi: [10.1103/PhysRevLett.100.242001](https://doi.org/10.1103/PhysRevLett.100.242001). arXiv: [0802.2470](https://arxiv.org/abs/0802.2470) [hep-ph].
- [74] M. Dasgupta et al. ‘Towards an understanding of jet substructure’. In: *JHEP* 09 (2013), p. 029. doi: [10.1007/JHEP09\(2013\)029](https://doi.org/10.1007/JHEP09(2013)029). arXiv: [1307.0007](https://arxiv.org/abs/1307.0007) [hep-ph].
- [75] C. Frye et al. ‘Factorization for groomed jet substructure beyond the next-to-leading logarithm’. In: *JHEP* 07 (2016), p. 064. doi: [10.1007/JHEP07\(2016\)064](https://doi.org/10.1007/JHEP07(2016)064). arXiv: [1603.09338](https://arxiv.org/abs/1603.09338) [hep-ph].
- [76] S. Marzani, L. Schunk and G. Soyez. ‘A study of jet mass distributions with grooming’. In: *JHEP* 07 (2017), p. 132. doi: [10.1007/JHEP07\(2017\)132](https://doi.org/10.1007/JHEP07(2017)132). arXiv: [1704.02210](https://arxiv.org/abs/1704.02210) [hep-ph].
- [77] Z.-B. Kang et al. ‘Soft drop groomed jet angularities at the LHC’. In: (2018). arXiv: [1811.06983](https://arxiv.org/abs/1811.06983) [hep-ph].
- [78] M. Cacciari and G. P. Salam. ‘Dispelling the N^3 myth for the k_t jet-finder’. In: *Phys. Lett. B* 641 (2006), pp. 57–61. doi: [10.1016/j.physletb.2006.08.037](https://doi.org/10.1016/j.physletb.2006.08.037). arXiv: [hep-ph/0512210](https://arxiv.org/abs/hep-ph/0512210) [hep-ph].

- [79] A. J. Larkoski, J. Thaler and W. J. Waalewijn. ‘Gaining (mutual) information about quark/gluon discrimination’. In: *JHEP* 11 (2014), p. 129. doi: [10.1007/JHEP11\(2014\)129](https://doi.org/10.1007/JHEP11(2014)129). arXiv: [1408.3122 \[hep-ph\]](https://arxiv.org/abs/1408.3122).
- [80] A. J. Larkoski, G. P. Salam and J. Thaler. ‘Energy correlation functions for jet substructure’. In: *JHEP* 06 (2013), p. 108. doi: [10.1007/JHEP06\(2013\)108](https://doi.org/10.1007/JHEP06(2013)108). arXiv: [1305.0007 \[hep-ph\]](https://arxiv.org/abs/1305.0007).
- [81] A. J. Larkoski, I. Moult and D. Neill. ‘Analytic boosted boson discrimination’. In: *JHEP* 05 (2016), p. 117. doi: [10.1007/JHEP05\(2016\)117](https://doi.org/10.1007/JHEP05(2016)117). arXiv: [1507.03018 \[hep-ph\]](https://arxiv.org/abs/1507.03018).
- [82] A. J. Larkoski, I. Moult and D. Neill. ‘Power counting to better jet observables’. In: *JHEP* 12 (2014), p. 009. doi: [10.1007/JHEP12\(2014\)009](https://doi.org/10.1007/JHEP12(2014)009). arXiv: [1409.6298 \[hep-ph\]](https://arxiv.org/abs/1409.6298).
- [83] J. Thaler and K. Van Tilburg. ‘Identifying boosted objects with N-subjettiness’. In: *JHEP* 03 (2011), p. 015. doi: [10.1007/JHEP03\(2011\)015](https://doi.org/10.1007/JHEP03(2011)015). arXiv: [1011.2268 \[hep-ph\]](https://arxiv.org/abs/1011.2268).
- [84] A. J. Larkoski, D. Neill and J. Thaler. ‘Jet shapes with the broadening axis’. In: *JHEP* 04 (2014), p. 017. doi: [10.1007/JHEP04\(2014\)017](https://doi.org/10.1007/JHEP04(2014)017). arXiv: [1401.2158 \[hep-ph\]](https://arxiv.org/abs/1401.2158).
- [85] ATLAS Collaboration. ‘A search for $t\bar{t}$ resonances using lepton-plus-jets events in proton-proton collisions at $\sqrt{s} = 8$ TeV with the ATLAS detector’. In: *JHEP* 08 (2015), p. 148. doi: [10.1007/JHEP08\(2015\)148](https://doi.org/10.1007/JHEP08(2015)148). arXiv: [1505.07018 \[hep-ex\]](https://arxiv.org/abs/1505.07018).
- [86] ATLAS Collaboration. ‘Measurements of normalized differential cross sections for $t\bar{t}$ production in pp collisions at $\sqrt{s} = 7$ TeV using the ATLAS detector’. In: *Phys. Rev. D* 90.7 (2014), p. 072004. doi: [10.1103/PhysRevD.90.072004](https://doi.org/10.1103/PhysRevD.90.072004). arXiv: [1407.0371 \[hep-ex\]](https://arxiv.org/abs/1407.0371).
- [87] ATLAS Collaboration. ‘In situ calibration of large- R jet energy and mass in 13 TeV proton-proton collisions with the ATLAS detector’. In: *Eur. Phys. J. C* 79.2 (2019), p. 135. doi: [10.1140/epjc/s10052-019-6632-8](https://doi.org/10.1140/epjc/s10052-019-6632-8). arXiv: [1807.09477 \[hep-ex\]](https://arxiv.org/abs/1807.09477).
- [88] ATLAS Collaboration. ‘Search for heavy particles decaying into top-quark pairs using lepton-plus-jets events in proton–proton collisions at $\sqrt{s} = 13$ TeV with the ATLAS detector’. In: *Eur. Phys. J. C* 78.7 (2018), p. 565. doi: [10.1140/epjc/s10052-018-5995-6](https://doi.org/10.1140/epjc/s10052-018-5995-6). arXiv: [1804.10823 \[hep-ex\]](https://arxiv.org/abs/1804.10823).
- [89] G. D’Agostini. ‘A multidimensional unfolding method based on Bayes’ theorem’. In: *Nucl. Instrum. Meth. A* 362 (1995), pp. 487–498. doi: [10.1016/0168-9002\(95\)00274-X](https://doi.org/10.1016/0168-9002(95)00274-X).
- [90] T. Adye. ‘Unfolding algorithms and tests using RooUnfold’. In: *Proceedings, PHYSTAT 2011 Workshop on Statistical Issues Related to Discovery Claims in Search Experiments and Unfolding, CERN, Geneva, Switzerland 17-20 January 2011*. CERN, Geneva: CERN, 2011, pp. 313–318. doi: [10.5170/CERN-2011-006.313](https://doi.org/10.5170/CERN-2011-006.313). arXiv: [1105.1160 \[physics.data-an\]](https://arxiv.org/abs/1105.1160).
- [91] <https://doi.org/10.17182/hepdata.89324>.
- [92] ATLAS Collaboration. *ATLAS Computing Acknowledgements 2016–2017*. ATL-GEN-PUB-2016-002. URL: <https://cds.cern.ch/record/2202407>.

The ATLAS Collaboration

M. Aaboud^{35d}, G. Aad¹⁰¹, B. Abbott¹²⁸, D.C. Abbott¹⁰², O. Abdinov^{13,*}, A. Abed Abud^{70a,70b}, D.K. Abhayasinghe⁹³, S.H. Abidi¹⁶⁷, O.S. AbouZeid⁴⁰, N.L. Abraham¹⁵⁶, H. Abramowicz¹⁶¹, H. Abreu¹⁶⁰, Y. Abulaiti⁶, B.S. Acharya^{66a,66b,o}, S. Adachi¹⁶³, L. Adam⁹⁹, C. Adam Bourdarios¹³², L. Adamczyk^{83a}, L. Adamek¹⁶⁷, J. Adelman¹²¹, M. Adersberger¹¹⁴, A. Adiguzel^{12c,ai}, S. Adorni⁵⁴, T. Adye¹⁴⁴, A.A. Affolder¹⁴⁶, Y. Afik¹⁶⁰, C. Agapopoulou¹³², M.N. Agaras³⁸, A. Aggarwal¹¹⁹, C. Agheorghiesei^{27c}, J.A. Aguilar-Saavedra^{140f,140a,ah}, F. Ahmadov⁷⁹, X. Ai^{15a}, G. Aielli^{73a,73b}, S. Akatsuka⁸⁵, T.P.A. Åkesson⁹⁶, E. Akilli⁵⁴, A.V. Akimov¹¹⁰, K. Al Khoury¹³², G.L. Alberghi^{23b,23a}, J. Albert¹⁷⁶, M.J. Alconada Verzini¹⁶¹, S. Alderweireldt¹¹⁹, M. Aleksa³⁶, I.N. Aleksandrov⁷⁹, C. Alexa^{27b}, D. Alexandre¹⁹, T. Alexopoulos¹⁰, A. Alfonsi¹²⁰, M. Alhroob¹²⁸, B. Ali¹⁴², G. Alimonti^{68a}, J. Alison³⁷, S.P. Alkire¹⁴⁸, C. Allaire¹³², B.M.M. Allbrooke¹⁵⁶, B.W. Allen¹³¹, P.P. Allport²¹, A. Aloisio^{69a,69b}, A. Alonso⁴⁰, F. Alonso⁸⁸, C. Alpigiani¹⁴⁸, A.A. Alshehri⁵⁷, M.I. Alstaty¹⁰¹, M. Alvarez Estevez⁹⁸, B. Alvarez Gonzalez³⁶, D. Álvarez Piqueras¹⁷⁴, M.G. Alvaggi^{69a,69b}, Y. Amaral Coutinho^{80b}, A. Ambler¹⁰³, L. Ambroz¹³⁵, C. Amelung²⁶, D. Amidei¹⁰⁵, S.P. Amor Dos Santos^{140a,140c}, S. Amoroso⁴⁶, C.S. Amrouche⁵⁴, F. An⁷⁸, C. Anastopoulos¹⁴⁹, N. Andari¹⁴⁵, T. Andeen¹¹, C.F. Anders^{61b}, J.K. Anders²⁰, A. Andreazza^{68a,68b}, V. Andrei^{61a}, C.R. Anelli¹⁷⁶, S. Angelidakis³⁸, I. Angelozzi¹²⁰, A. Angerami³⁹, A.V. Anisenkov^{122b,122a}, A. Annovi^{71a}, C. Antel^{61a}, M.T. Anthony¹⁴⁹, M. Antonelli⁵¹, D.J.A. Antrim¹⁷¹, F. Anulli^{72a}, M. Aoki⁸¹, J.A. Aparisi Pozo¹⁷⁴, L. Aperio Bella³⁶, G. Arabidze¹⁰⁶, J.P. Araque^{140a}, V. Araujo Ferraz^{80b}, R. Araujo Pereira^{80b}, A.T.H. Arce⁴⁹, F.A. Arduh⁸⁸, J-F. Arguin¹⁰⁹, S. Argyropoulos⁷⁷, J.-H. Arling⁴⁶, A.J. Armbruster³⁶, L.J. Armitage⁹², A. Armstrong¹⁷¹, O. Arnaez¹⁶⁷, H. Arnold¹²⁰, A. Artamonov^{111,*}, G. Artoni¹³⁵, S. Artz⁹⁹, S. Asai¹⁶³, N. Asbah⁵⁹, E.M. Asimakopoulou¹⁷², L. Asquith¹⁵⁶, K. Assamagan²⁹, R. Astalos^{28a}, R.J. Atkin^{33a}, M. Atkinson¹⁷³, N.B. Atlay¹⁵¹, H. Atmani¹³², K. Augsten¹⁴², G. Avolio³⁶, R. Avramidou^{60a}, M.K. Ayoub^{15a}, A.M. Azoulay^{168b}, G. Azuelos^{109,aw}, A.E. Baas^{61a}, M.J. Baca²¹, H. Bachacou¹⁴⁵, K. Bachas^{67a,67b}, M. Backes¹³⁵, F. Backman^{45a,45b}, P. Bagnaia^{72a,72b}, M. Bahmani⁸⁴, H. Bahrasemani¹⁵², A.J. Bailey¹⁷⁴, V.R. Bailey¹⁷³, J.T. Baines¹⁴⁴, M. Bajic⁴⁰, C. Bakalis¹⁰, O.K. Baker¹⁸³, P.J. Bakker¹²⁰, D. Bakshi Gupta⁸, S. Balaji¹⁵⁷, E.M. Baldin^{122b,122a}, P. Balek¹⁸⁰, F. Balli¹⁴⁵, W.K. Balunas¹³⁵, J. Balz⁹⁹, E. Banas⁸⁴, A. Bandyopadhyay²⁴, Sw. Banerjee^{181,j}, A.A.E. Bannoura¹⁸², L. Barak¹⁶¹, W.M. Barbe³⁸, E.L. Barberio¹⁰⁴, D. Barberis^{55b,55a}, M. Barbero¹⁰¹, T. Barillari¹¹⁵, M-S. Barisits³⁶, J. Barkeloo¹³¹, T. Barklow¹⁵³, R. Barnea¹⁶⁰, S.L. Barnes^{60c}, B.M. Barnett¹⁴⁴, R.M. Barnett¹⁸, Z. Barnovska-Blenessy^{60a}, A. Baroncelli^{60a}, G. Barone²⁹, A.J. Barr¹³⁵, L. Barranco Navarro¹⁷⁴, F. Barreiro⁹⁸, J. Barreiro Guimarães da Costa^{15a}, R. Bartoldus¹⁵³, G. Bartolini¹⁰¹, A.E. Barton⁸⁹, P. Bartos^{28a}, A. Basalaev⁴⁶, A. Bassalat^{132,qa}, R.L. Bates⁵⁷, S.J. Batista¹⁶⁷, S. Batlamous^{35e}, J.R. Batley³², B. Batool¹⁵¹, M. Battaglia¹⁴⁶, M. Bauce^{72a,72b}, F. Bauer¹⁴⁵, K.T. Bauer¹⁷¹, H.S. Bawa^{31,m}, J.B. Beacham⁴⁹, T. Beau¹³⁶, P.H. Beauchemin¹⁷⁰, P. Bechtle²⁴, H.C. Beck⁵³, H.P. Beck^{20,r}, K. Becker⁵², M. Becker⁹⁹, C. Becot⁴⁶, A. Beddall^{12d}, A.J. Beddall^{12a}, V.A. Bednyakov⁷⁹, M. Bedognetti¹²⁰, C.P. Bee¹⁵⁵, T.A. Beermann⁷⁶, M. Begalli^{80b}, M. Begel²⁹, A. Behera¹⁵⁵, J.K. Behr⁴⁶, F. Beisiegel²⁴, A.S. Bell⁹⁴, G. Bella¹⁶¹, L. Bellagamba^{23b}, A. Bellerive³⁴, P. Bellos⁹, K. Beloborodov^{122b,122a}, K. Belotskiy¹¹², N.L. Belyaev¹¹², O. Benary^{161,*}, D. Benchekroun^{35a}, N. Benekos¹⁰, Y. Benhammou¹⁶¹, D.P. Benjamin⁶, M. Benoit⁵⁴, J.R. Bensinger²⁶, S. Bentvelsen¹²⁰, L. Beresford¹³⁵, M. Beretta⁵¹, D. Berge⁴⁶, E. Bergeaas Kuutmann¹⁷², N. Berger⁵, B. Bergmann¹⁴², L.J. Bergsten²⁶, J. Beringer¹⁸, S. Berlendis⁷, N.R. Bernard¹⁰², G. Bernardi¹³⁶, C. Bernius¹⁵³, F.U. Bernlochner²⁴, T. Berry⁹³, P. Berta⁹⁹, C. Bertella^{15a}, G. Bertoli^{45a,45b}, I.A. Bertram⁸⁹, G.J. Besjes⁴⁰, O. Bessidskaia Bylund¹⁸², N. Besson¹⁴⁵, A. Bethani¹⁰⁰, S. Bethke¹¹⁵, A. Betti²⁴, A.J. Bevan⁹², J. Beyer¹¹⁵, R. Bi¹³⁹, R.M. Bianchi¹³⁹, O. Bibel¹¹⁴, D. Biedermann¹⁹, R. Bielski³⁶, K. Bierwagen⁹⁹, N.V. Biesuz^{71a,71b}, M. Biglietti^{74a}, T.R.V. Billoud¹⁰⁹, M. Bindi⁵³, A. Bingul^{12d}, C. Bini^{72a,72b},

S. Biondi^{23b,23a}, M. Birman¹⁸⁰, T. Bisanz⁵³, J.P. Biswal¹⁶¹, A. Bitadze¹⁰⁰, C. Bittrich⁴⁸, D.M. Bjergaard⁴⁹, J.E. Black¹⁵³, K.M. Black²⁵, T. Blazek^{28a}, I. Bloch⁴⁶, C. Blocker²⁶, A. Blue⁵⁷, U. Blumenschein⁹², G.J. Bobbink¹²⁰, V.S. Bobrovnikov^{122b,122a}, S.S. Bocchetta⁹⁶, A. Bocci⁴⁹, D. Boerner⁴⁶, D. Bogavac¹¹⁴, A.G. Bogdanchikov^{122b,122a}, C. Bohm^{45a}, V. Boisvert⁹³, P. Bokan^{53,172}, T. Bold^{83a}, A.S. Boldyrev¹¹³, A.E. Bolz^{61b}, M. Bomben¹³⁶, M. Bona⁹², J.S. Bonilla¹³¹, M. Boonekamp¹⁴⁵, H.M. Borecka-Bielska⁹⁰, A. Borisov¹²³, G. Borissov⁸⁹, J. Bortfeldt³⁶, D. Bortolotto¹³⁵, V. Bortolotto^{73a,73b}, D. Boscherini^{23b}, M. Bosman¹⁴, J.D. Bossio Sola³⁰, K. Bouaouda^{35a}, J. Boudreau¹³⁹, E.V. Bouhova-Thacker⁸⁹, D. Boumediene³⁸, S.K. Boutle⁵⁷, A. Boveia¹²⁶, J. Boyd³⁶, D. Boye^{33b}, I.R. Boyko⁷⁹, A.J. Bozson⁹³, J. Bracinik²¹, N. Brahimi¹⁰¹, G. Brandt¹⁸², O. Brandt^{61a}, F. Braren⁴⁶, U. Bratzler¹⁶⁴, B. Brau¹⁰², J.E. Brau¹³¹, W.D. Breaden Madden⁵⁷, K. Brendlinger⁴⁶, L. Brenner⁴⁶, R. Brenner¹⁷², S. Bressler¹⁸⁰, B. Brickwedde⁹⁹, D.L. Briglin²¹, D. Britton⁵⁷, D. Britzger¹¹⁵, I. Brock²⁴, R. Brock¹⁰⁶, G. Brooijmans³⁹, T. Brooks⁹³, W.K. Brooks^{147b}, E. Brost¹²¹, J.H. Broughton²¹, P.A. Bruckman de Renstrom⁸⁴, D. Bruncko^{28b}, A. Bruni^{23b}, G. Bruni^{23b}, L.S. Bruni¹²⁰, S. Bruno^{73a,73b}, B.H. Brunt³², M. Bruschi^{23b}, N. Bruscino¹³⁹, P. Bryant³⁷, L. Bryngemark⁹⁶, T. Buanes¹⁷, Q. Buat³⁶, P. Buchholz¹⁵¹, A.G. Buckley⁵⁷, I.A. Budagov⁷⁹, M.K. Bugge¹³⁴, F. Bührer⁵², O. Bulekov¹¹², T.J. Burch¹²¹, S. Burdin⁹⁰, C.D. Burgard¹²⁰, A.M. Burger¹²⁹, B. Burghgrave⁸, J.T.P. Burr⁴⁶, V. Büscher⁹⁹, E. Buschmann⁵³, P.J. Bussey⁵⁷, J.M. Butler²⁵, C.M. Buttar⁵⁷, J.M. Butterworth⁹⁴, P. Butti³⁶, W. Buttlinger³⁶, A. Buzatu¹⁵⁸, A.R. Buzykaev^{122b,122a}, G. Cabras^{23b,23a}, S. Cabrera Urbán¹⁷⁴, D. Caforio¹⁴², H. Cai¹⁷³, V.M.M. Cairo¹⁵³, O. Cakir^{4a}, N. Calace³⁶, P. Calafiura¹⁸, A. Calandri¹⁰¹, G. Calderini¹³⁶, P. Calfayan⁶⁵, G. Callea⁵⁷, L.P. Caloba^{80b}, S. Calvente Lopez⁹⁸, D. Calvet³⁸, S. Calvet³⁸, T.P. Calvet¹⁵⁵, M. Calvetti^{71a,71b}, R. Camacho Toro¹³⁶, S. Camarda³⁶, D. Camarero Munoz⁹⁸, P. Camarri^{73a,73b}, D. Cameron¹³⁴, R. Caminal Armadans¹⁰², C. Camincher³⁶, S. Campana³⁶, M. Campanelli⁹⁴, A. Camplani⁴⁰, A. Campoverde¹⁵¹, V. Canale^{69a,69b}, A. Canesse¹⁰³, M. Cano Bret^{60c}, J. Cantero¹²⁹, T. Cao¹⁶¹, Y. Cao¹⁷³, M.D.M. Capeans Garrido³⁶, M. Capua^{41b,41a}, R. Cardarelli^{73a}, F. Cardillo¹⁴⁹, I. Carli¹⁴³, T. Carli³⁶, G. Carlino^{69a}, B.T. Carlson¹³⁹, L. Carminati^{68a,68b}, R.M.D. Carney^{45a,45b}, S. Caron¹¹⁹, E. Carquin^{147b}, S. Carrá^{68a,68b}, J.W.S. Carter¹⁶⁷, M.P. Casado^{14,f}, A.F. Casha¹⁶⁷, D.W. Casper¹⁷¹, R. Castelijn¹²⁰, F.L. Castillo¹⁷⁴, V. Castillo Gimenez¹⁷⁴, N.F. Castro^{140a,140e}, A. Catinaccio³⁶, J.R. Catmore¹³⁴, A. Cattai³⁶, J. Caudron²⁴, V. Cavaliere²⁹, E. Cavallaro¹⁴, D. Cavalli^{68a}, M. Cavalli-Sforza¹⁴, V. Cavasinni^{71a,71b}, E. Celebi^{12b}, F. Ceradini^{74a,74b}, L. Cerdà Alberich¹⁷⁴, A.S. Cerqueira^{80a}, A. Cerri¹⁵⁶, L. Cerrito^{73a,73b}, F. Cerutti¹⁸, A. Cervelli^{23b,23a}, S.A. Cetin^{12b}, A. Chafaq^{35a}, D. Chakraborty¹²¹, S.K. Chan⁵⁹, W.S. Chan¹²⁰, W.Y. Chan⁹⁰, J.D. Chapman³², B. Chargeishvili^{159b}, D.G. Charlton²¹, C.C. Chau³⁴, C.A. Chavez Barajas¹⁵⁶, S. Che¹²⁶, A. Chegwidden¹⁰⁶, S. Chekanov⁶, S.V. Chekulaev^{168a}, G.A. Chelkov^{79,av}, M.A. Chelstowska³⁶, B. Chen⁷⁸, C. Chen^{60a}, C.H. Chen⁷⁸, H. Chen²⁹, J. Chen^{60a}, J. Chen³⁹, S. Chen¹³⁷, S.J. Chen^{15c}, X. Chen^{15b,au}, Y. Chen⁸², Y-H. Chen⁴⁶, H.C. Cheng^{63a}, H.J. Cheng^{15a,15d}, A. Cheplakov⁷⁹, E. Cheremushkina¹²³, R. Cherkaoui El Moursli^{35e}, E. Cheu⁷, K. Cheung⁶⁴, T.J.A. Chevaléries¹⁴⁵, L. Chevalier¹⁴⁵, V. Chiarella⁵¹, G. Chiarella^{71a}, G. Chiodini^{67a}, A.S. Chisholm^{36,21}, A. Chitan^{27b}, I. Chiu¹⁶³, Y.H. Chiu¹⁷⁶, M.V. Chizhov⁷⁹, K. Choi⁶⁵, A.R. Chomont¹³², S. Chouridou¹⁶², Y.S. Chow¹²⁰, M.C. Chu^{63a}, J. Chudoba¹⁴¹, A.J. Chuinard¹⁰³, J.J. Chwastowski⁸⁴, L. Chytka¹³⁰, D. Cinca⁴⁷, V. Cindro⁹¹, I.A. Cioară^{27b}, A. Ciocio¹⁸, F. Cirotto^{69a,69b}, Z.H. Citron¹⁸⁰, M. Citterio^{68a}, B.M. Ciungu¹⁶⁷, A. Clark⁵⁴, M.R. Clark³⁹, P.J. Clark⁵⁰, C. Clement^{45a,45b}, Y. Coadou¹⁰¹, M. Cobal^{66a,66c}, A. Coccaro^{55b}, J. Cochran⁷⁸, H. Cohen¹⁶¹, A.E.C. Coimbra¹⁸⁰, L. Colasurdo¹¹⁹, B. Cole³⁹, A.P. Colijn¹²⁰, J. Collot⁵⁸, P. Conde Muiño^{140a,g}, E. Coniavitis⁵², S.H. Connell^{33b}, I.A. Connelly⁵⁷, S. Constantinescu^{27b}, F. Conventi^{69a,ax}, A.M. Cooper-Sarkar¹³⁵, F. Cormier¹⁷⁵, K.J.R. Cormier¹⁶⁷, L.D. Corpe⁹⁴, M. Corradi^{72a,72b}, E.E. Corrigan⁹⁶, F. Corriveau^{103,ad}, A. Cortes-Gonzalez³⁶, M.J. Costa¹⁷⁴, F. Costanza⁵, D. Costanzo¹⁴⁹, G. Cowan⁹³, J.W. Cowley³², J. Crane¹⁰⁰, K. Cranmer¹²⁴, S.J. Crawley⁵⁷, R.A. Creager¹³⁷, S. Crépé-Renaudin⁵⁸, F. Crescioli¹³⁶, M. Cristinziani²⁴, V. Croft¹²⁰, G. Crosetti^{41b,41a}, A. Cueto⁵, T. Cuhadar Donszelmann¹⁴⁹,

A.R. Cukierman¹⁵³, S. Czekiera⁸⁴, P. Czodrowski³⁶, M.J. Da Cunha Sargedas De Sousa^{60b},
 J.V. Da Fonseca Pinto^{80b}, C. Da Via¹⁰⁰, W. Dabrowski^{83a}, T. Dado^{28a}, S. Dahbi^{35e}, T. Dai¹⁰⁵,
 C. Dallapiccola¹⁰², M. Dam⁴⁰, G. D'amen^{23b,23a}, J. Damp⁹⁹, J.R. Dandoy¹³⁷, M.F. Daneri³⁰,
 N.P. Dang^{181,j}, N.S. Dann¹⁰⁰, M. Danninger¹⁷⁵, V. Dao³⁶, G. Darbo^{55b}, O. Dartsi⁵, A. Dattagupta¹³¹,
 T. Daubney⁴⁶, S. D'Auria^{68a,68b}, W. Davey²⁴, C. David⁴⁶, T. Davidek¹⁴³, D.R. Davis⁴⁹, E. Dawe¹⁰⁴,
 I. Dawson¹⁴⁹, K. De⁸, R. De Asmundis^{69a}, A. De Benedetti¹²⁸, M. De Beurs¹²⁰, S. De Castro^{23b,23a},
 S. De Cecco^{72a,72b}, N. De Groot¹¹⁹, P. de Jong¹²⁰, H. De la Torre¹⁰⁶, A. De Maria^{15c}, D. De Pedis^{72a},
 A. De Salvo^{72a}, U. De Sanctis^{73a,73b}, M. De Santis^{73a,73b}, A. De Santo¹⁵⁶, K. De Vasconcelos Corga¹⁰¹,
 J.B. De Vivie De Regie¹³², C. Debenedetti¹⁴⁶, D.V. Dedovich⁷⁹, A.M. Deiana⁴², M. Del Gaudio^{41b,41a},
 J. Del Peso⁹⁸, Y. Delabat Diaz⁴⁶, D. Delgove¹³², F. Deliot¹⁴⁵, C.M. Delitzsch⁷, M. Della Pietra^{69a,69b},
 D. Della Volpe⁵⁴, A. Dell'Acqua³⁶, L. Dell'Asta²⁵, M. Delmastro⁵, C. Delporte¹³², P.A. Delsart⁵⁸,
 D.A. DeMarco¹⁶⁷, S. Demers¹⁸³, M. Demichev⁷⁹, G. Demontigny¹⁰⁹, S.P. Denisov¹²³, D. Denysiuk¹²⁰,
 L. D'Eramo¹³⁶, D. Derendarz⁸⁴, J.E. Derkaoui^{35d}, F. Derue¹³⁶, P. Dervan⁹⁰, K. Desch²⁴, C. Deterre⁴⁶,
 K. Dette¹⁶⁷, M.R. Devesa³⁰, P.O. Deviveiros³⁶, A. Dewhurst¹⁴⁴, S. Dhaliwal²⁶, F.A. Di Bello⁵⁴,
 A. Di Ciaccio^{73a,73b}, L. Di Ciaccio⁵, W.K. Di Clemente¹³⁷, C. Di Donato^{69a,69b}, A. Di Girolamo³⁶,
 G. Di Gregorio^{71a,71b}, B. Di Micco^{74a,74b}, R. Di Nardo¹⁰², K.F. Di Petrillo⁵⁹, R. Di Sipio¹⁶⁷,
 D. Di Valentino³⁴, C. Diaconu¹⁰¹, F.A. Dias⁴⁰, T. Dias Do Vale^{140a,140e}, M.A. Diaz^{147a}, J. Dickinson¹⁸,
 E.B. Diehl¹⁰⁵, J. Dietrich¹⁹, S. Díez Cornell⁴⁶, A. Dimitrievska¹⁸, W. Ding^{15b}, J. Dingfelder²⁴, F. Dittus³⁶,
 F. Djama¹⁰¹, T. Djobava^{159b}, J.I. Djuvsland¹⁷, M.A.B. Do Vale^{80c}, M. Dobre^{27b}, D. Dodsworth²⁶,
 C. Doglioni⁹⁶, J. Dolejsi¹⁴³, Z. Dolezal¹⁴³, M. Donadelli^{80d}, J. Donini³⁸, A. D'onofrio⁹², M. D'Onofrio⁹⁰,
 J. Dopke¹⁴⁴, A. Doria^{69a}, M.T. Dova⁸⁸, A.T. Doyle⁵⁷, E. Drechsler¹⁵², E. Dreyer¹⁵², T. Dreyer⁵³, Y. Du^{60b},
 Y. Duan^{60b}, F. Dubinin¹¹⁰, M. Dubovsky^{28a}, A. Dubreuil⁵⁴, E. Duchovni¹⁸⁰, G. Duckeck¹¹⁴,
 A. Ducourthial¹³⁶, O.A. Ducu^{109,x}, D. Duda¹¹⁵, A. Dudarev³⁶, A.C. Dudder⁹⁹, E.M. Duffield¹⁸,
 L. Duflot¹³², M. Dührssen³⁶, C. Dülsen¹⁸², M. Dumancic¹⁸⁰, A.E. Dumitriu^{27b}, A.K. Duncan⁵⁷,
 M. Dunford^{61a}, A. Duperrin¹⁰¹, H. Duran Yildiz^{4a}, M. Düren⁵⁶, A. Durglishvili^{159b}, D. Duschinger⁴⁸,
 B. Dutta⁴⁶, D. Duvnjak¹, G.I. Dyckes¹³⁷, M. Dyndal⁴⁶, S. Dysch¹⁰⁰, B.S. Dziedzic⁸⁴, K.M. Ecker¹¹⁵,
 R.C. Edgar¹⁰⁵, T. Eifert³⁶, G. Eigen¹⁷, K. Einsweiler¹⁸, T. Ekelof¹⁷², M. El Kacimi^{35c}, R. El Kosseifi¹⁰¹,
 V. Ellajosyula¹⁷², M. Ellert¹⁷², F. Ellinghaus¹⁸², A.A. Elliot⁹², N. Ellis³⁶, J. Elmsheuser²⁹, M. Elsing³⁶,
 D. Emeliyanov¹⁴⁴, A. Emerman³⁹, Y. Enari¹⁶³, J.S. Ennis¹⁷⁸, M.B. Epland⁴⁹, J. Erdmann⁴⁷, A. Ereditato²⁰,
 M. Escalier¹³², C. Escobar¹⁷⁴, O. Estrada Pastor¹⁷⁴, A.I. Etienne¹⁴⁵, E. Etzion¹⁶¹, H. Evans⁶⁵,
 A. Ezhilov¹³⁸, F. Fabbri⁵⁷, L. Fabbri^{23b,23a}, V. Fabiani¹¹⁹, G. Facini⁹⁴, R.M. Faisca Rodrigues Pereira^{140a},
 R.M. Fakhrutdinov¹²³, S. Falciano^{72a}, P.J. Falke⁵, S. Falke⁵, J. Faltova¹⁴³, Y. Fang^{15a}, Y. Fang^{15a},
 G. Fanourakis⁴⁴, M. Fanti^{68a,68b}, A. Farbin⁸, A. Farilla^{74a}, E.M. Farina^{70a,70b}, T. Farooque¹⁰⁶, S. Farrell¹⁸,
 S.M. Farrington¹⁷⁸, P. Farthouat³⁶, F. Fassi^{35e}, P. Fassnacht³⁶, D. Fassouliotis⁹, M. Faucci Giannelli⁵⁰,
 W.J. Fawcett³², L. Fayard¹³², O.L. Fedin^{138,p}, W. Fedorko¹⁷⁵, M. Feickert⁴², S. Feigl¹³⁴, L. Feligioni¹⁰¹,
 A. Fell¹⁴⁹, C. Feng^{60b}, E.J. Feng³⁶, M. Feng⁴⁹, M.J. Fenton⁵⁷, A.B. Fenyuk¹²³, J. Ferrando⁴⁶, A. Ferrari¹⁷²,
 P. Ferrari¹²⁰, R. Ferrari^{70a}, D.E. Ferreira de Lima^{61b}, A. Ferrer¹⁷⁴, D. Ferrere⁵⁴, C. Ferretti¹⁰⁵, F. Fiedler⁹⁹,
 A. Filipčič⁹¹, F. Filthaut¹¹⁹, K.D. Finelli²⁵, M.C.N. Fiolhais^{140a,140c,a}, L. Fiorini¹⁷⁴, C. Fischer¹⁴,
 F. Fischer¹¹⁴, W.C. Fisher¹⁰⁶, I. Fleck¹⁵¹, P. Fleischmann¹⁰⁵, R.R.M. Fletcher¹³⁷, T. Flick¹⁸²,
 B.M. Flierl¹¹⁴, L. Flores¹³⁷, L.R. Flores Castillo^{63a}, F.M. Follega^{75a,75b}, N. Fomin¹⁷, G.T. Forcolin^{75a,75b},
 A. Formica¹⁴⁵, F.A. Förster¹⁴, A.C. Forti¹⁰⁰, A.G. Foster²¹, D. Fournier¹³², H. Fox⁸⁹, S. Fracchia¹⁴⁹,
 P. Francavilla^{71a,71b}, M. Franchini^{23b,23a}, S. Franchino^{61a}, D. Francis³⁶, L. Franconi²⁰, M. Franklin⁵⁹,
 M. Frate¹⁷¹, A.N. Fray⁹², B. Freund¹⁰⁹, W.S. Freund^{80b}, E.M. Freundlich⁴⁷, D.C. Frizzell¹²⁸,
 D. Froidevaux³⁶, J.A. Frost¹³⁵, C. Fukunaga¹⁶⁴, E. Fullana Torregrosa¹⁷⁴, E. Fumagalli^{55b,55a},
 T. Fusayasu¹¹⁶, J. Fuster¹⁷⁴, A. Gabrielli^{23b,23a}, A. Gabrielli¹⁸, G.P. Gach^{83a}, S. Gadatsch⁵⁴, P. Gadow¹¹⁵,
 G. Gagliardi^{55b,55a}, L.G. Gagnon¹⁰⁹, C. Galea^{27b}, B. Galhardo^{140a,140c}, E.J. Gallas¹³⁵, B.J. Gallop¹⁴⁴,
 P. Gallus¹⁴², G. Galster⁴⁰, R. Gamboa Goni⁹², K.K. Gan¹²⁶, S. Ganguly¹⁸⁰, J. Gao^{60a}, Y. Gao⁹⁰,

Y.S. Gao^{31,m}, C. García¹⁷⁴, J.E. García Navarro¹⁷⁴, J.A. García Pascual^{15a}, C. Garcia-Argos⁵², M. Garcia-Sciveres¹⁸, R.W. Gardner³⁷, N. Garelli¹⁵³, S. Gargiulo⁵², V. Garonne¹³⁴, A. Gaudiello^{55b,55a}, G. Gaudio^{70a}, I.L. Gavrilenko¹¹⁰, A. Gavrilyuk¹¹¹, C. Gay¹⁷⁵, G. Gaycken²⁴, E.N. Gazis¹⁰, A.A. Geanta^{27b}, C.N.P. Gee¹⁴⁴, J. Geisen⁵³, M. Geisen⁹⁹, M.P. Geisler^{61a}, C. Gemme^{55b}, M.H. Genest⁵⁸, C. Geng¹⁰⁵, S. Gentile^{72a,72b}, S. George⁹³, T. Geralis⁴⁴, D. Gerbaudo¹⁴, L.O. Gerlach⁵³, G. Gessner⁴⁷, S. Ghasemi¹⁵¹, M. Ghasemi Bostanabad¹⁷⁶, A. Ghosh⁷⁷, B. Giacobbe^{23b}, S. Giagu^{72a,72b}, N. Giangiacomi^{23b,23a}, P. Giannetti^{71a}, A. Giannini^{69a,69b}, S.M. Gibson⁹³, M. Gignac¹⁴⁶, D. Gillberg³⁴, G. Gilles¹⁸², D.M. Gingrich^{3,aw}, M.P. Giordani^{66a,66c}, F.M. Giorgi^{23b}, P.F. Giraud¹⁴⁵, G. Giugliarelli^{66a,66c}, D. Giugni^{68a}, F. Giuli^{73a,73b}, M. Giulini^{61b}, S. Gkaitatzis¹⁶², I. Gkialas^{9,i}, E.L. Gkougkousis¹⁴, P. Gkountoumis¹⁰, L.K. Gladilin¹¹³, C. Glasman⁹⁸, J. Glatzer¹⁴, P.C.F. Glaysher⁴⁶, A. Glazov⁴⁶, M. Goblirsch-Kolb²⁶, S. Goldfarb¹⁰⁴, T. Golling⁵⁴, D. Golubkov¹²³, A. Gomes^{140a,140b}, R. Goncalves Gama⁵³, R. Gonçalo^{140a,140b}, G. Gonella⁵², L. Gonella²¹, A. Gongadze⁷⁹, F. Gonnella²¹, J.L. Gonski⁵⁹, S. González de la Hoz¹⁷⁴, S. Gonzalez-Sevilla⁵⁴, G.R. Gonzalvo Rodriguez¹⁷⁴, L. Goossens³⁶, P.A. Gorbounov¹¹¹, H.A. Gordon²⁹, B. Gorini³⁶, E. Gorini^{67a,67b}, A. Gorišek⁹¹, A.T. Goshaw⁴⁹, M.I. Gostkin⁷⁹, C.A. Gottardo²⁴, C.R. Goudet¹³², M. Gouighri^{35b}, D. Goujdami^{35c}, A.G. Goussiou¹⁴⁸, N. Govender^{33b,b}, C. Goy⁵, E. Gozani¹⁶⁰, I. Grabowska-Bold^{83a}, P.O.J. Gradin¹⁷², E.C. Graham⁹⁰, J. Gramling¹⁷¹, E. Gramstad¹³⁴, S. Grancagnolo¹⁹, M. Grandi¹⁵⁶, V. Gratchev¹³⁸, P.M. Gravila^{27f}, F.G. Gravili^{67a,67b}, C. Gray⁵⁷, H.M. Gray¹⁸, C. Grefe²⁴, K. Gregersen⁹⁶, I.M. Gregor⁴⁶, P. Grenier¹⁵³, K. Grevtsov⁴⁶, N.A. Grieser¹²⁸, J. Griffiths⁸, A.A. Grillo¹⁴⁶, K. Grimm^{31,l}, S. Grinstein^{14,y}, J.-F. Grivaz¹³², S. Groh⁹⁹, E. Gross¹⁸⁰, J. Grosse-Knetter⁵³, Z.J. Grout⁹⁴, C. Grud¹⁰⁵, A. Grummer¹¹⁸, L. Guan¹⁰⁵, W. Guan¹⁸¹, J. Guenther³⁶, A. Guerguichon¹³², F. Guescini^{168a}, D. Guest¹⁷¹, R. Gugel⁵², B. Gui¹²⁶, T. Guillemin⁵, S. Guindon³⁶, U. Gul⁵⁷, J. Guo^{60c}, W. Guo¹⁰⁵, Y. Guo^{60a,s}, Z. Guo¹⁰¹, R. Gupta⁴⁶, S. Gurbuz^{12c}, G. Gustavino¹²⁸, P. Gutierrez¹²⁸, C. Gutschow⁹⁴, C. Guyot¹⁴⁵, M.P. Guzik^{83a}, C. Gwenlan¹³⁵, C.B. Gwilliam⁹⁰, A. Haas¹²⁴, C. Haber¹⁸, H.K. Hadavand⁸, N. Haddad^{35e}, A. Hadef^{60a}, S. Hageböck³⁶, M. Hagihara¹⁶⁹, M. Haleem¹⁷⁷, J. Haley¹²⁹, G. Halladjian¹⁰⁶, G.D. Hallewell¹⁰¹, K. Hamacher¹⁸², P. Hamal¹³⁰, K. Hamano¹⁷⁶, H. Hamdaoui^{35e}, G.N. Hamity¹⁴⁹, K. Han^{60a,ak}, L. Han^{60a}, S. Han^{15a,15d}, K. Hanagaki^{81,v}, M. Hance¹⁴⁶, D.M. Handl¹¹⁴, B. Haney¹³⁷, R. Hankache¹³⁶, E. Hansen⁹⁶, J.B. Hansen⁴⁰, J.D. Hansen⁴⁰, M.C. Hansen²⁴, P.H. Hansen⁴⁰, E.C. Hanson¹⁰⁰, K. Hara¹⁶⁹, A.S. Hard¹⁸¹, T. Harenberg¹⁸², S. Harkusha¹⁰⁷, P.F. Harrison¹⁷⁸, N.M. Hartmann¹¹⁴, Y. Hasegawa¹⁵⁰, A. Hasib⁵⁰, S. Hassani¹⁴⁵, S. Haug²⁰, R. Hauser¹⁰⁶, L. Hauswald⁴⁸, L.B. Havener³⁹, M. Havranek¹⁴², C.M. Hawkes²¹, R.J. Hawkings³⁶, D. Hayden¹⁰⁶, C. Hayes¹⁵⁵, R.L. Hayes¹⁷⁵, C.P. Hays¹³⁵, J.M. Hays⁹², H.S. Hayward⁹⁰, S.J. Haywood¹⁴⁴, F. He^{60a}, M.P. Heath⁵⁰, V. Hedberg⁹⁶, L. Heelan⁸, S. Heer²⁴, K.K. Heidegger⁵², J. Heilman³⁴, S. Heim⁴⁶, T. Heim¹⁸, B. Heinemann^{46,ar}, J.J. Heinrich¹³¹, L. Heinrich³⁶, C. Heinz⁵⁶, J. Hejbal¹⁴¹, L. Helary^{61b}, A. Held¹⁷⁵, S. Hellesund¹³⁴, C.M. Helling¹⁴⁶, S. Hellman^{45a,45b}, C. Helsens³⁶, R.C.W. Henderson⁸⁹, Y. Heng¹⁸¹, S. Henkelmann¹⁷⁵, A.M. Henriques Correia³⁶, G.H. Herbert¹⁹, H. Herde²⁶, V. Herget¹⁷⁷, Y. Hernández Jiménez^{33c}, H. Herr⁹⁹, M.G. Herrmann¹¹⁴, T. Herrmann⁴⁸, G. Herten⁵², R. Hertenberger¹¹⁴, L. Hervas³⁶, T.C. Herwig¹³⁷, G.G. Hesketh⁹⁴, N.P. Hessey^{168a}, A. Higashida¹⁶³, S. Higashino⁸¹, E. Higón-Rodríguez¹⁷⁴, K. Hildebrand³⁷, E. Hill¹⁷⁶, J.C. Hill³², K.K. Hill²⁹, K.H. Hiller⁴⁶, S.J. Hillier²¹, M. Hils⁴⁸, I. Hinchliffe¹⁸, F. Hinterkeuser²⁴, M. Hirose¹³³, S. Hirose⁵², D. Hirschbuehl¹⁸², B. Hiti⁹¹, O. Hladík¹⁴¹, D.R. Hlaluku^{33c}, X. Hoad⁵⁰, J. Hobbs¹⁵⁵, N. Hod¹⁸⁰, M.C. Hodgkinson¹⁴⁹, A. Hoecker³⁶, F. Hoenig¹¹⁴, D. Hohn⁵², D. Hohov¹³², T.R. Holmes³⁷, M. Holzbock¹¹⁴, L.B.A.H Hommels³², S. Honda¹⁶⁹, T. Honda⁸¹, T.M. Hong¹³⁹, A. Hönl¹¹⁵, B.H. Hooberman¹⁷³, W.H. Hopkins⁶, Y. Horii¹¹⁷, P. Horn⁴⁸, A.J. Horton¹⁵², L.A. Horyn³⁷, J-Y. Hostachy⁵⁸, A. Hostiuc¹⁴⁸, S. Hou¹⁵⁸, A. Hoummada^{35a}, J. Howarth¹⁰⁰, J. Hoya⁸⁸, M. Hrabovsky¹³⁰, J. Hrdinka⁷⁶, I. Hristova¹⁹, J. Hrvnac¹³², A. Hrynevich¹⁰⁸, T. Hrynn'ova⁵, P.J. Hsu⁶⁴, S.-C. Hsu¹⁴⁸, Q. Hu²⁹, S. Hu^{60c}, Y. Huang^{15a}, Z. Hubacek¹⁴², F. Hubaut¹⁰¹, M. Huebner²⁴, F. Huegging²⁴, T.B. Huffman¹³⁵, M. Huhtinen³⁶, R.F.H. Hunter³⁴, P. Huo¹⁵⁵, A.M. Hupe³⁴, N. Huseynov^{79,af}, J. Huston¹⁰⁶, J. Huth⁵⁹,

R. Hyneman¹⁰⁵, S. Hyrych^{28a}, G. Iacobucci⁵⁴, G. Iakovidis²⁹, I. Ibragimov¹⁵¹, L. Iconomidou-Fayard¹³², Z. Idrissi^{35e}, P. Iengo³⁶, R. Ignazzi⁴⁰, O. Igonkina^{120,aa,*}, R. Iguchi¹⁶³, T. Iizawa⁵⁴, Y. Ikegami⁸¹, M. Ikeno⁸¹, D. Iliadis¹⁶², N. Ilie¹¹⁹, F. Iltzsche⁴⁸, G. Introzzi^{70a,70b}, M. Iodice^{74a}, K. Iordanidou³⁹, V. Ippolito^{72a,72b}, M.F. Isacson¹⁷², N. Ishijima¹³³, M. Ishino¹⁶³, M. Ishitsuka¹⁶⁵, W. Islam¹²⁹, C. Issever¹³⁵, S. Isti¹⁶⁰, F. Ito¹⁶⁹, J.M. Iturbe Ponce^{63a}, R. Iuppa^{75a,75b}, A. Ivina¹⁸⁰, H. Iwasaki⁸¹, J.M. Izen⁴³, V. Izzo^{69a}, P. Jacka¹⁴¹, P. Jackson¹, R.M. Jacobs²⁴, V. Jain², G. Jäkel¹⁸², K.B. Jakobi⁹⁹, K. Jakobs⁵², S. Jakobsen⁷⁶, T. Jakoubek¹⁴¹, J. Jamieson⁵⁷, D.O. Jamin¹²⁹, R. Jansky⁵⁴, J. Janssen²⁴, M. Janus⁵³, P.A. Janus^{83a}, G. Jarlskog⁹⁶, N. Javadov^{79,af}, T. Javůrek³⁶, M. Javurkova⁵², F. Jeanneau¹⁴⁵, L. Jeanty¹³¹, J. Jejelava^{159a,ag}, A. Jelinskas¹⁷⁸, P. Jenni^{52,c}, J. Jeong⁴⁶, N. Jeong⁴⁶, S. Jézéquel⁵, H. Ji¹⁸¹, J. Jia¹⁵⁵, H. Jiang⁷⁸, Y. Jiang^{60a}, Z. Jiang^{153,q}, S. Jiggins⁵², F.A. Jimenez Morales³⁸, J. Jimenez Pena¹⁷⁴, S. Jin^{15c}, A. Jinaru^{27b}, O. Jinnouchi¹⁶⁵, H. Jivan^{33c}, P. Johansson¹⁴⁹, K.A. Johns⁷, C.A. Johnson⁶⁵, K. Jon-And^{45a,45b}, R.W.L. Jones⁸⁹, S.D. Jones¹⁵⁶, S. Jones⁷, T.J. Jones⁹⁰, J. Jongmanns^{61a}, P.M. Jorge^{140a,140b}, J. Jovicevic^{168a}, X. Ju¹⁸, J.J. Junggeburth¹¹⁵, A. Juste Rozas^{14,y}, A. Kaczmarska⁸⁴, M. Kado¹³², H. Kagan¹²⁶, M. Kagan¹⁵³, T. Kaji¹⁷⁹, E. Kajomovitz¹⁶⁰, C.W. Kalderon⁹⁶, A. Kaluza⁹⁹, A. Kamenshchikov¹²³, L. Kanjir⁹¹, Y. Kano¹⁶³, V.A. Kantserov¹¹², J. Kanzaki⁸¹, L.S. Kaplan¹⁸¹, D. Kar^{33c}, M.J. Kareem^{168b}, E. Karentzos¹⁰, S.N. Karpov⁷⁹, Z.M. Karpova⁷⁹, V. Kartvelishvili⁸⁹, A.N. Karyukhin¹²³, L. Kashif¹⁸¹, R.D. Kass¹²⁶, A. Kastanas^{45a,45b}, Y. Kataoka¹⁶³, C. Kato^{60d,60c}, J. Katzy⁴⁶, K. Kawade⁸², K. Kawagoe⁸⁷, T. Kawaguchi¹¹⁷, T. Kawamoto¹⁶³, G. Kawamura⁵³, E.F. Kay¹⁷⁶, V.F. Kazanin^{122b,122a}, R. Keeler¹⁷⁶, R. Kehoe⁴², J.S. Keller³⁴, E. Kellermann⁹⁶, J.J. Kempster²¹, J. Kendrick²¹, O. Kepka¹⁴¹, S. Kersten¹⁸², B.P. Kerševan⁹¹, S. Ketabchi Haghigat¹⁶⁷, R.A. Keyes¹⁰³, M. Khader¹⁷³, F. Khalil-Zada¹³, A. Khanov¹²⁹, A.G. Kharlamov^{122b,122a}, T. Kharlamova^{122b,122a}, E.E. Khoda¹⁷⁵, A. Khodinov¹⁶⁶, T.J. Khoo⁵⁴, E. Khramov⁷⁹, J. Khubua^{159b}, S. Kido⁸², M. Kiehn⁵⁴, C.R. Kilby⁹³, Y.K. Kim³⁷, N. Kimura^{66a,66c}, O.M. Kind¹⁹, B.T. King^{90,*}, D. Kirchmeier⁴⁸, J. Kirk¹⁴⁴, A.E. Kiryunin¹¹⁵, T. Kishimoto¹⁶³, V. Kitali⁴⁶, O. Kivernyk⁵, E. Kladiva^{28b,*}, T. Klapdor-Kleingrothaus⁵², M.H. Klein¹⁰⁵, M. Klein⁹⁰, U. Klein⁹⁰, K. Kleinknecht⁹⁹, P. Klimek¹²¹, A. Klimentov²⁹, T. Klingl²⁴, T. Klioutchnikova³⁶, F.F. Klitzner¹¹⁴, P. Kluit¹²⁰, S. Kluth¹¹⁵, E. Kneringer⁷⁶, E.B.F.G. Knoops¹⁰¹, A. Knue⁵², D. Kobayashi⁸⁷, T. Kobayashi¹⁶³, M. Kobel⁴⁸, M. Kocian¹⁵³, P. Kodys¹⁴³, P.T. Koenig²⁴, T. Koffas³⁴, N.M. Köhler¹¹⁵, T. Koi¹⁵³, M. Kolb^{61b}, I. Koletsou⁵, T. Kondo⁸¹, N. Kondrashova^{60c}, K. Köneke⁵², A.C. König¹¹⁹, T. Kono¹²⁵, R. Konoplich^{124,an}, V. Konstantinides⁹⁴, N. Konstantinidis⁹⁴, B. Konya⁹⁶, R. Kopeliansky⁶⁵, S. Koperny^{83a}, K. Korcyl⁸⁴, K. Kordas¹⁶², G. Koren¹⁶¹, A. Korn⁹⁴, I. Korolkov¹⁴, E.V. Korolkova¹⁴⁹, N. Korotkova¹¹³, O. Kortner¹¹⁵, S. Kortner¹¹⁵, T. Kosek¹⁴³, V.V. Kostyukhin²⁴, A. Kotwal⁴⁹, A. Koulouris¹⁰, A. Kourkoumeli-Charalampidi^{70a,70b}, C. Kourkoumelis⁹, E. Kourlitis¹⁴⁹, V. Kouskoura²⁹, A.B. Kowalewska⁸⁴, R. Kowalewski¹⁷⁶, C. Kozakai¹⁶³, W. Kozanecki¹⁴⁵, A.S. Kozhin¹²³, V.A. Kramarenko¹¹³, G. Kramberger⁹¹, D. Krasnopevtsev^{60a}, M.W. Krasny¹³⁶, A. Krasznahorkay³⁶, D. Krauss¹¹⁵, J.A. Kremer^{83a}, J. Kretschmar⁹⁰, P. Krieger¹⁶⁷, A. Krishnan^{61b}, K. Krizka¹⁸, K. Kroeninger⁴⁷, H. Kroha¹¹⁵, J. Kroll¹⁴¹, J. Kroll¹³⁷, J. Krstic¹⁶, U. Kruchonak⁷⁹, H. Krüger²⁴, N. Krumnack⁷⁸, M.C. Kruse⁴⁹, T. Kubota¹⁰⁴, S. Kuday^{4b}, J.T. Kuechler⁴⁶, S. Kuehn³⁶, A. Kugel^{61a}, T. Kuhl⁴⁶, V. Kukhtin⁷⁹, R. Kukla¹⁰¹, Y. Kulchitsky^{107,aj}, S. Kuleshov^{147b}, Y.P. Kulinch¹⁷³, M. Kuna⁵⁸, T. Kunigo⁸⁵, A. Kupco¹⁴¹, T. Kupfer⁴⁷, O. Kuprash⁵², H. Kurashige⁸², L.L. Kurchaninov^{168a}, Y.A. Kurochkin¹⁰⁷, A. Kurova¹¹², M.G. Kurth^{15a,15d}, E.S. Kuwertz³⁶, M. Kuze¹⁶⁵, A.K. Kvam¹⁴⁸, J. Kvita¹³⁰, T. Kwan¹⁰³, A. La Rosa¹¹⁵, J.L. La Rosa Navarro^{80d}, L. La Rotonda^{41b,41a}, F. La Ruffa^{41b,41a}, C. Lacasta¹⁷⁴, F. Lacava^{72a,72b}, D.P.J. Lack¹⁰⁰, H. Lacker¹⁹, D. Lacour¹³⁶, E. Ladygin⁷⁹, R. Lafaye⁵, B. Laforge¹³⁶, T. Lagouri^{33c}, S. Lai⁵³, S. Lammers⁶⁵, W. Lampl⁷, E. Lançon²⁹, U. Landgraf⁵², M.P.J. Landon⁹², M.C. Lanfermann⁵⁴, V.S. Lang⁴⁶, J.C. Lange⁵³, R.J. Langenberg³⁶, A.J. Lankford¹⁷¹, F. Lanni²⁹, K. Lantzsch²⁴, A. Lanza^{70a}, A. Lapertosa^{55b,55a}, S. Laplace¹³⁶, J.F. Laporte¹⁴⁵, T. Lari^{68a}, F. Lasagni Manghi^{23b,23a}, M. Lassnig³⁶, T.S. Lau^{63a}, A. Laudrain¹³², A. Laurier³⁴, M. Lavorgna^{69a,69b}, M. Lazzaroni^{68a,68b}, B. Le¹⁰⁴, O. Le Dertz¹³⁶, E. Le Guirriec¹⁰¹, M. LeBlanc⁷, T. LeCompte⁶,

F. Ledroit-Guillon⁵⁸, C.A. Lee²⁹, G.R. Lee¹⁷, L. Lee⁵⁹, S.C. Lee¹⁵⁸, S.J. Lee³⁴, B. Lefebvre^{168a},
 M. Lefebvre¹⁷⁶, F. Legger¹¹⁴, C. Leggett¹⁸, K. Lehmann¹⁵², N. Lehmann¹⁸², G. Lehmann Miotto³⁶,
 W.A. Leight⁴⁶, A. Leisos^{162,w}, M.A.L. Leite^{80d}, R. Leitner¹⁴³, D. Lellouch^{180,*}, K.J.C. Leney⁴², T. Lenz²⁴,
 B. Lenzi³⁶, R. Leone⁷, S. Leone^{71a}, C. Leonidopoulos⁵⁰, A. Leopold¹³⁶, G. Lerner¹⁵⁶, C. Leroy¹⁰⁹,
 R. Les¹⁶⁷, C.G. Lester³², M. Levchenko¹³⁸, J. Levêque⁵, D. Levin¹⁰⁵, L.J. Levinson¹⁸⁰, D.J. Lewis²¹,
 B. Li^{15b}, B. Li¹⁰⁵, C-Q. Li^{60a,am}, F. Li^{60c}, H. Li^{60a}, H. Li^{60b}, J. Li^{60c}, K. Li¹⁵³, L. Li^{60c}, M. Li^{15a},
 Q. Li^{15a,15d}, Q.Y. Li^{60a}, S. Li^{60d,60c}, X. Li⁴⁶, Y. Li⁴⁶, Z. Liang^{15a}, B. Liberti^{73a}, A. Liblong¹⁶⁷, K. Lie^{63c},
 S. Liem¹²⁰, C.Y. Lin³², K. Lin¹⁰⁶, T.H. Lin⁹⁹, R.A. Linck⁶⁵, J.H. Lindon²¹, A.L. Lionti⁵⁴, E. Lipeles¹³⁷,
 A. Lipniacka¹⁷, M. Lisovyi^{61b}, T.M. Liss^{173,at}, A. Lister¹⁷⁵, A.M. Litke¹⁴⁶, J.D. Little⁸, B. Liu⁷⁸, B.L. Liu⁶,
 H.B. Liu²⁹, H. Liu¹⁰⁵, J.B. Liu^{60a}, J.K.K. Liu¹³⁵, K. Liu¹³⁶, M. Liu^{60a}, P. Liu¹⁸, Y. Liu^{15a,15d}, Y.L. Liu¹⁰⁵,
 Y.W. Liu^{60a}, M. Livan^{70a,70b}, A. Lleres⁵⁸, J. Llorente Merino^{15a}, S.L. Lloyd⁹², C.Y. Lo^{63b}, F. Lo Sterzo⁴²,
 E.M. Lobodzinska⁴⁶, P. Loch⁷, S. Loffredo^{73a,73b}, T. Lohse¹⁹, K. Lohwasser¹⁴⁹, M. Lokajicek¹⁴¹,
 J.D. Long¹⁷³, R.E. Long⁸⁹, L. Longo³⁶, K.A.Looper¹²⁶, J.A. Lopez^{147b}, I. Lopez Paz¹⁰⁰,
 A. Lopez Solis¹⁴⁹, J. Lorenz¹¹⁴, N. Lorenzo Martinez⁵, M. Losada²², P.J. Lösel¹¹⁴, A. Lösle⁵², X. Lou⁴⁶,
 X. Lou^{15a}, A. Lounis¹³², J. Love⁶, P.A. Love⁸⁹, J.J. Lozano Bahilo¹⁷⁴, H. Lu^{63a}, M. Lu^{60a}, Y.J. Lu⁶⁴,
 H.J. Lubatti¹⁴⁸, C. Luci^{72a,72b}, A. Lucotte⁵⁸, C. Luedtke⁵², F. Luehring⁶⁵, I. Luise¹³⁶, L. Luminari^{72a},
 B. Lund-Jensen¹⁵⁴, M.S. Lutz¹⁰², D. Lynn²⁹, R. Lysak¹⁴¹, E. Lytken⁹⁶, F. Lyu^{15a}, V. Lyubushkin⁷⁹,
 T. Lyubushkina⁷⁹, H. Ma²⁹, L.L. Ma^{60b}, Y. Ma^{60b}, G. Maccarrone⁵¹, A. Macchiolo¹¹⁵,
 C.M. Macdonald¹⁴⁹, J. Machado Miguens^{137,140b}, D. Madaffari¹⁷⁴, R. Madar³⁸, W.F. Mader⁴⁸,
 N. Madysa⁴⁸, J. Maeda⁸², K. Maekawa¹⁶³, S. Maeland¹⁷, T. Maeno²⁹, M. Maerker⁴⁸, A.S. Maevskiy¹¹³,
 V. Magerl⁵², N. Magini⁷⁸, D.J. Mahon³⁹, C. Maidantchik^{80b}, T. Maier¹¹⁴, A. Maio^{140a,140b,140d}, K. Maj⁸⁴,
 O. Majersky^{28a}, S. Majewski¹³¹, Y. Makida⁸¹, N. Makovec¹³², B. Malaescu¹³⁶, Pa. Malecki⁸⁴,
 V.P. Maleev¹³⁸, F. Malek⁵⁸, U. Mallik⁷⁷, D. Malon⁶, C. Malone³², S. Maltezos¹⁰, S. Malyukov⁷⁹,
 J. Mamuzic¹⁷⁴, G. Mancini⁵¹, I. Mandić⁹¹, L. Manhaes de Andrade Filho^{80a}, I.M. Maniatis¹⁶²,
 J. Manjarres Ramos⁴⁸, K.H. Mankinen⁹⁶, A. Mann¹¹⁴, A. Manousos⁷⁶, B. Mansoulie¹⁴⁵, I. Manthos¹⁶²,
 S. Manzoni¹²⁰, A. Marantis¹⁶², G. Marceca³⁰, L. Marchese¹³⁵, G. Marchiori¹³⁶, M. Marcisovsky¹⁴¹,
 C. Marcon⁹⁶, C.A. Marin Tobon³⁶, M. Marjanovic³⁸, Z. Marshall¹⁸, M.U.F Martensson¹⁷²,
 S. Marti-Garcia¹⁷⁴, C.B. Martin¹²⁶, T.A. Martin¹⁷⁸, V.J. Martin⁵⁰, B. Martin dit Latour¹⁷, M. Martinez^{14,y},
 V.I. Martinez Outschoorn¹⁰², S. Martin-Haugh¹⁴⁴, V.S. Martoiu^{27b}, A.C. Martyniuk⁹⁴, A. Marzin³⁶,
 L. Masetti⁹⁹, T. Mashimo¹⁶³, R. Mashinistov¹¹⁰, J. Masik¹⁰⁰, A.L. Maslennikov^{122b,122a}, L.H. Mason¹⁰⁴,
 L. Massa^{73a,73b}, P. Massarotti^{69a,69b}, P. Mastrandrea^{71a,71b}, A. Mastroberardino^{41b,41a}, T. Masubuchi¹⁶³,
 A. Matic¹¹⁴, P. Mättig²⁴, J. Maurer^{27b}, B. Maček⁹¹, D.A. Maximov^{122b,122a}, R. Mazini¹⁵⁸, I. Maznas¹⁶²,
 S.M. Mazza¹⁴⁶, S.P. Mc Kee¹⁰⁵, T.G. McCarthy¹¹⁵, L.I. McClymont⁹⁴, W.P. McCormack¹⁸,
 E.F. McDonald¹⁰⁴, J.A. McFayden³⁶, M.A. McKay⁴², K.D. McLean¹⁷⁶, S.J. McMahon¹⁴⁴,
 P.C. McNamara¹⁰⁴, C.J. McNicol¹⁷⁸, R.A. McPherson^{176,ad}, J.E. Mdhluli^{33c}, Z.A. Meadows¹⁰²,
 S. Meehan¹⁴⁸, T. Megy⁵², S. Mehlhase¹¹⁴, A. Mehta⁹⁰, T. Meideck⁵⁸, B. Meirose⁴³, D. Melini¹⁷⁴,
 B.R. Mellado Garcia^{33c}, J.D. Mellenthin⁵³, M. Melo^{28a}, F. Meloni⁴⁶, A. Melzer²⁴, S.B. Menary¹⁰⁰,
 E.D. Mendes Gouveia^{140a,140e}, L. Meng³⁶, X.T. Meng¹⁰⁵, S. Menke¹¹⁵, E. Meoni^{41b,41a}, S. Mergelmeyer¹⁹,
 S.A.M. Merkt¹³⁹, C. Merlassino²⁰, P. Mermod⁵⁴, L. Merola^{69a,69b}, C. Meroni^{68a}, O. Meshkov¹¹³,
 J.K.R. Meshreki¹⁵¹, A. Messina^{72a,72b}, J. Metcalfe⁶, A.S. Mete¹⁷¹, C. Meyer⁶⁵, J. Meyer¹⁶⁰, J-P. Meyer¹⁴⁵,
 H. Meyer Zu Theenhausen^{61a}, F. Miano¹⁵⁶, R.P. Middleton¹⁴⁴, L. Mijović⁵⁰, G. Mikenberg¹⁸⁰,
 M. Mikestikova¹⁴¹, M. Mikuž⁹¹, H. Mildner¹⁴⁹, M. Milesi¹⁰⁴, A. Milic¹⁶⁷, D.A. Millar⁹², D.W. Miller³⁷,
 A. Milov¹⁸⁰, D.A. Milstead^{45a,45b}, R.A. Mina^{153,q}, A.A. Minaenko¹²³, M. Miñano Moya¹⁷⁴,
 I.A. Minashvili^{159b}, A.I. Mincer¹²⁴, B. Mindur^{83a}, M. Mineev⁷⁹, Y. Minegishi¹⁶³, Y. Ming¹⁸¹, L.M. Mir¹⁴,
 A. Mirto^{67a,67b}, K.P. Mistry¹³⁷, T. Mitani¹⁷⁹, J. Mitrevski¹¹⁴, V.A. Mitsou¹⁷⁴, M. Mittal^{60c}, A. Miucci²⁰,
 P.S. Miyagawa¹⁴⁹, A. Mizukami⁸¹, J.U. Mjörnmark⁹⁶, T. Mkrtchyan¹⁸⁴, M. Mlynarikova¹⁴³, T. Moa^{45a,45b},
 K. Mochizuki¹⁰⁹, P. Mogg⁵², S. Mohapatra³⁹, R. Moles-Valls²⁴, M.C. Mondragon¹⁰⁶, K. Mönig⁴⁶,

J. Monk⁴⁰, E. Monnier¹⁰¹, A. Montalbano¹⁵², J. Montejo Berlingen³⁶, M. Montella⁹⁴, F. Monticelli⁸⁸, S. Monzani^{68a}, N. Morange¹³², D. Moreno²², M. Moreno Llácer³⁶, P. Morettini^{55b}, M. Morgenstern¹²⁰, S. Morgenstern⁴⁸, D. Mori¹⁵², M. Morii⁵⁹, M. Morinaga¹⁷⁹, V. Morisbak¹³⁴, A.K. Morley³⁶, G. Mornacchi³⁶, A.P. Morris⁹⁴, L. Morvaj¹⁵⁵, P. Moschovakos¹⁰, B. Moser¹²⁰, M. Mosidze^{159b}, H.J. Moss¹⁴⁹, J. Moss^{31,n}, K. Motohashi¹⁶⁵, E. Mountricha³⁶, E.J.W. Moyse¹⁰², S. Muanza¹⁰¹, F. Mueller¹¹⁵, J. Mueller¹³⁹, R.S.P. Mueller¹¹⁴, D. Muenstermann⁸⁹, G.A. Mullier⁹⁶, J.L. Munoz Martinez¹⁴, F.J. Munoz Sanchez¹⁰⁰, P. Murin^{28b}, W.J. Murray^{178,144}, A. Murrone^{68a,68b}, M. Muškinja¹⁸, C. Mwewa^{33a}, A.G. Myagkov^{123,a0}, J. Myers¹³¹, M. Myska¹⁴², B.P. Nachman¹⁸, O. Nackenhorst⁴⁷, A.Nag Nag⁴⁸, K. Nagai¹³⁵, K. Nagano⁸¹, Y. Nagasaka⁶², M. Nagel⁵², E. Nagy¹⁰¹, A.M. Nairz³⁶, Y. Nakahama¹¹⁷, K. Nakamura⁸¹, T. Nakamura¹⁶³, I. Nakano¹²⁷, H. Nanjo¹³³, F. Napolitano^{61a}, R.F. Naranjo Garcia⁴⁶, R. Narayan¹¹, D.I. Narrias Villar^{61a}, I. Naryshkin¹³⁸, T. Naumann⁴⁶, G. Navarro²², H.A. Neal^{105,*}, P.Y. Nechaeva¹¹⁰, F. Nechansky⁴⁶, T.J. Neep²¹, A. Negri^{70a,70b}, M. Negrini^{23b}, S. Nektarijevic¹¹⁹, C. Nellist⁵³, M.E. Nelson¹³⁵, S. Nemecek¹⁴¹, P. Nemethy¹²⁴, M. Nessi^{36,e}, M.S. Neubauer¹⁷³, M. Neumann¹⁸², P.R. Newman²¹, T.Y. Ng^{63c}, Y.S. Ng¹⁹, Y.W.Y. Ng¹⁷¹, H.D.N. Nguyen¹⁰¹, T. Nguyen Manh¹⁰⁹, E. Nibigira³⁸, R.B. Nickerson¹³⁵, R. Nicolaidou¹⁴⁵, D.S. Nielsen⁴⁰, J. Nielsen¹⁴⁶, N. Nikiforou¹¹, V. Nikolaenko^{123,a0}, I. Nikolic-Audit¹³⁶, K. Nikolopoulos²¹, P. Nilsson²⁹, H.R. Nindhito⁵⁴, Y. Ninomiya⁸¹, A. Nisati^{72a}, N. Nishu^{60c}, R. Nisius¹¹⁵, I. Nitsche⁴⁷, T. Nitta¹⁷⁹, T. Nobe¹⁶³, Y. Noguchi⁸⁵, M. Nomachi¹³³, I. Nomidis¹³⁶, M.A. Nomura²⁹, M. Nordberg³⁶, N. Norjoharuddeen¹³⁵, T. Novak⁹¹, O. Novgorodova⁴⁸, R. Novotny¹⁴², L. Nozka¹³⁰, K. Ntekas¹⁷¹, E. Nurse⁹⁴, F. Nuti¹⁰⁴, F.G. Oakham^{34,aw}, H. Oberlack¹¹⁵, J. Ocariz¹³⁶, A. Ochi⁸², I. Ochoa³⁹, J.P. Ochoa-Ricoux^{147a}, K. O'Connor²⁶, S. Oda⁸⁷, S. Odaka⁸¹, S. Oerdekk⁵³, A. Ogrodnik^{83a}, A. Oh¹⁰⁰, S.H. Oh⁴⁹, C.C. Ohm¹⁵⁴, H. Oide^{55b,55a}, M.L. Ojeda¹⁶⁷, H. Okawa¹⁶⁹, Y. Okazaki⁸⁵, Y. Okumura¹⁶³, T. Okuyama⁸¹, A. Olariu^{27b}, L.F. Oleiro Seabra^{140a}, S.A. Olivares Pino^{147a}, D. Oliveira Damazio²⁹, J.L. Oliver¹, M.J.R. Olsson¹⁷¹, A. Olszewski⁸⁴, J. Olszowska⁸⁴, D.C. O'Neil¹⁵², A. Onofre^{140a,140e}, K. Onogi¹¹⁷, P.U.E. Onyisi¹¹, H. Oppen¹³⁴, M.J. Oreglia³⁷, G.E. Orellana⁸⁸, D. Orestano^{74a,74b}, N. Orlando¹⁴, R.S. Orr¹⁶⁷, B. Osculati^{55b,55a,*}, V. O'Shea⁵⁷, R. Ospanov^{60a}, G. Otero y Garzon³⁰, H. Otono⁸⁷, M. Ouchrif^{35d}, F. Ould-Saada¹³⁴, A. Ouraou¹⁴⁵, Q. Ouyang^{15a}, M. Owen⁵⁷, R.E. Owen²¹, V.E. Ozcan^{12c}, N. Ozturk⁸, J. Pacalt¹³⁰, H.A. Pacey³², K. Pachal⁴⁹, A. Pacheco Pages¹⁴, C. Padilla Aranda¹⁴, S. Pagan Griso¹⁸, M. Paganini¹⁸³, G. Palacino⁶⁵, S. Palazzo⁵⁰, S. Palestini³⁶, M. Palka^{83b}, D. Pallin³⁸, I. Panagoulias¹⁰, C.E. Pandini³⁶, J.G. Panduro Vazquez⁹³, P. Pani⁴⁶, G. Panizzo^{66a,66c}, L. Paolozzi⁵⁴, C. Papadatos¹⁰⁹, K. Papageorgiou^{9,i}, A. Paramonov⁶, D. Paredes Hernandez^{63b}, S.R. Paredes Saenz¹³⁵, B. Parida¹⁶⁶, T.H. Park¹⁶⁷, A.J. Parker⁸⁹, M.A. Parker³², F. Parodi^{55b,55a}, E.W.P. Parrish¹²¹, J.A. Parsons³⁹, U. Parzefall⁵², L. Pascual Dominguez¹³⁶, V.R. Pascuzzi¹⁶⁷, J.M.P. Pasner¹⁴⁶, E. Pasqualucci^{72a}, S. Passaggio^{55b}, F. Pastore⁹³, P. Pasuwant^{45a,45b}, S. Pataria⁹⁹, J.R. Pater¹⁰⁰, A. Pathak¹⁸¹, T. Pauly³⁶, B. Pearson¹¹⁵, M. Pedersen¹³⁴, L. Pedraza Diaz¹¹⁹, R. Pedro^{140a,140b}, S.V. Peleganchuk^{122b,122a}, O. Penc¹⁴¹, C. Peng^{15a}, H. Peng^{60a}, B.S. Peralva^{80a}, M.M. Perego¹³², A.P. Pereira Peixoto^{140a,140e}, D.V. Perekiltsa²⁹, F. Peri¹⁹, L. Perini^{68a,68b}, H. Pernegger³⁶, S. Perrella^{69a,69b}, V.D. Peshekhanov^{79,*}, K. Peters⁴⁶, R.F.Y. Peters¹⁰⁰, B.A. Petersen³⁶, T.C. Petersen⁴⁰, E. Petit⁵⁸, A. Petridis¹, C. Petridou¹⁶², P. Petroff¹³², M. Petrov¹³⁵, F. Petrucci^{74a,74b}, M. Pettee¹⁸³, N.E. Pettersson¹⁰², K. Petukhova¹⁴³, A. Peyaud¹⁴⁵, R. Pezoa^{147b}, T. Pham¹⁰⁴, F.H. Phillips¹⁰⁶, P.W. Phillips¹⁴⁴, M.W. Phipps¹⁷³, G. Piacquadio¹⁵⁵, E. Pianori¹⁸, A. Picazio¹⁰², R.H. Pickles¹⁰⁰, R. Piegaia³⁰, D. Pietreanu^{27b}, J.E. Pilcher³⁷, A.D. Pilkington¹⁰⁰, M. Pinamonti^{73a,73b}, J.L. Pinfold³, M. Pitt¹⁸⁰, L. Pizzimento^{73a,73b}, M.-A. Pleier²⁹, V. Pleskot¹⁴³, E. Plotnikova⁷⁹, D. Pluth⁷⁸, P. Podberezko^{122b,122a}, R. Poettgen⁹⁶, R. Poggi⁵⁴, L. Poggioli¹³², I. Pogrebnyak¹⁰⁶, D. Pohl²⁴, I. Pokharel⁵³, G. Polesello^{70a}, A. Poley¹⁸, A. Policicchio^{72a,72b}, R. Polifka³⁶, A. Polini^{23b}, C.S. Pollard⁴⁶, V. Polychronakos²⁹, D. Ponomarenko¹¹², L. Pontecorvo³⁶, S. Popa^{27a}, G.A. Popeneciu^{27d}, D.M. Portillo Quintero¹³⁶, S. Pospisil¹⁴², K. Potamianos⁴⁶, I.N. Potrap⁷⁹, C.J. Potter³², H. Potti¹¹,

T. Poulsen⁹⁶, J. Poveda³⁶, T.D. Powell¹⁴⁹, G. Pownall⁴⁶, M.E. Pozo Astigarraga³⁶, P. Pralavorio¹⁰¹, S. Prell⁷⁸, D. Price¹⁰⁰, M. Primavera^{67a}, S. Prince¹⁰³, M.L. Proffitt¹⁴⁸, N. Proklova¹¹², K. Prokofiev^{63c}, F. Prokoshin^{147b}, S. Protopopescu²⁹, J. Proudfoot⁶, M. Przybycien^{83a}, A. Puri¹⁷³, P. Puzo¹³², J. Qian¹⁰⁵, Y. Qin¹⁰⁰, A. Quadt⁵³, M. Queitsch-Maitland⁴⁶, A. Qureshi¹, P. Rados¹⁰⁴, F. Ragusa^{68a,68b}, G. Rahal⁹⁷, J.A. Raine⁵⁴, S. Rajagopalan²⁹, A. Ramirez Morales⁹², K. Ran^{15a,15d}, T. Rashid¹³², S. Raspopov⁵, M.G. Ratti^{68a,68b}, D.M. Rauch⁴⁶, F. Rauscher¹¹⁴, S. Rave⁹⁹, B. Ravina¹⁴⁹, I. Ravinovich¹⁸⁰, J.H. Rawling¹⁰⁰, M. Raymond³⁶, A.L. Read¹³⁴, N.P. Readioff⁵⁸, M. Reale^{67a,67b}, D.M. Rebuzzi^{70a,70b}, A. Redelbach¹⁷⁷, G. Redlinger²⁹, R.G. Reed^{33c}, K. Reeves⁴³, L. Rehnisch¹⁹, J. Reichert¹³⁷, D. Reikher¹⁶¹, A. Reiss⁹⁹, A. Rej¹⁵¹, C. Rembser³⁶, H. Ren^{15a}, M. Rescigno^{72a}, S. Resconi^{68a}, E.D. Ressegueie¹³⁷, S. Rettie¹⁷⁵, E. Reynolds²¹, O.L. Rezanova^{122b,122a}, P. Reznicek¹⁴³, E. Ricci^{75a,75b}, R. Richter¹¹⁵, S. Richter⁴⁶, E. Richter-Was^{83b}, O. Ricken²⁴, M. Ridel¹³⁶, P. Rieck¹¹⁵, C.J. Riegel¹⁸², O. Rifki⁴⁶, M. Rijssenbeek¹⁵⁵, A. Rimoldi^{70a,70b}, M. Rimoldi²⁰, L. Rinaldi^{23b}, G. Ripellino¹⁵⁴, B. Ristic⁸⁹, E. Ritsch³⁶, I. Riu¹⁴, J.C. Rivera Vergara^{147a}, F. Rizatdinova¹²⁹, E. Rizvi⁹², C. Rizzi³⁶, R.T. Roberts¹⁰⁰, S.H. Robertson^{103,ad}, M. Robin⁴⁶, D. Robinson³², J.E.M. Robinson⁴⁶, A. Robson⁵⁷, E. Rocco⁹⁹, C. Roda^{71a,71b}, Y. Rodina¹⁰¹, S. Rodriguez Bosca¹⁷⁴, A. Rodriguez Perez¹⁴, D. Rodriguez Rodriguez¹⁷⁴, A.M. Rodríguez Vera^{168b}, S. Roe³⁶, O. Røhne¹³⁴, R. Röhrlig¹¹⁵, C.P.A. Roland⁶⁵, J. Roloff⁵⁹, A. Romaniouk¹¹², M. Romano^{23b,23a}, N. Rompotis⁹⁰, M. Ronzani¹²⁴, L. Roos¹³⁶, S. Rosati^{72a}, K. Rosbach⁵², N-A. Rosien⁵³, G. Rosin¹⁰², B.J. Rosser¹³⁷, E. Rossi⁴⁶, E. Rossi^{74a,74b}, E. Rossi^{69a,69b}, L.P. Rossi^{55b}, L. Rossini^{68a,68b}, J.H.N. Rosten³², R. Rosten¹⁴, M. Rotaru^{27b}, J. Rothberg¹⁴⁸, D. Rousseau¹³², D. Roy^{33c}, A. Rozanov¹⁰¹, Y. Rozen¹⁶⁰, X. Ruan^{33c}, F. Rubbo¹⁵³, F. Rühr⁵², A. Ruiz-Martinez¹⁷⁴, A. Rummler³⁶, Z. Rurikova⁵², N.A. Rusakovich⁷⁹, H.L. Russell¹⁰³, L. Rustige^{38,47}, J.P. Rutherford⁷, E.M. Rüttinger^{46,k}, Y.F. Ryabov^{138,*}, M. Rybar³⁹, G. Rybkin¹³², A. Ryzhov¹²³, G.F. Rzehorž⁵³, P. Sabatini⁵³, G. Sabato¹²⁰, S. Sacerdoti¹³², H.F-W. Sadrozinski¹⁴⁶, R. Sadykov⁷⁹, F. Safai Tehrani^{72a}, B. Safarzadeh Samani¹⁵⁶, P. Saha¹²¹, S. Saha¹⁰³, M. Sahinsoy^{61a}, A. Sahu¹⁸², M. Saimpert⁴⁶, M. Saito¹⁶³, T. Saito¹⁶³, H. Sakamoto¹⁶³, A. Sakharov^{124,an}, D. Salamani⁵⁴, G. Salamanna^{74a,74b}, J.E. Salazar Loyola^{147b}, P.H. Sales De Bruin¹⁷², D. Salihagic^{115,*}, A. Salnikov¹⁵³, J. Salt¹⁷⁴, D. Salvatore^{41b,41a}, F. Salvatore¹⁵⁶, A. Salvucci^{63a,63b,63c}, A. Salzburger³⁶, J. Samarati³⁶, D. Sammel⁵², D. Sampsonidis¹⁶², D. Sampsonidou¹⁶², J. Sánchez¹⁷⁴, A. Sanchez Pineda^{66a,66c}, H. Sandaker¹³⁴, C.O. Sander⁴⁶, M. Sandhoff¹⁸², C. Sandoval²², D.P.C. Sankey¹⁴⁴, M. Sannino^{55b,55a}, Y. Sano¹¹⁷, A. Sansoni⁵¹, C. Santoni³⁸, H. Santos^{140a,140b}, S.N. Santpur¹⁸, A. Santra¹⁷⁴, A. Sapronov⁷⁹, J.G. Saraiva^{140a,140d}, O. Sasaki⁸¹, K. Sato¹⁶⁹, E. Sauvan⁵, P. Savard^{167,aw}, N. Savic¹¹⁵, R. Sawada¹⁶³, C. Sawyer¹⁴⁴, L. Sawyer^{95,al}, C. Sbarra^{23b}, A. Sbrizzi^{23a}, T. Scanlon⁹⁴, J. Schaarschmidt¹⁴⁸, P. Schacht¹¹⁵, B.M. Schachtner¹¹⁴, D. Schaefer³⁷, L. Schaefer¹³⁷, J. Schaeffer⁹⁹, S. Schaepe³⁶, U. Schäfer⁹⁹, A.C. Schaffer¹³², D. Schaile¹¹⁴, R.D. Schamberger¹⁵⁵, N. Scharmberg¹⁰⁰, V.A. Schegelsky¹³⁸, D. Scheirich¹⁴³, F. Schenck¹⁹, M. Schernau¹⁷¹, C. Schiavi^{55b,55a}, S. Schier¹⁴⁶, L.K. Schildgen²⁴, Z.M. Schillaci²⁶, E.J. Schioppa³⁶, M. Schioppa^{41b,41a}, K.E. Schleicher⁵², S. Schlenker³⁶, K.R. Schmidt-Sommerfeld¹¹⁵, K. Schmieden³⁶, C. Schmitt⁹⁹, S. Schmitt⁴⁶, S. Schmitz⁹⁹, J.C. Schmoeckel⁴⁶, U. Schnoor⁵², L. Schoeffel¹⁴⁵, A. Schoening^{61b}, E. Schopf¹³⁵, M. Schott⁹⁹, J.F.P. Schouwenberg¹¹⁹, J. Schovancova³⁶, S. Schramm⁵⁴, F. Schroeder¹⁸², A. Schulte⁹⁹, H-C. Schultz-Coulon^{61a}, M. Schumacher⁵², B.A. Schumm¹⁴⁶, Ph. Schune¹⁴⁵, A. Schwartzman¹⁵³, T.A. Schwarz¹⁰⁵, Ph. Schwemling¹⁴⁵, R. Schwienhorst¹⁰⁶, A. Sciandra²⁴, G. Sciolla²⁶, M. Scornajenghi^{41b,41a}, F. Scuri^{71a}, F. Scutti¹⁰⁴, L.M. Scyboz¹¹⁵, C.D. Sebastiani^{72a,72b}, P. Seema¹⁹, S.C. Seidel¹¹⁸, A. Seiden¹⁴⁶, T. Seiss³⁷, J.M. Seixas^{80b}, G. Sekhniaidze^{69a}, K. Sekhon¹⁰⁵, S.J. Sekula⁴², N. Semprini-Cesari^{23b,23a}, S. Sen⁴⁹, S. Senkin³⁸, C. Serfon⁷⁶, L. Serin¹³², L. Serkin^{66a,66b}, M. Sessa^{60a}, H. Severini¹²⁸, T. Šfiligoj⁹¹, F. Sforza¹⁷⁰, A. Sfyrla⁵⁴, E. Shabalina⁵³, J.D. Shahinian¹⁴⁶, N.W. Shaikh^{45a,45b}, D. Shaked Renous¹⁸⁰, L.Y. Shan^{15a}, R. Shang¹⁷³, J.T. Shank²⁵, M. Shapiro¹⁸, A. Sharma¹³⁵, A.S. Sharma¹, P.B. Shatalov¹¹¹, K. Shaw¹⁵⁶, S.M. Shaw¹⁰⁰, A. Shcherbakova¹³⁸,

Y. Shen¹²⁸, N. Sherafati³⁴, A.D. Sherman²⁵, P. Sherwood⁹⁴, L. Shi^{158,as}, S. Shimizu⁸¹, C.O. Shimmin¹⁸³, Y. Shimogama¹⁷⁹, M. Shimojima¹¹⁶, I.P.J. Shipsey¹³⁵, S. Shirabe⁸⁷, M. Shiyakova^{79,ab}, J. Shlomi¹⁸⁰, A. Shmeleva¹¹⁰, M.J. Shochet³⁷, J. Shojaei¹⁰⁴, D.R. Shope¹²⁸, S. Shrestha¹²⁶, E. Shulga¹⁸⁰, P. Sicho¹⁴¹, A.M. Sickles¹⁷³, P.E. Sidebo¹⁵⁴, E. Sideras Haddad^{33c}, O. Sidiropoulou³⁶, A. Sidoti^{23b,23a}, F. Siegert⁴⁸, Dj. Sijacki¹⁶, M.Jr. Silva¹⁸¹, M.V. Silva Oliveira^{80a}, S.B. Silverstein^{45a}, S. Simion¹³², E. Simioni⁹⁹, M. Simon⁹⁹, R. Simoniello⁹⁹, P. Sinervo¹⁶⁷, N.B. Sinev¹³¹, M. Sioli^{23b,23a}, I. Siral¹⁰⁵, S.Yu. Sivoklokov¹¹³, J. Sjölin^{45a,45b}, E. Skorda⁹⁶, P. Skubic¹²⁸, M. Slawinska⁸⁴, K. Sliwa¹⁷⁰, R. Slovak¹⁴³, V. Smakhtin¹⁸⁰, B.H. Smart¹⁴⁴, J. Smiesko^{28a}, N. Smirnov¹¹², S.Yu. Smirnov¹¹², Y. Smirnov¹¹², L.N. Smirnova^{113,t}, O. Smirnova⁹⁶, J.W. Smith⁵³, M. Smizanska⁸⁹, K. Smolek¹⁴², A. Smykiewicz⁸⁴, A.A. Snesarev¹¹⁰, H.L. Snoek¹²⁰, I.M. Snyder¹³¹, S. Snyder²⁹, R. Sobie^{176,ad}, A.M. Soffa¹⁷¹, A. Soffer¹⁶¹, A. Søgaard⁵⁰, F. Sohns⁵³, G. Sokhrannyi⁹¹, C.A. Solans Sanchez³⁶, E.Yu. Soldatov¹¹², U. Soldevila¹⁷⁴, A.A. Solodkov¹²³, A. Soloshenko⁷⁹, O.V. Solovyanov¹²³, V. Solovyev¹³⁸, P. Sommer¹⁴⁹, H. Son¹⁷⁰, W. Song¹⁴⁴, W.Y. Song^{168b}, A. Sopczak¹⁴², F. Sopkova^{28b}, C.L. Sotiropoulou^{71a,71b}, S. Sottocornola^{70a,70b}, R. Soualah^{66a,66c,h}, A.M. Soukharev^{122b,122a}, D. South⁴⁶, S. Spagnolo^{67a,67b}, M. Spalla¹¹⁵, M. Spangenberg¹⁷⁸, F. Spanò⁹³, D. Sperlich¹⁹, T.M. Speker^{61a}, R. Spighi^{23b}, G. Spigo³⁶, L.A. Spiller¹⁰⁴, M. Spina¹⁵⁶, D.P. Spiteri⁵⁷, M. Spousta¹⁴³, A. Stabile^{68a,68b}, B.L. Stamas¹²¹, R. Stamen^{61a}, M. Stamenkovic¹²⁰, S. Stamm¹⁹, E. Stancka⁸⁴, R.W. Stanek⁶, B. Stanislaus¹³⁵, M.M. Stanitzki⁴⁶, M. Stankaityte¹³⁵, B. Stapf¹²⁰, E.A. Starchenko¹²³, G.H. Stark¹⁴⁶, J. Stark⁵⁸, S.H. Stark⁴⁰, P. Staroba¹⁴¹, P. Starovoitov^{61a}, S. Stärz¹⁰³, R. Staszewski⁸⁴, G. Stavropoulos⁴⁴, M. Stegler⁴⁶, P. Steinberg²⁹, B. Stelzer¹⁵², H.J. Stelzer³⁶, O. Stelzer-Chilton^{168a}, H. Stenzel⁵⁶, T.J. Stevenson¹⁵⁶, G.A. Stewart³⁶, M.C. Stockton³⁶, G. Stoicea^{27b}, M. Stolarski^{140a}, P. Stolte⁵³, S. Stonjek¹¹⁵, A. Straessner⁴⁸, J. Strandberg¹⁵⁴, S. Strandberg^{45a,45b}, M. Strauss¹²⁸, P. Strizenec^{28b}, R. Ströhmer¹⁷⁷, D.M. Strom¹³¹, R. Stroynowski⁴², A. Strubig⁵⁰, S.A. Stucci²⁹, B. Stugu¹⁷, J. Stupak¹²⁸, N.A. Styles⁴⁶, D. Su¹⁵³, S. Suchek^{61a}, Y. Sugaya¹³³, V.V. Sulin¹¹⁰, M.J. Sullivan⁹⁰, D.M.S. Sultan⁵⁴, S. Sultansoy^{4c}, T. Sumida⁸⁵, S. Sun¹⁰⁵, X. Sun³, K. Suruliz¹⁵⁶, C.J.E. Suster¹⁵⁷, M.R. Sutton¹⁵⁶, S. Suzuki⁸¹, M. Svatos¹⁴¹, M. Swiatlowski³⁷, S.P. Swift², A. Sydorenko⁹⁹, I. Sykora^{28a}, M. Sykora¹⁴³, T. Sykora¹⁴³, D. Ta⁹⁹, K. Tackmann^{46,z}, J. Taenzer¹⁶¹, A. Taffard¹⁷¹, R. Tafirout^{168a}, E. Tahirovic⁹², H. Takai²⁹, R. Takashima⁸⁶, K. Takeda⁸², T. Takeshita¹⁵⁰, E.P. Takeva⁵⁰, Y. Takubo⁸¹, M. Talby¹⁰¹, A.A. Talyshev^{122b,122a}, N.M. Tamir¹⁶¹, J. Tanaka¹⁶³, M. Tanaka¹⁶⁵, R. Tanaka¹³², B.B. Tannenwald¹²⁶, S. Tapia Araya¹⁷³, S. Tapprogge⁹⁹, A. Tarek Abouelfadl Mohamed¹³⁶, S. Tarem¹⁶⁰, G. Tarna^{27b,d}, G.F. Tartarelli^{68a}, P. Tas¹⁴³, M. Tasevsky¹⁴¹, T. Tashiro⁸⁵, E. Tassi^{41b,41a}, A. Tavares Delgado^{140a,140b}, Y. Tayalati^{35e}, A.J. Taylor⁵⁰, G.N. Taylor¹⁰⁴, P.T.E. Taylor¹⁰⁴, W. Taylor^{168b}, A.S. Tee⁸⁹, R. Teixeira De Lima¹⁵³, P. Teixeira-Dias⁹³, H. Ten Kate³⁶, J.J. Teoh¹²⁰, S. Terada⁸¹, K. Terashi¹⁶³, J. Terron⁹⁸, S. Terzo¹⁴, M. Testa⁵¹, R.J. Teuscher^{167,ad}, S.J. Thais¹⁸³, T. Theveneaux-Pelzer⁴⁶, F. Thiele⁴⁰, D.W. Thomas⁹³, J.O. Thomas⁴², J.P. Thomas²¹, A.S. Thompson⁵⁷, P.D. Thompson²¹, L.A. Thomsen¹⁸³, E. Thomson¹³⁷, Y. Tian³⁹, R.E. Ticse Torres⁵³, V.O. Tikhomirov^{110,ap}, Yu.A. Tikhonov^{122b,122a}, S. Timoshenko¹¹², P. Tipton¹⁸³, S. Tisserant¹⁰¹, K. Todome^{23b,23a}, S. Todorova-Nova⁵, S. Todt⁴⁸, J. Tojo⁸⁷, S. Tokár^{28a}, K. Tokushuku⁸¹, E. Tolley¹²⁶, K.G. Tomiwa^{33c}, M. Tomoto¹¹⁷, L. Tompkins^{153,q}, B. Tong⁵⁹, P. Tornambe¹⁰², E. Torrence¹³¹, H. Torres⁴⁸, E. Torró Pastor¹⁴⁸, C. Tosciri¹³⁵, J. Toth^{101,ac}, D.R. Tovey¹⁴⁹, C.J. Treado¹²⁴, T. Trefzger¹⁷⁷, F. Tresoldi¹⁵⁶, A. Tricoli²⁹, I.M. Trigger^{168a}, S. Trincaz-Duvoid¹³⁶, W. Trischuk¹⁶⁷, B. Trocmé⁵⁸, A. Trofymov¹³², C. Troncon^{68a}, M. Trovatelli¹⁷⁶, F. Trovato¹⁵⁶, L. Truong^{33b}, M. Trzebinski⁸⁴, A. Trzupek⁸⁴, F. Tsai⁴⁶, J.C.-L. Tseng¹³⁵, P.V. Tsiareshka^{107,aj}, A. Tsirigotis¹⁶², N. Tsirintanis⁹, V. Tsiskaridze¹⁵⁵, E.G. Tskhadadze^{159a}, M. Tsopoulou¹⁶², I.I. Tsukerman¹¹¹, V. Tsulaia¹⁸, S. Tsuno⁸¹, D. Tsybychev¹⁵⁵, Y. Tu^{63b}, A. Tudorache^{27b}, V. Tudorache^{27b}, T.T. Tulbure^{27a}, A.N. Tuna⁵⁹, S. Turchikhin⁷⁹, D. Turgeman¹⁸⁰, I. Turk Cakir^{4b,u}, R.J. Turner²¹, R.T. Turra^{68a}, P.M. Tuts³⁹, S. Tzamarias¹⁶², E. Tzovara⁹⁹, G. Ucchielli⁴⁷, I. Ueda⁸¹, M. Ughetto^{45a,45b}, F. Ukegawa¹⁶⁹, G. Unal³⁶, A. Undrus²⁹, G. Unel¹⁷¹, F.C. Ungaro¹⁰⁴, Y. Unno⁸¹, K. Uno¹⁶³, J. Urban^{28b}, P. Urquijo¹⁰⁴, G. Usai⁸,

J. Usui⁸¹, L. Vacavant¹⁰¹, V. Vacek¹⁴², B. Vachon¹⁰³, K.O.H. Vadla¹³⁴, A. Vaidya⁹⁴, C. Valderanis¹¹⁴, E. Valdes Santurio^{45a,45b}, M. Valente⁵⁴, S. Valentineti^{23b,23a}, A. Valero¹⁷⁴, L. Valéry⁴⁶, R.A. Vallance²¹, A. Vallier³⁶, J.A. Valls Ferrer¹⁷⁴, T.R. Van Daalen¹⁴, P. Van Gemmeren⁶, I. Van Vulpen¹²⁰, M. Vanadia^{73a,73b}, W. Vandelli³⁶, A. Vaniachine¹⁶⁶, R. Vari^{72a}, E.W. Varnes⁷, C. Varni^{55b,55a}, T. Varol⁴², D. Varouchas¹³², K.E. Varvell¹⁵⁷, M.E. Vasile^{27b}, G.A. Vasquez¹⁷⁶, J.G. Vasquez¹⁸³, F. Vazeille³⁸, D. Vazquez Furelos¹⁴, T. Vazquez Schroeder³⁶, J. Veatch⁵³, V. Vecchio^{74a,74b}, L.M. Veloce¹⁶⁷, F. Veloso^{140a,140c}, S. Veneziano^{72a}, A. Ventura^{67a,67b}, N. Venturi³⁶, A. Verbytskyi¹¹⁵, V. Vercesi^{70a}, M. Verducci^{74a,74b}, C.M. Vergel Infante⁷⁸, C. Vergis²⁴, W. Verkerke¹²⁰, A.T. Vermeulen¹²⁰, J.C. Vermeulen¹²⁰, M.C. Vetterli^{152,aw}, N. Viaux Maira^{147b}, M. Vicente Barreto Pinto⁵⁴, I. Vichou^{173,*}, T. Vickey¹⁴⁹, O.E. Vickey Boeriu¹⁴⁹, G.H.A. Viehhauser¹³⁵, L. Vigani¹³⁵, M. Villa^{23b,23a}, M. Villaplana Perez^{68a,68b}, E. Vilucchi⁵¹, M.G. Vinchter³⁴, V.B. Vinogradov⁷⁹, A. Vishwakarma⁴⁶, C. Vittori^{23b,23a}, I. Vivarelli¹⁵⁶, M. Vogel¹⁸², P. Vokac¹⁴², G. Volpi¹⁴, S.E. von Buddenbrock^{33c}, E. Von Toerne²⁴, V. Vorobel¹⁴³, K. Vorobev¹¹², M. Vos¹⁷⁴, J.H. Vossebeld⁹⁰, N. Vranjes¹⁶, M. Vranjes Milosavljevic¹⁶, V. Vrba¹⁴², M. Vreeswijk¹²⁰, R. Vuillermet³⁶, I. Vukotic³⁷, P. Wagner²⁴, W. Wagner¹⁸², J. Wagner-Kuhr¹¹⁴, H. Wahlberg⁸⁸, S. Wahrmund⁴⁸, K. Wakamiya⁸², V.M. Walbrecht¹¹⁵, J. Walder⁸⁹, R. Walker¹¹⁴, S.D. Walker⁹³, W. Walkowiak¹⁵¹, V. Wallangen^{45a,45b}, A.M. Wang⁵⁹, C. Wang^{60b}, F. Wang¹⁸¹, H. Wang¹⁸, H. Wang³, J. Wang¹⁵⁷, J. Wang^{61b}, P. Wang⁴², Q. Wang¹²⁸, R.-J. Wang¹³⁶, R. Wang^{60a}, R. Wang⁶, S.M. Wang¹⁵⁸, W.T. Wang^{60a}, W. Wang^{15c,ae}, W.X. Wang^{60a,ae}, Y. Wang^{60a,am}, Z. Wang^{60c}, C. Wanotayaroj⁴⁶, A. Warburton¹⁰³, C.P. Ward³², D.R. Wardrope⁹⁴, A. Washbrook⁵⁰, A.T. Watson²¹, M.F. Watson²¹, G. Watts¹⁴⁸, B.M. Waugh⁹⁴, A.F. Webb¹¹, S. Webb⁹⁹, C. Weber¹⁸³, M.S. Weber²⁰, S.A. Weber³⁴, S.M. Weber^{61a}, A.R. Weidberg¹³⁵, J. Weingarten⁴⁷, M. Weirich⁹⁹, C. Weiser⁵², P.S. Wells³⁶, T. Wenaus²⁹, T. Wengler³⁶, S. Wenig³⁶, N. Wermes²⁴, M.D. Werner⁷⁸, P. Werner³⁶, M. Wessels^{61a}, T.D. Weston²⁰, K. Whalen¹³¹, N.L. Whallon¹⁴⁸, A.M. Wharton⁸⁹, A.S. White¹⁰⁵, A. White⁸, M.J. White¹, R. White^{147b}, D. Whiteson¹⁷¹, B.W. Whitmore⁸⁹, F.J. Wickens¹⁴⁴, W. Wiedenmann¹⁸¹, M. Wielers¹⁴⁴, C. Wiglesworth⁴⁰, L.A.M. Wiik-Fuchs⁵², F. Wilk¹⁰⁰, H.G. Wilkens³⁶, L.J. Wilkins⁹³, H.H. Williams¹³⁷, S. Williams³², C. Willis¹⁰⁶, S. Willocq¹⁰², J.A. Wilson²¹, I. Wingerter-Seez⁵, E. Winkels¹⁵⁶, F. Winklmeier¹³¹, O.J. Winston¹⁵⁶, B.T. Winter⁵², M. Wittgen¹⁵³, M. Wobisch⁹⁵, A. Wolf⁹⁹, T.M.H. Wolf¹²⁰, R. Wolff¹⁰¹, R.W. Wölker¹³⁵, J. Wollrath⁵², M.W. Wolter⁸⁴, H. Wolters^{140a,140c}, V.W.S. Wong¹⁷⁵, N.L. Woods¹⁴⁶, S.D. Worm²¹, B.K. Wosiek⁸⁴, K.W. Woźniak⁸⁴, K. Wraight⁵⁷, S.L. Wu¹⁸¹, X. Wu⁵⁴, Y. Wu^{60a}, T.R. Wyatt¹⁰⁰, B.M. Wynne⁵⁰, S. Xella⁴⁰, Z. Xi¹⁰⁵, L. Xia¹⁷⁸, D. Xu^{15a}, H. Xu^{60a,d}, L. Xu²⁹, T. Xu¹⁴⁵, W. Xu¹⁰⁵, Z. Xu^{60b}, Z. Xu¹⁵³, B. Yabsley¹⁵⁷, S. Yacoob^{33a}, K. Yajima¹³³, D.P. Yallup⁹⁴, D. Yamaguchi¹⁶⁵, Y. Yamaguchi¹⁶⁵, A. Yamamoto⁸¹, T. Yamanaka¹⁶³, F. Yamane⁸², M. Yamatani¹⁶³, T. Yamazaki¹⁶³, Y. Yamazaki⁸², Z. Yan²⁵, H.J. Yang^{60c,60d}, H.T. Yang¹⁸, S. Yang⁷⁷, X. Yang^{60b,58}, Y. Yang¹⁶³, Z. Yang¹⁷, W-M. Yao¹⁸, Y.C. Yap⁴⁶, Y. Yasu⁸¹, E. Yatsenko^{60c,60d}, J. Ye⁴², S. Ye²⁹, I. Yeletskikh⁷⁹, E. Yigitbasi²⁵, E. Yildirim⁹⁹, K. Yorita¹⁷⁹, K. Yoshihara¹³⁷, C.J.S. Young³⁶, C. Young¹⁵³, J. Yu⁷⁸, X. Yue^{61a}, S.P.Y. Yuen²⁴, B. Zabinski⁸⁴, G. Zacharis¹⁰, E. Zaffaroni⁵⁴, J. Zahreddine¹³⁶, R. Zaidan¹⁴, A.M. Zaitsev^{123,ao}, T. Zakareishvili^{159b}, N. Zakharchuk³⁴, S. Zambito⁵⁹, D. Zanzi³⁶, D.R. Zaripovas⁵⁷, S.V. Zeißner⁴⁷, C. Zeitnitz¹⁸², G. Zemaitytė¹³⁵, J.C. Zeng¹⁷³, O. Zenin¹²³, T. Ženiš^{28a}, D. Zerwas¹³², M. Zgubić¹³⁵, D.F. Zhang^{15b}, F. Zhang¹⁸¹, G. Zhang^{60a}, G. Zhang^{15b}, H. Zhang^{15c}, J. Zhang⁶, L. Zhang^{15c}, L. Zhang^{60a}, M. Zhang¹⁷³, R. Zhang^{60a}, R. Zhang²⁴, X. Zhang^{60b}, Y. Zhang^{15a,15d}, Z. Zhang^{63a}, Z. Zhang¹³², P. Zhao⁴⁹, Y. Zhao^{60b}, Z. Zhao^{60a}, A. Zhemchugov⁷⁹, Z. Zheng¹⁰⁵, D. Zhong¹⁷³, B. Zhou¹⁰⁵, C. Zhou¹⁸¹, M.S. Zhou^{15a,15d}, M. Zhou¹⁵⁵, N. Zhou^{60c}, Y. Zhou⁷, C.G. Zhu^{60b}, H.L. Zhu^{60a}, H. Zhu^{15a}, J. Zhu¹⁰⁵, Y. Zhu^{60a}, X. Zhuang^{15a}, K. Zhukov¹¹⁰, V. Zhulanov^{122b,122a}, D. Ziemińska⁶⁵, N.I. Zimine⁷⁹, S. Zimmermann⁵², Z. Zinonos¹¹⁵, M. Ziolkowski¹⁵¹, L. Živković¹⁶, G. Zobernig¹⁸¹, A. Zoccoli^{23b,23a}, K. Zoch⁵³, T.G. Zorbas¹⁴⁹, R. Zou³⁷, L. Zwaliński³⁶.

- ¹Department of Physics, University of Adelaide, Adelaide; Australia.
- ²Physics Department, SUNY Albany, Albany NY; United States of America.
- ³Department of Physics, University of Alberta, Edmonton AB; Canada.
- ^{4(a)}Department of Physics, Ankara University, Ankara; ^(b)Istanbul Aydin University, Istanbul; ^(c)Division of Physics, TOBB University of Economics and Technology, Ankara; Turkey.
- ⁵LAPP, Université Grenoble Alpes, Université Savoie Mont Blanc, CNRS/IN2P3, Annecy; France.
- ⁶High Energy Physics Division, Argonne National Laboratory, Argonne IL; United States of America.
- ⁷Department of Physics, University of Arizona, Tucson AZ; United States of America.
- ⁸Department of Physics, University of Texas at Arlington, Arlington TX; United States of America.
- ⁹Physics Department, National and Kapodistrian University of Athens, Athens; Greece.
- ¹⁰Physics Department, National Technical University of Athens, Zografou; Greece.
- ¹¹Department of Physics, University of Texas at Austin, Austin TX; United States of America.
- ^{12(a)}Bahcesehir University, Faculty of Engineering and Natural Sciences, Istanbul; ^(b)Istanbul Bilgi University, Faculty of Engineering and Natural Sciences, Istanbul; ^(c)Department of Physics, Bogazici University, Istanbul; ^(d)Department of Physics Engineering, Gaziantep University, Gaziantep; Turkey.
- ¹³Institute of Physics, Azerbaijan Academy of Sciences, Baku; Azerbaijan.
- ¹⁴Institut de Física d'Altes Energies (IFAE), Barcelona Institute of Science and Technology, Barcelona; Spain.
- ^{15(a)}Institute of High Energy Physics, Chinese Academy of Sciences, Beijing; ^(b)Physics Department, Tsinghua University, Beijing; ^(c)Department of Physics, Nanjing University, Nanjing; ^(d)University of Chinese Academy of Science (UCAS), Beijing; China.
- ¹⁶Institute of Physics, University of Belgrade, Belgrade; Serbia.
- ¹⁷Department for Physics and Technology, University of Bergen, Bergen; Norway.
- ¹⁸Physics Division, Lawrence Berkeley National Laboratory and University of California, Berkeley CA; United States of America.
- ¹⁹Institut für Physik, Humboldt Universität zu Berlin, Berlin; Germany.
- ²⁰Albert Einstein Center for Fundamental Physics and Laboratory for High Energy Physics, University of Bern, Bern; Switzerland.
- ²¹School of Physics and Astronomy, University of Birmingham, Birmingham; United Kingdom.
- ²²Facultad de Ciencias y Centro de Investigaciones, Universidad Antonio Nariño, Bogota; Colombia.
- ^{23(a)}INFN Bologna and Universita' di Bologna, Dipartimento di Fisica; ^(b)INFN Sezione di Bologna; Italy.
- ²⁴Physikalisches Institut, Universität Bonn, Bonn; Germany.
- ²⁵Department of Physics, Boston University, Boston MA; United States of America.
- ²⁶Department of Physics, Brandeis University, Waltham MA; United States of America.
- ^{27(a)}Transilvania University of Brasov, Brasov; ^(b)Horia Hulubei National Institute of Physics and Nuclear Engineering, Bucharest; ^(c)Department of Physics, Alexandru Ioan Cuza University of Iasi, Iasi; ^(d)National Institute for Research and Development of Isotopic and Molecular Technologies, Physics Department, Cluj-Napoca; ^(e)University Politehnica Bucharest, Bucharest; ^(f)West University in Timisoara, Timisoara; Romania.
- ^{28(a)}Faculty of Mathematics, Physics and Informatics, Comenius University, Bratislava; ^(b)Department of Subnuclear Physics, Institute of Experimental Physics of the Slovak Academy of Sciences, Kosice; Slovak Republic.
- ²⁹Physics Department, Brookhaven National Laboratory, Upton NY; United States of America.
- ³⁰Departamento de Física, Universidad de Buenos Aires, Buenos Aires; Argentina.
- ³¹California State University, CA; United States of America.
- ³²Cavendish Laboratory, University of Cambridge, Cambridge; United Kingdom.
- ^{33(a)}Department of Physics, University of Cape Town, Cape Town; ^(b)Department of Mechanical

Engineering Science, University of Johannesburg, Johannesburg;^(c)School of Physics, University of the Witwatersrand, Johannesburg; South Africa.

³⁴Department of Physics, Carleton University, Ottawa ON; Canada.

^{35(a)}Faculté des Sciences Ain Chock, Réseau Universitaire de Physique des Hautes Energies - Université Hassan II, Casablanca;^(b)Faculté des Sciences, Université Ibn-Tofail, Kénitra;^(c)Faculté des Sciences Semlalia, Université Cadi Ayyad, LPHEA-Marrakech;^(d)Faculté des Sciences, Université Mohamed Premier and LPTPM, Oujda;^(e)Faculté des sciences, Université Mohammed V, Rabat; Morocco.

³⁶CERN, Geneva; Switzerland.

³⁷Enrico Fermi Institute, University of Chicago, Chicago IL; United States of America.

³⁸LPC, Université Clermont Auvergne, CNRS/IN2P3, Clermont-Ferrand; France.

³⁹Nevis Laboratory, Columbia University, Irvington NY; United States of America.

⁴⁰Niels Bohr Institute, University of Copenhagen, Copenhagen; Denmark.

^{41(a)}Dipartimento di Fisica, Università della Calabria, Rende;^(b)INFN Gruppo Collegato di Cosenza, Laboratori Nazionali di Frascati; Italy.

⁴²Physics Department, Southern Methodist University, Dallas TX; United States of America.

⁴³Physics Department, University of Texas at Dallas, Richardson TX; United States of America.

⁴⁴National Centre for Scientific Research "Demokritos", Agia Paraskevi; Greece.

^{45(a)}Department of Physics, Stockholm University;^(b)Oskar Klein Centre, Stockholm; Sweden.

⁴⁶Deutsches Elektronen-Synchrotron DESY, Hamburg and Zeuthen; Germany.

⁴⁷Lehrstuhl für Experimentelle Physik IV, Technische Universität Dortmund, Dortmund; Germany.

⁴⁸Institut für Kern- und Teilchenphysik, Technische Universität Dresden, Dresden; Germany.

⁴⁹Department of Physics, Duke University, Durham NC; United States of America.

⁵⁰SUPA - School of Physics and Astronomy, University of Edinburgh, Edinburgh; United Kingdom.

⁵¹INFN e Laboratori Nazionali di Frascati, Frascati; Italy.

⁵²Physikalisches Institut, Albert-Ludwigs-Universität Freiburg, Freiburg; Germany.

⁵³II. Physikalisches Institut, Georg-August-Universität Göttingen, Göttingen; Germany.

⁵⁴Département de Physique Nucléaire et Corpusculaire, Université de Genève, Genève; Switzerland.

^{55(a)}Dipartimento di Fisica, Università di Genova, Genova;^(b)INFN Sezione di Genova; Italy.

⁵⁶II. Physikalisches Institut, Justus-Liebig-Universität Giessen, Giessen; Germany.

⁵⁷SUPA - School of Physics and Astronomy, University of Glasgow, Glasgow; United Kingdom.

⁵⁸LPSC, Université Grenoble Alpes, CNRS/IN2P3, Grenoble INP, Grenoble; France.

⁵⁹Laboratory for Particle Physics and Cosmology, Harvard University, Cambridge MA; United States of America.

^{60(a)}Department of Modern Physics and State Key Laboratory of Particle Detection and Electronics, University of Science and Technology of China, Hefei;^(b)Institute of Frontier and Interdisciplinary Science and Key Laboratory of Particle Physics and Particle Irradiation (MOE), Shandong University, Qingdao;^(c)School of Physics and Astronomy, Shanghai Jiao Tong University, KLPPAC-MoE, SKLPPC, Shanghai;^(d)Tsung-Dao Lee Institute, Shanghai; China.

^{61(a)}Kirchhoff-Institut für Physik, Ruprecht-Karls-Universität Heidelberg, Heidelberg;^(b)Physikalisches Institut, Ruprecht-Karls-Universität Heidelberg, Heidelberg; Germany.

⁶²Faculty of Applied Information Science, Hiroshima Institute of Technology, Hiroshima; Japan.

^{63(a)}Department of Physics, Chinese University of Hong Kong, Shatin, N.T., Hong Kong;^(b)Department of Physics, University of Hong Kong, Hong Kong;^(c)Department of Physics and Institute for Advanced Study, Hong Kong University of Science and Technology, Clear Water Bay, Kowloon, Hong Kong; China.

⁶⁴Department of Physics, National Tsing Hua University, Hsinchu; Taiwan.

⁶⁵Department of Physics, Indiana University, Bloomington IN; United States of America.

^{66(a)}INFN Gruppo Collegato di Udine, Sezione di Trieste, Udine;^(b)ICTP, Trieste;^(c)Dipartimento

- Politecnico di Ingegneria e Architettura, Università di Udine, Udine; Italy.
- ^{67(a)}INFN Sezione di Lecce;^(b)Dipartimento di Matematica e Fisica, Università del Salento, Lecce; Italy.
- ^{68(a)}INFN Sezione di Milano;^(b)Dipartimento di Fisica, Università di Milano, Milano; Italy.
- ^{69(a)}INFN Sezione di Napoli;^(b)Dipartimento di Fisica, Università di Napoli, Napoli; Italy.
- ^{70(a)}INFN Sezione di Pavia;^(b)Dipartimento di Fisica, Università di Pavia, Pavia; Italy.
- ^{71(a)}INFN Sezione di Pisa;^(b)Dipartimento di Fisica E. Fermi, Università di Pisa, Pisa; Italy.
- ^{72(a)}INFN Sezione di Roma;^(b)Dipartimento di Fisica, Sapienza Università di Roma, Roma; Italy.
- ^{73(a)}INFN Sezione di Roma Tor Vergata;^(b)Dipartimento di Fisica, Università di Roma Tor Vergata, Roma; Italy.
- ^{74(a)}INFN Sezione di Roma Tre;^(b)Dipartimento di Matematica e Fisica, Università Roma Tre, Roma; Italy.
- ^{75(a)}INFN-TIFPA;^(b)Università degli Studi di Trento, Trento; Italy.
- ⁷⁶Institut für Astro- und Teilchenphysik, Leopold-Franzens-Universität, Innsbruck; Austria.
- ⁷⁷University of Iowa, Iowa City IA; United States of America.
- ⁷⁸Department of Physics and Astronomy, Iowa State University, Ames IA; United States of America.
- ⁷⁹Joint Institute for Nuclear Research, Dubna; Russia.
- ^{80(a)}Departamento de Engenharia Elétrica, Universidade Federal de Juiz de Fora (UFJF), Juiz de Fora;^(b)Universidade Federal do Rio De Janeiro COPPE/EE/IF, Rio de Janeiro;^(c)Universidade Federal de São João del Rei (UFSJ), São João del Rei;^(d)Instituto de Física, Universidade de São Paulo, São Paulo; Brazil.
- ⁸¹KEK, High Energy Accelerator Research Organization, Tsukuba; Japan.
- ⁸²Graduate School of Science, Kobe University, Kobe; Japan.
- ^{83(a)}AGH University of Science and Technology, Faculty of Physics and Applied Computer Science, Krakow;^(b)Marian Smoluchowski Institute of Physics, Jagiellonian University, Krakow; Poland.
- ⁸⁴Institute of Nuclear Physics Polish Academy of Sciences, Krakow; Poland.
- ⁸⁵Faculty of Science, Kyoto University, Kyoto; Japan.
- ⁸⁶Kyoto University of Education, Kyoto; Japan.
- ⁸⁷Research Center for Advanced Particle Physics and Department of Physics, Kyushu University, Fukuoka ; Japan.
- ⁸⁸Instituto de Física La Plata, Universidad Nacional de La Plata and CONICET, La Plata; Argentina.
- ⁸⁹Physics Department, Lancaster University, Lancaster; United Kingdom.
- ⁹⁰Oliver Lodge Laboratory, University of Liverpool, Liverpool; United Kingdom.
- ⁹¹Department of Experimental Particle Physics, Jožef Stefan Institute and Department of Physics, University of Ljubljana, Ljubljana; Slovenia.
- ⁹²School of Physics and Astronomy, Queen Mary University of London, London; United Kingdom.
- ⁹³Department of Physics, Royal Holloway University of London, Egham; United Kingdom.
- ⁹⁴Department of Physics and Astronomy, University College London, London; United Kingdom.
- ⁹⁵Louisiana Tech University, Ruston LA; United States of America.
- ⁹⁶Fysiska institutionen, Lunds universitet, Lund; Sweden.
- ⁹⁷Centre de Calcul de l’Institut National de Physique Nucléaire et de Physique des Particules (IN2P3), Villeurbanne; France.
- ⁹⁸Departamento de Física Teorica C-15 and CIAFF, Universidad Autónoma de Madrid, Madrid; Spain.
- ⁹⁹Institut für Physik, Universität Mainz, Mainz; Germany.
- ¹⁰⁰School of Physics and Astronomy, University of Manchester, Manchester; United Kingdom.
- ¹⁰¹CPPM, Aix-Marseille Université, CNRS/IN2P3, Marseille; France.
- ¹⁰²Department of Physics, University of Massachusetts, Amherst MA; United States of America.
- ¹⁰³Department of Physics, McGill University, Montreal QC; Canada.
- ¹⁰⁴School of Physics, University of Melbourne, Victoria; Australia.

- ¹⁰⁵Department of Physics, University of Michigan, Ann Arbor MI; United States of America.
- ¹⁰⁶Department of Physics and Astronomy, Michigan State University, East Lansing MI; United States of America.
- ¹⁰⁷B.I. Stepanov Institute of Physics, National Academy of Sciences of Belarus, Minsk; Belarus.
- ¹⁰⁸Research Institute for Nuclear Problems of Byelorussian State University, Minsk; Belarus.
- ¹⁰⁹Group of Particle Physics, University of Montreal, Montreal QC; Canada.
- ¹¹⁰P.N. Lebedev Physical Institute of the Russian Academy of Sciences, Moscow; Russia.
- ¹¹¹Institute for Theoretical and Experimental Physics of the National Research Centre Kurchatov Institute, Moscow; Russia.
- ¹¹²National Research Nuclear University MEPhI, Moscow; Russia.
- ¹¹³D.V. Skobeltsyn Institute of Nuclear Physics, M.V. Lomonosov Moscow State University, Moscow; Russia.
- ¹¹⁴Fakultät für Physik, Ludwig-Maximilians-Universität München, München; Germany.
- ¹¹⁵Max-Planck-Institut für Physik (Werner-Heisenberg-Institut), München; Germany.
- ¹¹⁶Nagasaki Institute of Applied Science, Nagasaki; Japan.
- ¹¹⁷Graduate School of Science and Kobayashi-Maskawa Institute, Nagoya University, Nagoya; Japan.
- ¹¹⁸Department of Physics and Astronomy, University of New Mexico, Albuquerque NM; United States of America.
- ¹¹⁹Institute for Mathematics, Astrophysics and Particle Physics, Radboud University Nijmegen/Nikhef, Nijmegen; Netherlands.
- ¹²⁰Nikhef National Institute for Subatomic Physics and University of Amsterdam, Amsterdam; Netherlands.
- ¹²¹Department of Physics, Northern Illinois University, DeKalb IL; United States of America.
- ^{122(a)}Budker Institute of Nuclear Physics and NSU, SB RAS, Novosibirsk;^(b)Novosibirsk State University Novosibirsk; Russia.
- ¹²³Institute for High Energy Physics of the National Research Centre Kurchatov Institute, Protvino; Russia.
- ¹²⁴Department of Physics, New York University, New York NY; United States of America.
- ¹²⁵Ochanomizu University, Otsuka, Bunkyo-ku, Tokyo; Japan.
- ¹²⁶Ohio State University, Columbus OH; United States of America.
- ¹²⁷Faculty of Science, Okayama University, Okayama; Japan.
- ¹²⁸Homer L. Dodge Department of Physics and Astronomy, University of Oklahoma, Norman OK; United States of America.
- ¹²⁹Department of Physics, Oklahoma State University, Stillwater OK; United States of America.
- ¹³⁰Palacký University, RCPTM, Joint Laboratory of Optics, Olomouc; Czech Republic.
- ¹³¹Center for High Energy Physics, University of Oregon, Eugene OR; United States of America.
- ¹³²LAL, Université Paris-Sud, CNRS/IN2P3, Université Paris-Saclay, Orsay; France.
- ¹³³Graduate School of Science, Osaka University, Osaka; Japan.
- ¹³⁴Department of Physics, University of Oslo, Oslo; Norway.
- ¹³⁵Department of Physics, Oxford University, Oxford; United Kingdom.
- ¹³⁶LPNHE, Sorbonne Université, Université de Paris, CNRS/IN2P3, Paris; France.
- ¹³⁷Department of Physics, University of Pennsylvania, Philadelphia PA; United States of America.
- ¹³⁸Konstantinov Nuclear Physics Institute of National Research Centre "Kurchatov Institute", PNPI, St. Petersburg; Russia.
- ¹³⁹Department of Physics and Astronomy, University of Pittsburgh, Pittsburgh PA; United States of America.
- ^{140(a)}Laboratório de Instrumentação e Física Experimental de Partículas - LIP, Lisbon;^(b)Departamento de Física, Faculdade de Ciências, Universidade de Lisboa, Lisbon;^(c)Departamento de Física, Universidade de

- Coimbra, Coimbra;^(d)Centro de Física Nuclear da Universidade de Lisboa, Lisbon;^(e)Departamento de Física, Universidade do Minho, Braga;^(f)Universidad de Granada, Granada (Spain);^(g)Dep Física and CEFITEC of Faculdade de Ciências e Tecnologia, Universidade Nova de Lisboa, Caparica;^(h)Av. Rovisco Pais, 1 1049-001 Lisbon, Portugal; Portugal.
- ¹⁴¹Institute of Physics of the Czech Academy of Sciences, Prague; Czech Republic.
- ¹⁴²Czech Technical University in Prague, Prague; Czech Republic.
- ¹⁴³Charles University, Faculty of Mathematics and Physics, Prague; Czech Republic.
- ¹⁴⁴Particle Physics Department, Rutherford Appleton Laboratory, Didcot; United Kingdom.
- ¹⁴⁵IRFU, CEA, Université Paris-Saclay, Gif-sur-Yvette; France.
- ¹⁴⁶Santa Cruz Institute for Particle Physics, University of California Santa Cruz, Santa Cruz CA; United States of America.
- ^{147(a)}Departamento de Física, Pontificia Universidad Católica de Chile, Santiago;^(b)Departamento de Física, Universidad Técnica Federico Santa María, Valparaíso; Chile.
- ¹⁴⁸Department of Physics, University of Washington, Seattle WA; United States of America.
- ¹⁴⁹Department of Physics and Astronomy, University of Sheffield, Sheffield; United Kingdom.
- ¹⁵⁰Department of Physics, Shinshu University, Nagano; Japan.
- ¹⁵¹Department Physik, Universität Siegen, Siegen; Germany.
- ¹⁵²Department of Physics, Simon Fraser University, Burnaby BC; Canada.
- ¹⁵³SLAC National Accelerator Laboratory, Stanford CA; United States of America.
- ¹⁵⁴Physics Department, Royal Institute of Technology, Stockholm; Sweden.
- ¹⁵⁵Departments of Physics and Astronomy, Stony Brook University, Stony Brook NY; United States of America.
- ¹⁵⁶Department of Physics and Astronomy, University of Sussex, Brighton; United Kingdom.
- ¹⁵⁷School of Physics, University of Sydney, Sydney; Australia.
- ¹⁵⁸Institute of Physics, Academia Sinica, Taipei; Taiwan.
- ^{159(a)}E. Andronikashvili Institute of Physics, Iv. Javakhishvili Tbilisi State University, Tbilisi;^(b)High Energy Physics Institute, Tbilisi State University, Tbilisi; Georgia.
- ¹⁶⁰Department of Physics, Technion, Israel Institute of Technology, Haifa; Israel.
- ¹⁶¹Raymond and Beverly Sackler School of Physics and Astronomy, Tel Aviv University, Tel Aviv; Israel.
- ¹⁶²Department of Physics, Aristotle University of Thessaloniki, Thessaloniki; Greece.
- ¹⁶³International Center for Elementary Particle Physics and Department of Physics, University of Tokyo, Tokyo; Japan.
- ¹⁶⁴Graduate School of Science and Technology, Tokyo Metropolitan University, Tokyo; Japan.
- ¹⁶⁵Department of Physics, Tokyo Institute of Technology, Tokyo; Japan.
- ¹⁶⁶Tomsk State University, Tomsk; Russia.
- ¹⁶⁷Department of Physics, University of Toronto, Toronto ON; Canada.
- ^{168(a)}TRIUMF, Vancouver BC;^(b)Department of Physics and Astronomy, York University, Toronto ON; Canada.
- ¹⁶⁹Division of Physics and Tomonaga Center for the History of the Universe, Faculty of Pure and Applied Sciences, University of Tsukuba, Tsukuba; Japan.
- ¹⁷⁰Department of Physics and Astronomy, Tufts University, Medford MA; United States of America.
- ¹⁷¹Department of Physics and Astronomy, University of California Irvine, Irvine CA; United States of America.
- ¹⁷²Department of Physics and Astronomy, University of Uppsala, Uppsala; Sweden.
- ¹⁷³Department of Physics, University of Illinois, Urbana IL; United States of America.
- ¹⁷⁴Instituto de Física Corpuscular (IFIC), Centro Mixto Universidad de Valencia - CSIC, Valencia; Spain.
- ¹⁷⁵Department of Physics, University of British Columbia, Vancouver BC; Canada.

- ¹⁷⁶Department of Physics and Astronomy, University of Victoria, Victoria BC; Canada.
- ¹⁷⁷Fakultät für Physik und Astronomie, Julius-Maximilians-Universität Würzburg, Würzburg; Germany.
- ¹⁷⁸Department of Physics, University of Warwick, Coventry; United Kingdom.
- ¹⁷⁹Waseda University, Tokyo; Japan.
- ¹⁸⁰Department of Particle Physics, Weizmann Institute of Science, Rehovot; Israel.
- ¹⁸¹Department of Physics, University of Wisconsin, Madison WI; United States of America.
- ¹⁸²Fakultät für Mathematik und Naturwissenschaften, Fachgruppe Physik, Bergische Universität Wuppertal, Wuppertal; Germany.
- ¹⁸³Department of Physics, Yale University, New Haven CT; United States of America.
- ¹⁸⁴Yerevan Physics Institute, Yerevan; Armenia.
- ^a Also at Borough of Manhattan Community College, City University of New York, New York NY; United States of America.
- ^b Also at Centre for High Performance Computing, CSIR Campus, Rosebank, Cape Town; South Africa.
- ^c Also at CERN, Geneva; Switzerland.
- ^d Also at CPPM, Aix-Marseille Université, CNRS/IN2P3, Marseille; France.
- ^e Also at Département de Physique Nucléaire et Corpusculaire, Université de Genève, Genève; Switzerland.
- ^f Also at Departament de Fisica de la Universitat Autònoma de Barcelona, Barcelona; Spain.
- ^g Also at Departamento de Física, Instituto Superior Técnico, Universidade de Lisboa, Lisboa; Portugal.
- ^h Also at Department of Applied Physics and Astronomy, University of Sharjah, Sharjah; United Arab Emirates.
- ⁱ Also at Department of Financial and Management Engineering, University of the Aegean, Chios; Greece.
- ^j Also at Department of Physics and Astronomy, University of Louisville, Louisville, KY; United States of America.
- ^k Also at Department of Physics and Astronomy, University of Sheffield, Sheffield; United Kingdom.
- ^l Also at Department of Physics, California State University, East Bay; United States of America.
- ^m Also at Department of Physics, California State University, Fresno; United States of America.
- ⁿ Also at Department of Physics, California State University, Sacramento; United States of America.
- ^o Also at Department of Physics, King's College London, London; United Kingdom.
- ^p Also at Department of Physics, St. Petersburg State Polytechnical University, St. Petersburg; Russia.
- ^q Also at Department of Physics, Stanford University, Stanford CA; United States of America.
- ^r Also at Department of Physics, University of Fribourg, Fribourg; Switzerland.
- ^s Also at Department of Physics, University of Michigan, Ann Arbor MI; United States of America.
- ^t Also at Faculty of Physics, M.V. Lomonosov Moscow State University, Moscow; Russia.
- ^u Also at Giresun University, Faculty of Engineering, Giresun; Turkey.
- ^v Also at Graduate School of Science, Osaka University, Osaka; Japan.
- ^w Also at Hellenic Open University, Patras; Greece.
- ^x Also at Horia Hulubei National Institute of Physics and Nuclear Engineering, Bucharest; Romania.
- ^y Also at Institutio Catalana de Recerca i Estudis Avancats, ICREA, Barcelona; Spain.
- ^z Also at Institut für Experimentalphysik, Universität Hamburg, Hamburg; Germany.
- ^{aa} Also at Institute for Mathematics, Astrophysics and Particle Physics, Radboud University Nijmegen/Nikhef, Nijmegen; Netherlands.
- ^{ab} Also at Institute for Nuclear Research and Nuclear Energy (INRNE) of the Bulgarian Academy of Sciences, Sofia; Bulgaria.
- ^{ac} Also at Institute for Particle and Nuclear Physics, Wigner Research Centre for Physics, Budapest; Hungary.
- ^{ad} Also at Institute of Particle Physics (IPP), Vancouver; Canada.

- ae* Also at Institute of Physics, Academia Sinica, Taipei; Taiwan.
- af* Also at Institute of Physics, Azerbaijan Academy of Sciences, Baku; Azerbaijan.
- ag* Also at Institute of Theoretical Physics, Ilia State University, Tbilisi; Georgia.
- ah* Also at Instituto de Fisica Teorica, IFT-UAM/CSIC, Madrid; Spain.
- ai* Also at Istanbul University, Dept. of Physics, Istanbul; Turkey.
- aj* Also at Joint Institute for Nuclear Research, Dubna; Russia.
- ak* Also at LAL, Université Paris-Sud, CNRS/IN2P3, Université Paris-Saclay, Orsay; France.
- al* Also at Louisiana Tech University, Ruston LA; United States of America.
- am* Also at LPNHE, Sorbonne Université, Université de Paris, CNRS/IN2P3, Paris; France.
- an* Also at Manhattan College, New York NY; United States of America.
- ao* Also at Moscow Institute of Physics and Technology State University, Dolgoprudny; Russia.
- ap* Also at National Research Nuclear University MEPhI, Moscow; Russia.
- aq* Also at Physics Department, An-Najah National University, Nablus; Palestine.
- ar* Also at Physikalisches Institut, Albert-Ludwigs-Universität Freiburg, Freiburg; Germany.
- as* Also at School of Physics, Sun Yat-sen University, Guangzhou; China.
- at* Also at The City College of New York, New York NY; United States of America.
- au* Also at The Collaborative Innovation Center of Quantum Matter (CICQM), Beijing; China.
- av* Also at Tomsk State University, Tomsk, and Moscow Institute of Physics and Technology State University, Dolgoprudny; Russia.
- aw* Also at TRIUMF, Vancouver BC; Canada.
- ax* Also at Universita di Napoli Parthenope, Napoli; Italy.
- * Deceased